

LAS

Jahresbericht / Annual Report 2019



Neubau des "Anwendungszentrums Fluidynamik" (Quelle: AWB Architekten, Dresden)



Prof. Dr.-Ing. Christoph Egbers
Lehrstuhl Aerodynamik und Strömungslehre (LAS)
Institut für Verkehrstechnik
Fakultät 3
Maschinenbau, Elektro- und Energiesysteme
BTU Cottbus-Senftenberg
Siemens-Halske-Ring 15a
03046 Cottbus



Brandenburgische
Technische Universität
Cottbus - Senftenberg

Vorwort

Der *Lehrstuhl Aerodynamik und Strömungslehre (LAS)* wurde im Juli 2000 mit der Berufung von Dr.-Ing. Christoph Egbers an die Brandenburgische Technische Universität (BTU) Cottbus neu gegründet. Der Lehrstuhl gehört zum *Institut für Verkehrstechnik (IVT)*, welches im Jahr 1999 gegründet wurde. Diesem Institut gehören z.Zt. folgende Lehrstühle an:

- LS Aerodynamik und Strömungslehre (LAS)
- LS Technische Mechanik und Fahrzeugdynamik
- LS Strukturmechanik und Fahrzeugschwingungen
- LS Verbrennungskraftmaschinen und Flugantriebe
- LS Fahrzeugtechnik- und Antriebe
- LS Technische Akustik
- LS Triebwerksdesign
- LS Numerische Strömungs- und Gasdynamik
- LS Bildgebende Messverfahren (neu: gemeinsame Berufung DLR-BTU)

Der Lehrstuhl für Aerodynamik und Strömungslehre (LAS) beschäftigt 27 Mitarbeiter/innen und ist in vier Abteilungen gegliedert, in denen z.Zt. folgende Forschungsthemen bearbeitet werden:

Aerodynamik

- Triebwerks-Flügel-Wechselwirkungen
- Grenzschichtströmungen
- Strömungsbeeinflussung

Strömungsmechanik

- Strukturbildung und Stabilität in hydrodynamischen Systemen
- Rotierende Strömungen
- Turbulente Strömungen
- Geophysikalisch motivierte Strömungen
- Meteorologisch motivierte Strömungen
- Gleitlagerströmungen
- Partikelströmungen
- Thermoelektrohydrodynamik (TEHD)

Raumfahrtanwendungen

- Fluid-Experimente unter Schwerelosigkeit (Raumstation ISS, Parabelflüge, Fallturm)

Messtechnik

- Entwicklung von Strömungsmessverfahren zur Strömungsbeeinflussung
- Partikelmesstechnik
- Zeitreihenanalyse und nichtlineare Datenanalyse
- Koppelung von PIV und Thermographie (simultane Temperatur- und Geschwindigkeitsmessung)

Ich bedanke mich mit diesem Jahresbericht bei meinen Mitarbeiterinnen und Mitarbeitern für die sehr erfolgreich geleistete Arbeit am Lehrstuhl sowie bei unseren Kooperationspartnern und bei allen Förderinstitutionen, von denen der Lehrstuhl Aerodynamik und Strömungslehre (LAS) an der BTU Cottbus-Senftenberg Projektförderung erhalten hat.

Cottbus, im Juni 2019

Prof. Dr.-Ing. Christoph Egbers

Inhaltsverzeichnis / Index

Mitarbeiter am Lehrstuhl Aeordynamik und Strömungslehre (LAS) / Staff at the Chair of Aerodynamics and Fluid Mechanics (LAS)	6
Internationale Kooperationen und Partner / International contacts and co-operation	7
Fluid-Centrum / Fluid-Center	8
Neubau "Anwendungszentrum Fluid Dynamik (AZFD) / New Building „Center of Applied Fluid Dynamics“	9
EUHiT-Netzwerk / Scientific network activities (EUHiT)	12
Lehre / Courses	14
Seminare / workshops	16
Forschungseinrichtungen des Lehrstuhls / Research Facilities	20
Aktuelle Forschungsschwerpunkte / Current research topics	22
Aerodynamics	22
Fluid Mechanics	40
Space Research	60
Computer-Technologie	72
Veröffentlichungen / Publications and contributions to conferences	74
BSc/MSc-, Diplomarbeiten, Promotionen, Habilitationen / Examinations and theses	80
Anfahrt / How to get there?	82

Mitarbeiter / Staff at the Chair of Aerodynamics and Fluid Mechanics

Prof. Dr.-Ing. Christoph Egbers	Leiter des Lehrstuhls
Silke Kaschwich	Sekretariat
Wissenschaftliche Mitarbeiter	Aufgabengebiet
M.Sc. Zeinab Hallol	Strömungsmechanik (Doktorandin)
apl. Prof. Dr. rer. nat. habil. Uwe Harlander	Strömungsmechanik, Meteorologie
M.Sc. Gazi Hasanuzzaman	Aerodynamik (Doktorand)
M.Sc. Peter Haun	Strömungsmechanik (Doktorand)
Dr. rer. nat. Andreas Krebs	Rechneradministration CFTMM und HLRN
Dr.-Ing. Martin Meier	Raumfahrtanwendungen (Postdoc)
M.Sc. Gabriel Meletti	Strömungsmechanik (Doktorand)
Dipl.-Phys. Sebastian Merbold	Strömungsmechanik (Doktorand)
Dr. Antoine Meyer	Strömungsmechanik (Postdoc)
Dr.-Ing. Vasyl Motuz	Aerodynamik, (Postdoc)
M.Sc. Stefan Richter	Aerodynamik (Doktorand)
M.Sc. Costanza Rodda	Strömungsmechanik (Doktorandin)
Dr.-Ing. Torsten Seelig	Strömungsmechanik (Postdoc)
M. Sc. Amir Shahirpour	Strömungsmechanik Numerik (Doktorand)
Dr. Peter Szabo	Strömungsmechanik (Postdoc)
Dr.-Ing. Vadim Travnikov	Strömungsmechanik (Postdoc)
Dipl.-Ing. Wenchao Xu	Strömungsmechanik (Doktorand)
M.Sc. Mohammed Yousry	Aerodynamik (Doktorand)
Prof. Dr.-Ing. El-Sayed Zanoun	Aerodynamik
Dr. Mag. rer. nat. Florian Zaussinger	Strömungsmechanik (Postdoc)
Technische Mitarbeiter	Aufgabengebiet
Dipl.-Ing. Wolfgang Beyer	Labore, Messtechnik, rotierende Strömungen
M. Sc. Markus Helbig	Parabelflug-/TEXUS-Experimente
B. Eng. Florian Prüfer	Parabelflug-/TEXUS-Experimente
Dipl.-Ing. Ludwig Stapelfeld	Labore, Windkanäle, Messtechnik
Dipl.-Ing. Andreas Stöckert	Systemadministration, Messtechnik
Dipl.-Ing. Heinz-Jörg Wengler	Labor- und Werkstattbetrieb

Wissenschaftliche Kooperationen und Partner

Scientific contacts and co-operation with industrial partner

Prof. Dr. Detlef Lohse	Physics of Fluids, University of Twente, The Netherlands
Prof. Dr. Vincent Heuveline	URZ, Heidelberg, Universität Heidelberg
Prof. Dr. Leo Maas	The Royal Netherlands Institute for Sea Research (NIOZ), Dept. of Phys. Oceanography, Texel, The Netherlands
Prof. Dr. Peter Read	Dept. of Atmospheric, Oceanic and Planetary Physics University of Oxford, UK
Dr. Wolf-Gerrit Früh	Heriot-Watt University, Edinburgh, UK
Prof. Dr. Rainer Hollerbach	Dept. of Mathematics, University of Leeds, UK
Prof. Dr. Daniel Lathrop	Institute for Physical Sciences and Technology, University of Maryland, USA
Prof. Dr. Richard M. Lueptow	Dept. of Mech. Engineering Northwestern University, Chicago, USA
Prof. Dr. Laurette Tuckerman	ESPCI, Paris, France
Prof. Dr. Patrice LeGal	IRPHE, Université Marseille, France
Prof. Dr. Innocent Mutabazi	LOMC, CNRS Université du Havre, France
Prof. Dr. Pascal Chossat	Directeur Centre International de Rencontres Mathématiques, Luminy (Marseille), France
Prof. Dr. Philippe Cardin	Institut des Sciences de la Terre, Grenoble, France
Prof. Dr. Antony Randriamampianina	CNRS, Université Marseille, France
Prof. Dr. Reinhard Hüttl	Leiter GFZ, Potsdam
Prof. Dr. rer. nat. Doris Breuer	DLR-Inst. (Planetary Atmospheres), Berlin
Prof. Dr. Bruno Eckhardt	Fachbereich Physik, Philipps Universität Marburg
Prof. Dr.-Ing. habil. Antonio Delgado	Lehrstuhl für Strömungsmechanik Universität Erlangen-Nürnberg
Prof. Dr. Jörg Schumacher	Institut für Thermo- und Fluidodynamik, TU Ilmenau
Prof. Dr. rer. nat. habil. Andre Thess	Institut für Technische Thermodynamik, DLR, Stuttgart
Prof. Dr. Andreas Tilgner	Institut für Geophysik., Universität Göttingen
Prof. Dr. Eberhard Bodenschatz	MPI für Dynamik und Selbstorganisation, Göttingen
Prof. Dr.-Ing. Ulrich Riebel	Lehrstuhl für Mech. Verfahrenstechnik, BTU Cottbus

Fluid-Centrum / Fluid-Center

Das Fluid-Centrum des Lehrstuhls Aerodynamik und Strömungslehre wurde 2004 in Betrieb genommen. Dort sind folgende Labore sowie Prüf- und Versuchsstände des Lehrstuhls untergebracht

Halle I (Aerodynamik- und Aeroakustik-Halle, 400qm):

- Großer Rohrströmungskanal (Cottbus Large Pipe Test Facility, CoLa-Pipe)
- Kleiner Rohrströmungskanal (Cottbus Small Pipe Test Facility, CoSma-Pipe)
- Kleiner Lehr- und Forschungswindkanal für hochpräzise Strömungskalibration
- Windkanal für Fahrzeugmodell- bzw. Flugzeughalbmodelluntersuchungen
- Aeroakustik-Prüfstand/Freistrahlbläse

Halle II (Strömungsprüfstands- / Raumfahrt-Halle, 400qm):

- Labore für rotierende Strömungen (150 qm)
- Laserlabor (75 qm)
- Strömungsprüfstandslabore (75 qm)
- Bodenstation und Vorbereitungsraum für Raumfahrtexperimente (100 qm)



Ansicht des Fluid-Centrums (Aerodynamik- und Strömungsprüfstandshalle)

Neubau des „Anwendungszentrums Fluidodynamik“ New Building „Center of Applied Fluid Dynamics“



EUROPÄISCHE UNION
Europäischer Fonds für
regionale Entwicklung

Zusammenfassung

Ziel des Ende 2017 genehmigten EFRE-Vorhabens in Höhe von 7.2 Mio. € ist der Neubau des "Anwendungszentrums Fluidodynamik", eines neuen Labor- und Bürogebäudes, neben dem Fluid-Centrum (LH3D) der Brandenburgischen Technischen Universität Cottbus-Senftenberg (BTU) auf dem Zentralcampus in Cottbus. Das neue Gebäude soll die Anzahl der Projekte, insbesondere die Kooperationsvorhaben im Bereich der Energietechnik mit der regionalen Industrie und damit den Technologietransfer maßgeblich erhöhen. Einen vergleichbaren Standort in Brandenburg gibt es nicht. Neben neuen Büros für die bisher in verschiedenen Gebäuden verteilten Mitarbeiter der Lehrstühle LAS, LTA und LNSG sowie dem CFTM² wird auch Platz für 7 weitere Labore geschaffen. Dies sind u. a. ein Labor für Parabelflug-Vorbereitung, ein Labor für akustische Messtechnik und ein Laserlabor. Damit wird das neue Anwendungszentrum zu einem zentralen Forschungspartner für die Energietechnik in der Region und überregional. Baubeginn war Februar 2018, Fertigstellung und Übernahme der BTU ist für Oktober 2019 geplant.

Ansichten



Ziele des Bau-Vorhabens

Am Lehrstuhl für Aerodynamik und Strömungslehre (LAS, Institut für Verkehrstechnik, BTU Cottbus-Senftenberg) werden national und international anerkannte grundlagen- und anwendungsorientierte Forschungsarbeiten auf dem Gebiet der experimentellen, theoretischen und numerischen Strömungsmechanik, Aerodynamik sowie Messtechnik durchgeführt.

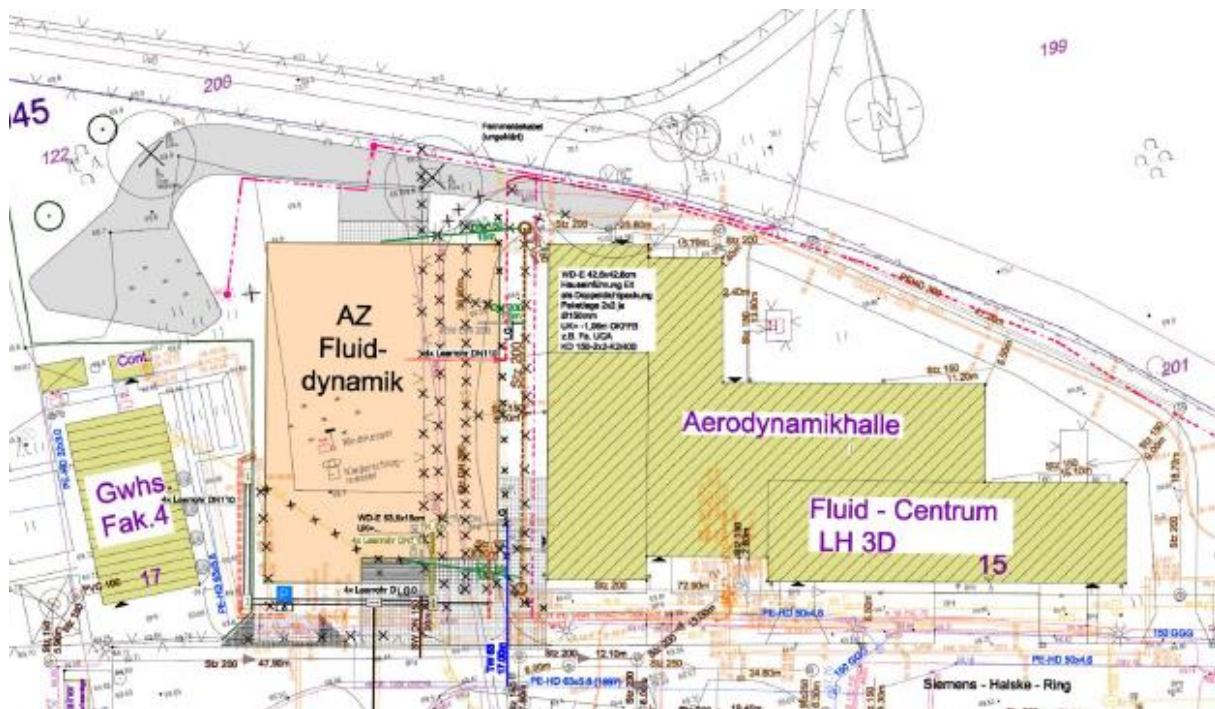
Der Lehrstuhl gehört ebenso wie die beiden anderen mitbeantragenden Lehrstühle für Technische Akustik (LTA) und Numerische Strömungs- und Gasdynamik, (LNSG), zum BTU-weiten Zentrum für Strömungs- und Transportphänomene, Modellierung und Messtechnik (CFTM²). Das Fluid-Centrum mit seiner Laborhalle steht dabei zentral im Mittelpunkt interdisziplinärer Forschung der beteiligten und weiteren BTU-Lehrstühle.

Neubau des „Anwendungszentrums Fluidodynamik“ New Building „Center of Applied Fluid Dynamics“



EUROPÄISCHE UNION
Europäischer Fonds für
regionale Entwicklung

Das hier beantragte „Anwendungszentrum Fluidodynamik“ ist auf dem Zentralcampus der BTU direkt neben dem bestehenden Fluid-Centrum geplant.



Der Neubau soll neben neuen Büros für die bisher in verschiedenen Gebäuden verteilten Mitarbeiter von LAS, LTA und LNSG sowie dem CFTM2 auch dringend benötigten Platz für weitere Labore im Bereich angewandter Forschung schaffen. Dies sind im Einzelnen folgende Labore mit je ca. 40-50 qm:

- Physikalisch-chemisches (Fluid-)Labor
mit einer Reinheitsklasse D nach EG-GMP-Leitfaden, Annex 1 (bzw. ca. 7 nach EN ISO 14644-1) zur Messung / Charakterisierung von sensiblen Fluideigenschaften, wie z.B. Dichte, Brechzahl, Grenz- und Oberflächenspannung, Viskosität etc.
- Labor zur Modell- und Messvorbereitung
für aeroakustische und aerodynamische Experimente.
- Laserlabor
mit Abdunkelung für Strömungsmessungen mit laseroptischen Messverfahren, z.B. PIV-/LIF-/LDA-Messtechnik (Laser Klasse 3 und 4).
- Labor für Hochspannungsversuche an Flüssigkeiten
mit interner Abschirmung. Durchführung industrie- und anwendungsnahe experimenteller Forschung zur Strömungskontrolle und zur Verbesserung von Wärmetauschern als Spin-Off des GEOFLOW-Raumfahrtprojekts.
- Labor für Parabelflugvorbereitung
zur Vorbereitung anwendungsorientierter Experimente zur Schwerelosigkeitsforschung, z.B. Schaumdynamik, Tropfendynamik usw. mit Industriebezug.

Neubau des „Anwendungszentrums Fluidodynamik“ New Building „Center of Applied Fluid Dynamics“



EUROPÄISCHE UNION
Europäischer Fonds für
regionale Entwicklung

- Labor für akustische Messtechnik
zur Vorbereitung umfangreicher Messaufbauten für die Charakterisierung von Schallquellen an Maschinen und Fahrzeugen.
- Labor für konstruktive Lärminderung
mit verschiedenen Versuchsaufbauten zum anwendungsnahen Testen lärmarmen Maschinen- und Fahrzeugkomponenten.

Zur Forschungsprogrammatische des LAS gehören gleichermaßen grundlagenorientierte wie anwendungsnahe Untersuchungen zu rotierenden, geschichteten und grenzschichtnahen Strömungen mit Anwendungen in Natur und Technik. Seit 17 Jahren stehen dabei Untersuchungen (experimentell, theoretisch, numerisch) von Stabilität, Strukturbildung und Turbulenzentstehung in rotierenden und geschichteten Fluidsystemen sowie von hochturbulenten Rohr- und Windkanalströmungen im Vordergrund. Dazu wurde seit Inbetriebnahme des Fluid-Centrums im Jahr 2004 eine Reihe von hochwertigen wissenschaftlichen Experimentalanlagen mit adäquater Messtechnik aufgebaut, die inzwischen auch von der Industrie nachgefragt werden. So werden zunehmend zahlreiche anwendungsorientierte Projekte zu aerodynamischen und strömungstechnischen Themen in enger Kooperation mit der Industrie bundesweit (z.B. im Rahmen von AIF, ZIM, FVV) durchgeführt. Dies schließt insbesondere auch bilaterale Kooperationsprojekte mit regionalen Firmen ein, wie z.B. Vattenfall Europe (theoretische und numerische Auslegung und Optimierung von Energiespeichersystemen), HKW Cottbus, (Optimierung von Kohletransport im Kraftwerksprozess), SGW Werder Filtertechnik (Optimierung von Filteranlagen für Bahntechnik) oder DB Cottbus (Optimierung der Abgasführung). Die Abbildungen 1 und 2 geben einen Überblick über die aktuellen Forschungsthemen des LAS und des LTA.

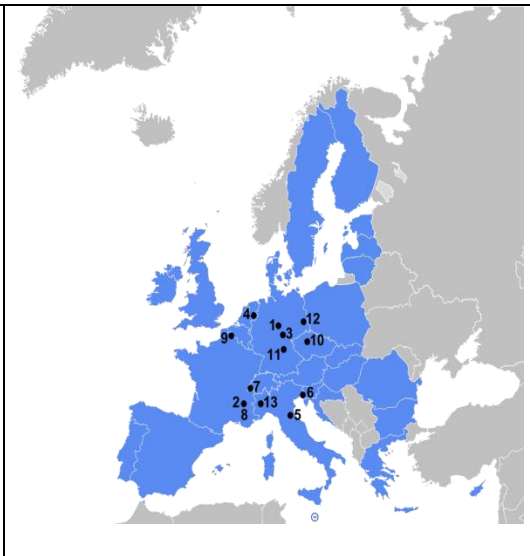
In der Laborhalle 3D (Fluid-Centrum) werden die Versuchsanlagen laufend weiterentwickelt, an den Stand der Forschung sowie an die Industrieforderungen angepasst. Es sind inzwischen zahlreiche neue Experimente hinzugekommen und der Nutzungsgrad durch regionale Industrievorhaben, aber auch mit internationaler wissenschaftlicher Beteiligung hat sich massiv erhöht. Deshalb ist ein weiteres Labor- und Bürogebäude für aerodynamische, aeroakustische und fluidmechanische anwendungsnahe Forschung dringend notwendig. Am Lehrstuhl LAS sind aktuell acht durch die Deutsche Forschungsgemeinschaft (DFG) und andere Fördermittelgeber (ESA, EU, BMWi, AiF, Industrie) geförderte Vorhaben angesiedelt. Das hier beantragte Anwendungszentrum soll als zentraler regionaler Ansprechpartner für fluiddynamische Untersuchungen in der Energietechnik die Anzahl der Projekte, insbesondere die Kooperationsvorhaben mit der regionalen Industrie maßgeblich weiter erhöhen und damit auch den Technologietransfer in die Region nachhaltig sicherstellen. Einen vergleichbaren Standort in Brandenburg gibt es nicht; die nächsten wissenschaftlichen Einrichtungen mit ähnlicher Ausstattung jedoch anderen Forschungsschwerpunkten sind an der TU Berlin und der TU Dresden zu finden. Fachwissenschaftlich ähnliche Zentren gibt es an den Universitäten Bremen, Erlangen und Karlsruhe sowie Twente in den Niederlanden.

Aktuell sind ca. 40 Mitarbeiter, davon ca. 30 Wissenschaftler am LAS, LTA sowie LNSG tätig. Die Mitarbeiter, Laborräume und zugehörige Rechnerclusterräume sind zurzeit provisorisch in drei Gebäuden (LG3A, LG3, LH3D) auf dem Zentralcampus der BTU untergebracht. Das neue Gebäude am Fluid-Centrum wird alle Mitarbeiterbüros und die industrienahen Forschungslabore vereinigen.

**Scientific network activities (EUHiT), www.euhit.org
European High-performance Infrastructures in Turbulence**

Infrastructures:

1. Göttingen Turbulence Facilities (GTF)
2. Grenoble Helium Infrastructures (GHI)
3. Barrel of Ilmenau (BOI)
4. Twente Turbulence Facility (TTF)
5. CICLoPE
6. High Rayleigh number Cryogenic Facility (HRCF)
7. CERN Cryogenic Turbulence facility (GReC)
8. CORIOLIS rotating platform
9. LML boundary layer wind tunnel
10. Czech Cryogenic Turbulence Facility (CCTF)
11. Refractive Index Matched Tunnel (RIMT)
12. Cottbus Geophysics Experiments (CoGeoF)
13. Turin Rotating Platform (TurLab)
14. Digital Library of Turbulence Data (DLTD)



Within **EUHiT-programme, (2013-2017)**, **CoGeoF** and **CoLaPipeF** have been established by the BTU Cottbus-Senftenberg, Department of Aerodynamics and Fluid Mechanics within the Center of Flow and Transport Modeling and Measurement (**CFTM2**). **CoGeoF** and **CoLaPipeF** are part of the Fluid-Center located on the Campus of BTU. The Fluid-Center is operational since 2004. The CFTM2 was founded 2008 as an initiative to bundle the BTU activities on fluid transport processes and to promote the interdisciplinary exchange within the University and with the industry. Guest apartments for visiting scientists are located close to the University Campus.

(a) Cottbus Geophysical Experiments Facility (CoGeoF):

Experiments on rotating platforms suited for applications in the geophysical context:

- Rotating differentially heated annulus to study geostrophic turbulence,
- Inertial wave tanks to study wave turbulence relevant in the geophysical and astrophysical context, two different geometries (annulus and spherical shell) allow a flexible experimental design,
- Taylor-Couette-systems with a flexible design to study turbulence with astrophysical applications,
- Measurement systems: stereo PIV, Tomo PIV, LIF, LDA, infrared thermography, the facilities can provide simultaneous thermography/PIV, LIF/PIV measurements.

(b) Cottbus Large Pipe Test Facility (CoLaPipe)

- Closed-return air pipe facility with constant temperature conditions, high spatial resolution (up to 300mm) at high turbulence levels (Karman number $R^+ = 1.9 \cdot 10^4$), 27 m long measurement tunnel with movable measurement subsections of 0.25, 0.5, 0.75 and 2m length respectively, optical assessment of the tunnel,
- Measurement techniques: HWA, LDA, PIV, pressure probes, surface microphones.

Scientific network activities (EUHiT), www.euhit.org European High-performance Infrastructures in Turbulence

Recent experiments from external scientists at BTU facilities (EUHIT 2013-2017):

- **CoGeoF1 (baroclinic wave tank):**
 - Spatial and spectral features of the onset of turbulence in baroclinic flow; Project leader: W.-G. Früh, Univ. of Edinburgh, UK
 - Detection of inertia gravity waves in a water-filled rotating baroclinic wave; Project leader: A. Randriamampianina, Univ. Marseille, France
 - The baroclinic instability of an initially stratified layer; Project leader: P. LeGal, Univ. Aix-Marseille, France
 - Extremes in a Changing Climate - a Laboratory Approach, Project leader: Miklos Vincze, Hungarian Academy of Sciences, MTA-ELTE Theoretical Physics Research group, Budapest, Hungary
- **CoGeoF2a,b (spherical gap and QBO-experiment):**
 - Inertial mode excitation: The role of critical layers; Project leader: S.A. Triana, Univ. Leuven, Belgium
- **CoGeoF2b (QBO-experiment):**
 - Investigations of the transitional and turbulent flows in rotor/stator cavities; Project leader: E. M. Tuluszka-Sznitko, TU Poznan, Poland
- **CoGeoF3 (Taylor-Couette experiment):**
 - Turbulent Taylor-Couette Torque Measurement; Project leader: I. Mutabazi, B. Martinez Arias, Univ. Le Havre, France
 - Measurement of the boundary layer in turbulent Taylor-Couette flow at small radius ratios; Project leader: D. Lohse, R. C. A. van der Veen, Univ. Twente, Netherlands
- **CoLaPipe (large pipe test facility):**
 - Turbulence development of the high Reynolds number flow in the CoLaPipe, Project leader: Jorge Peixinho, CNRS & Université du Havre, Le Havre, France
 - Comparative turbulence statistics in pipe flows, Project leader: Tommaso Fiorini, Università di Bologna, Dipartimento Ingegneria Industriale, Forlì, Italy
 - High-Dynamic-Range Measurements in Pipe Flows at High Reynolds Numbers, Project leader: Andrea Ianiro, Universidad Carlos III de Madrid, Bioengineering and Aerospace Engineering Department, Leganes, Spain

Recent experiments from BTU scientists at external facilities EUHIT(2013-2017):

- **LML Boundary Layer Wind Tunnel** (Laboratoire de Mécanique de Lille, Villeneuve d'Ascq, France): Enhanced Turbulent Outer Peak using uniform Micro-Blowing Technique, Project leader: Gazi Hasanuzzaman, Vasyil Motuz, Sebastian Merbold & Christoph Egbers (BTU), Christophe Cuvier & Jean-Marc Foucaut (Laboratoire de Mécanique de Lille, Villeneuve d'Ascq, France), 2017
- **Twente Turbulence Facilities, University of Twente**, Formation of large scale vortices in the torque maximum region in Taylor-Couette flow, Project leader: Andreas Froitzheim, Sebastian Merbold & Christoph Egbers (BTU), 2017
- **CICLOPE: Center for International Cooperation in Long Pipe Experiments**, Spectral scaling of turbulence in CICLOPE at high Reynolds numbers, Project leader: Emir Öngüner, El-Sayed Zanoun & Christoph Egbers (BTU), 2016

Lehre / Courses offered

Vorlesungen des Lehrstuhls für Aerodynamik und Strömungslehre im SS 2019

Strömungslehre (2 SWS VL + 2 SWS UE)

Prof. Egbers / Dr. Zaussinger

- Grundlagen (Stoffgrößen und physikalische Eigenschaften von Fluiden)
- Hydrostatik (Druck, Auftrieb)
- Kinematik der Flüssigkeiten (Kontinuitätsgleichung)
- Kinetik der Fluide (Bernoulli-Gleichung, Massenerhaltung, Impulssatz, Drehimpuls)
- Materialgleichungen (Navier-Stokes Gleichungen, Newtonsche Fluide)
- Schichtenströmungen (Couette-, Poiseuille-Strömung)
- Grenzschichttheorie
- Ausgewählte Strömungsbeispiele

Fahrzeug-Aerodynamik I (2 SWS VL + 2 SWS UE)

Prof. Egbers / M.Sc. Peter Haun

- Grundlagen der Strömungslehre
- Übertragbarkeitsregeln von Modellmessungen auf Originalausführungen
- Fahrzeugaerodynamik und Design
- Windkanaltechnik
- Messtechnik in der Fahrzeugaerodynamik

Raumfahrtanwendungen (2 SWS VL + 2 SWS UE)

Prof. Egbers / Dr. Martin Meier

- Physikalische Grundlagen der Schwerelosigkeit
- Übersicht zu Forschung unter Schwerelosigkeit
- Verschiedene Experimentierplattformen (Fallturm, Parabelflüge, TEXUS, ISS)

Analyse und Visualisierung von Strömungen mit MATLAB (2 SWS VL + 2 SWS UE)

apl. Prof. Harlander

- MATLAB Tutorial
- Strömungslehre Tutorial
- Statistische Analyse von Strömungsdaten
- Zeitreihenanalyse
- bi- und multivariate Verfahren; nichtlineare Verfahren
- Visualisierung von Strömungen
- Darstellung statistischer Ergebnisse

CFD für Ingenieure (2 SWS VL + 2 SWS UE)

Dr. Zaussinger

- Einführung in die CFD und Methoden in der Industrie
- Praxisnahe Modellierung von strömungsmechanischen Problemstellungen
- Simulation und Auswertung mit gängigen CFD Tools (Fluent, CFX, OpenFoam)
- Aufbereitung, Analyse und Präsentation der Ergebnisse

Lehre / Courses offered

Vorlesungen des Lehrstuhls für Aerodynamik und Strömungslehre im WS 2019

Numerische Strömungsmechanik (2 SWS VL + 2 SWS UE)

Dr. Zaussinger

Einführung, was ist ein CFD-Code; Aufbau und Struktur des Open Source Programmes "OpenFOAM"; Durchführung von Simulationen mit "OpenFOAM"; Grundgleichungen inkompressibler, kompressibler Fluide, von Turbulenzmodelle und Mehrphasenströmungen und deren Umsatz in "OpenFOAM"; Aspekte numerischer Diskretisierung und Implementierung in "OpenFOAM"; Post-processing mit dem Visualisierungsprogramm "ParaView";

Höhere Strömungsmechanik (2 SWS VL + 2 SWS UE)

Prof. Egbers / Dr. Zaussinger

Einführung, Theoretische Grundlagen; Methoden der Stabilitätsanalyse; Methoden der Zeitreihenanalyse und Chaosdynamik; Modell-Systeme (Strömungsinstabilitäten in Natur und Technik); Experimentelle Methoden; Praktische Beispiele (Rayleigh-Bénard-Konvektion, Taylor-Couette-Strömungen), Turbulente Strömungen

Strömungsmesstechnik (2 SWS VL + 2 SWS UE)

Prof. Egbers / Dr.-Ing. Vasyly Motuz

- Verfahren zur Sichtbarmachung von Strömungen / Übersicht zu optischen Messverfahren
- LDA-, PIV- und PTV-Strömungsmessverfahren
- Flüssigkristall-Messtechnik
- Farbinjektion
- Hitzdraht- und Heißfilm-Technik
- Verfahren zur Messung von Zustandsgrößen (Temperatur, Druck, Feuchte)
- Windkanalmesstechnik (6-Komponentenwaage, Drucksonden, Drucksensitive Farben)

Aerothermodynamik (2 SWS VL + 2 SWS UE)

Prof. Egbers / M.Sc. Peter Haun

Einführung; Kompressible Strömungen (Gasdynamik), Grenzschichtströmungen, Übersicht über die Tragflügeltheorie; Singularitätenverfahren für Überschallströmungen; Energiesatz für materielles Volumen, Energiesatz für Stromfaden, Gibbsche Gleichung und Entropieungleichung, Ideale Gase, Thermische und kalorische Zustandsgleichung, Schallgeschwindigkeit und Schallausbreitung, Bernoulli Gleichung für ideales Gas, Isentrope stationäre Stromfadentheorie, Flächen-/Geschwindigkeitsbeziehung, Durchflussfunktion, Verdichtungsstoß, Lavaldüse

Wellen in Flüssigkeiten (2 SWS VL + 2 SWS UE)

apl. Prof. Harlander

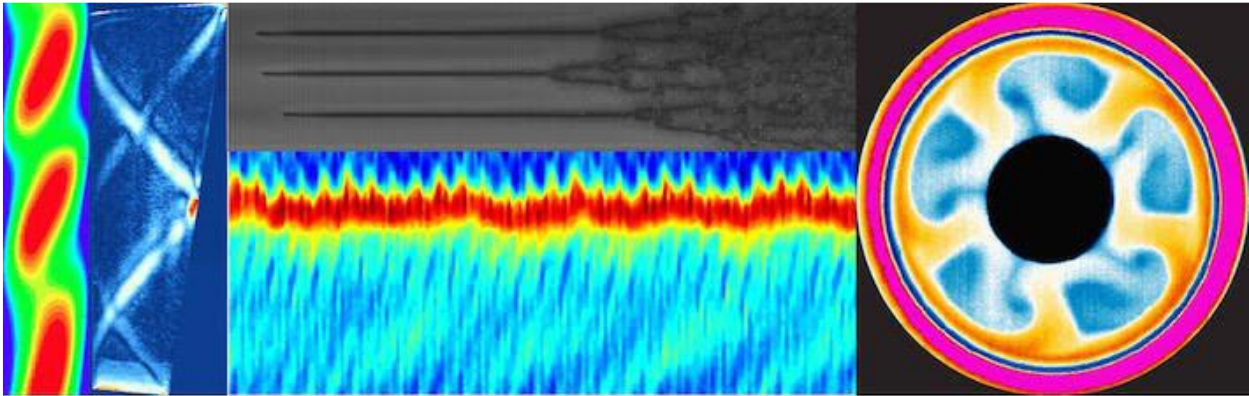
- Oberflächenwellen
- Reflexion und Refraktion
- WKB Analyse
- Flachwasserwellen, Interne Schwerewellen, Planetare Wellen, Trägheitswellen
- Numerische Verfahren zur Lösung von Wellenphänomenen

Parallel Rechnen (2 SWS VL + 2 SWS UE)

Dr. Krebs

- Die Studierenden lernen grundlegende Konzepte paralleler Rechnerarchitektur (Hardwareaspekt) und der parallelen Programmierung (Softwareaspekt) kennen. Typische Aufgabenstellungen numerischer Simulation aus den Bereichen Computational Physics, CFD und Image Processing können selbständig parallel implementiert werden.

Seminare / workshops



LIA-ISTROF* workshop 2019

Scientific committee:

- Christoph Egbers
- Innocent Mutabazi
- Andreas Tilgner
- Laurette Tuckerman

Local organisation committee:

- Christoph Egbers
- Costanza Rodda
- Antoine Meyer



* LIA-ISTROF: Laboratory International Association: Instabilities of stratified and rotating fluids (CNRS funded)

LIA-ISTROF SCHEDULE 19th June

8:30-9:00	Registration
Session 1: Waves	Chair: Antoine Meyer
9:00 – 9:30	Welcome
9:30 - 9:50	Patrice Le Gal: Resonances of Internal Gravity Waves in Stratified Shear Flows
9:50 – 10:10	Costanza Rodda: Differentially heated rotating annulus experiments to study gravity wave emission from jets and fronts
10:10 – 10:30	Maxime Brunet: Linear and nonlinear regimes of an inertial wave attractor
10:30 – 10:50	Wenchao Xu: Inertial mode interactions in a rotating tilted cylindrical annulus with free surface
Session 2: Waves	Chair: Wenchao Xu
11:20 – 11:40	Gabriel Meletti: Latest comparisons of experimental results and high performance non-linear numerical simulation on stratified rotational instabilities
11:40 – 12:00	Uwe Harlander: Stewartson layer instability in a wide-gap spherical Couette experiment: Rossby number dependence
12:00 – 12:20	Joris Labarbe/Oleg Kirillov: Instability windows of Chandrasekhar-Friedman-Schutz instability

Seminare / workshops

Session 3: TEHD

Chair: Patrice Le Gal

13:50 – 14:10

Peter Szabo: Thermomagnetic convection in thermally heated baroclinic annulus

14:10 - 14:30

Innocent Mutabazi: Thermal convection induced by centrifugal and dielectrophoretic buoyancies in cylindrical annular cavities: a general review of recent results

14:30 – 14:50

Antoine Meyer: Thermo-electro-hydrodynamic instability of a dielectric fluid in a vertical cylindrical annulus: Earth's gravity and weightless conditions

14:50 – 15:10

Elhadj Barry: Linear stability analysis of thermoelectric convection in a vertical rectangular cavity with a horizontal temperature gradient and a high frequency voltage

15:10 – 15:30

Harunori Yoshikawa: Dielectric-heating-induced thermal convection in isothermal parallel plane capacitors.

Session 4: AtmoFlow

Chair: Costanza Rodda

15:50 – 16:10

Fred Feudel: Bifurcations in rotating spherical shell convection under the influence of a weak differential rotation between the inner and outer spheres

16:10 - 16:30

Florian Zaussinger: GeoFlow I and GeoFlow II: A review

16:30 – 16:50

Vadim Travnikov: Dielectrical heating effect on the convective flow in the spherical gap

16:50 – 17:10

Peter Haun: Technical requirements and realization of the AtmoFlow experiment.

17:10 – 17:30

Andreas Tilgner: Flows in precessing cubes

18:00 – 19:00

Laboratories tour / Scientific committee

LIA-ISTROF SCHEDULE 20th June

Session 5: TC

Chair: Harunori Yoshikawa

9:00 – 9:20	Grégoire Lemoult: Directed percolation in pipe flow
9:20 - 9:40	Marlene Crumeyrolle - Smieszek: Convection of a phase change material in a rectangular cavity: numerical investigation.
9:40 – 10:00	Mohamed Mouzaoui: Convection of phase change material in a rectangular cavity: an experimental investigation.
10:00 – 10:20	Abdessamad Talioua: Statistical analysis in the turbulent counter-rotating Taylor-Couette flow
10:20 – 10:40	Sebastian Merbold: Transport process of large-scale circulation and turbulent fluctuations in wide gap Taylor-Couette flow.

Session 6: TC

Chair: Sebastian Merbold

11:10 – 11:30	Arnaud Prigent: Experimental and numerical study of the flow produced in a vertical Taylor-Couette system submitted to a large radial temperature gradient
11:30 – 11:50	Harminder Singh: A large Thermal Turbulent Taylor-Couette facility: Investigation of the turbulence induced by simultaneous action of rotation and radial temperature gradient
11:50 – 12:20	Conclusions



Brandenburg
University of Technology
Cottbus - Senftenberg



Infrastruktur des Lehrstuhls / Laboratories and research facilities

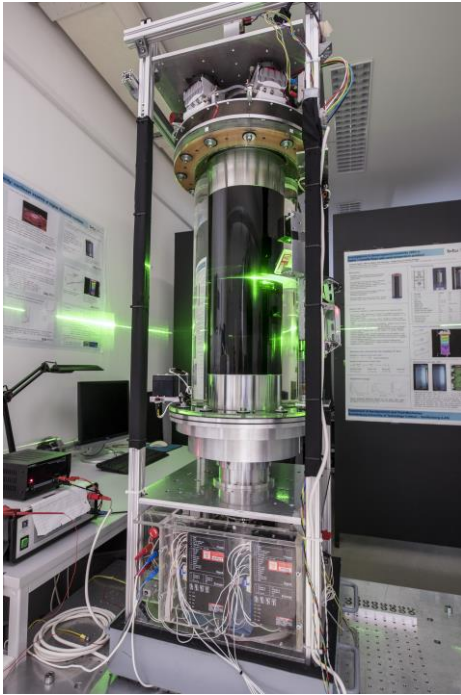
Laboreinrichtungen	Laboratory facilities
<ul style="list-style-type: none"> • Labor für exp. Strömungsmechanik • Elektronik-/Messtechnik-Labor • Mechanik-Labor • Laser-Labor • Labor für Weltraumexperimente • Rechnerraum 	<ul style="list-style-type: none"> • Fluid laboratory • Electronic laboratory • Mechanical workshop • Laseroptical laboratory • Space experiments laboratory • Computation room

Experimenteinrichtungen	Experiment facilities
<ul style="list-style-type: none"> • Taylor-Couette Apparaturen (DFG) • Strato-Rotations-Experiment (DFG) • QBO-Experiment / Rotor-Stator (DFG) • Kugelspalt-Anlagen (DLR, DFG) • Rayleigh-Bénard Experiment (BTU) • Rotierende Zylinder-Konus-Apparaturen • Barokliner Wellentank (DFG) • MS-GWave Tank (DFG) • Turbulente Rohrströmung (DFG) • Lehr-und Forschungswindkanal (BTU) • Aeroakustik-Freistrahler-Prüfstand 	<ul style="list-style-type: none"> • Taylor Couette apparatus (DFG) • Strato-Rotational experiment (DFG) • QBO-experiment, rotor-stator (DFG) • Spherical gap flow experiment (DLR, DFG) • Rotating Rayleigh-Bénard tank (BTU) • Rotating cone facilities • Baroclinic-wave tank facility (DFG) • MS-GWave tank (DFG) • Turbulent pipe flow facility (DFG) • Wind tunnel (aerodynamics, BTU) • Aeroacoustic-Test-Facility

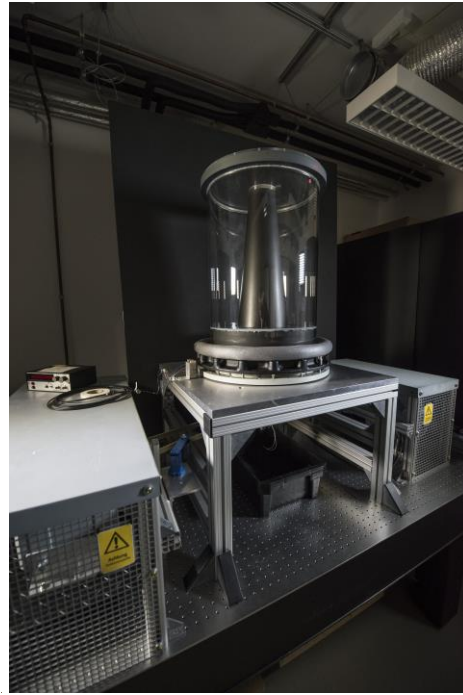
Messtechnik	Measuring techniques
<ul style="list-style-type: none"> • Laserlichtschnitt-Technik • PIV-Technik (2D-Messungen) • LIF-Technik • LDA-Technik (2D-Messung) • He-Ne Laser, Ar-Ion Laser • Schlieren-/Schattenverfahren und Interferometrie • Heissfilm- und Hitzdraht-Technik • Ölfilm-Methode • Thermographie 	<ul style="list-style-type: none"> • Laser light sheet technique • PIV-technique (2D velocity measurements) • LIF technique • LDA-techniques (2D measurements) • He-Ne laser, Ar-Ion laser • Shadowgraph- Schlieren and interferometer optics • Hotfilm- and hot wire measuring technique • Oilfilm-technique • Thermography

Numerik / Software	Numerics / Software
<ul style="list-style-type: none"> • 3D zeitabhängige Codes zur Berechnung isothermer und thermisch getriebener Strömungen, FORTRAN • Zeitreihenanalyse- und nicht-lineare Analysemethoden • AUTOCAD, ProE • OpenFOAM • FLUENT, Matlab • PV wave, Tecplot (Visualisierung) 	<ul style="list-style-type: none"> • 3D time dependent computational code (isothermal and thermal flows), FORTRAN • Time series analysis- and non-linear analysis tools • AUTOCAD, ProE • OpenFOAM • FLUENT, Matlab • PV wave, Tecplot (visualization)

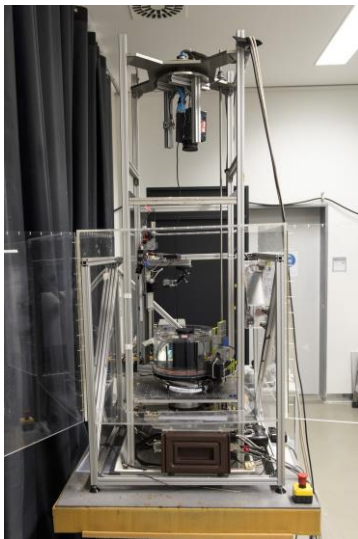
Infrastruktur des Lehrstuhls / Laboratories and research facilities



Taylor-Couette-experiment (SRI)



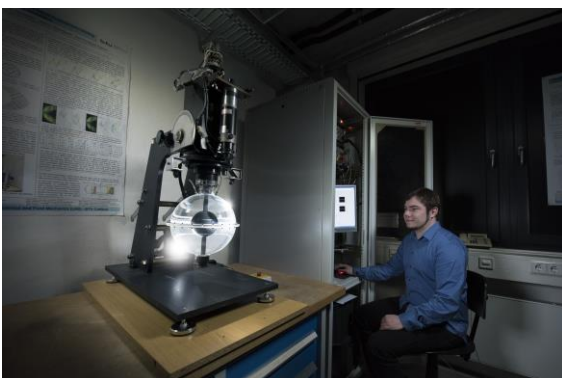
Taylor-Couette experiment (QBO)



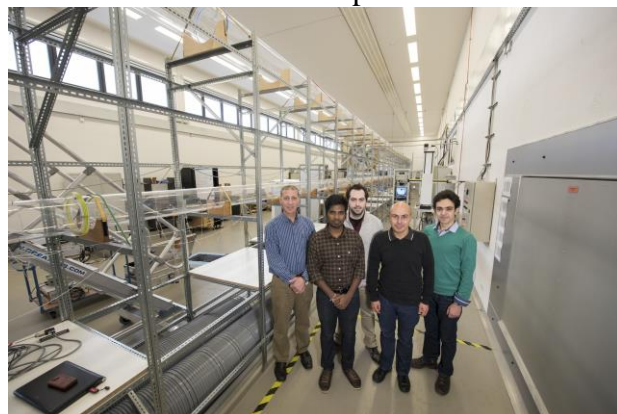
Baroclinic wave tank



MS-GWaves experiment



Concentric spherical gap apparatus



Cottbus Large Pipe Test Facility CoLa-Pipe

Aktuelle Forschungsschwerpunkte / Current research topics

A Aerodynamics

A1 Features of Pipe Flow at high Reynolds numbers

E.-S. Zanoun, & Ch. Egbers (DFG-SPP 1881, EG100/24-1, 2)

Introduction

Pipe flow remains one of the most interesting research topics among fluid mechanics researchers as it has a wide range of engineering applications. Therefore, intensive experimental, theoretical, and computational studies of the pipe flow are indeed well progressing over decades. Major part of these studies is focusing on the pipe flow structure, momentum transport, energy balance and scaling, providing large sets of data and considerable insight into physics of wall-bounded turbulent flows, see e.g. Refs. [1–3]. In this short report, we are briefly addressing the following two points in pipe flow:

- Scaling of the streamwise mean velocity and Reynolds normal stress
- Estimating sizes of the large and very large scale motions, i.e. LSM & VLSM

To highlight the two issues raised above, the large pipe facility (CoLa-Pipe) located in Brandenburg University of Technology (BTU-Cottbus-Senftenberg), has been utilized. The facility, see Fig.1, is a closed return equipped with water cooler to carry out measurements for shear Reynolds number in the range $1.5 \times 10^3 < R^+ < 2 \times 10^4$ ($6 \times 10^4 < Re_b < 10^6$), where R^+ is defined as $R^+ = R/\ell_c$, R is the pipe radius, $\ell_c = \nu/u_\tau$ is the viscous length scale, u_τ is the wall friction velocity, and ν is fluid kinematic viscosity, while Re_b is defined based on the bulk velocity, U_b , and the pipe diameter, D .

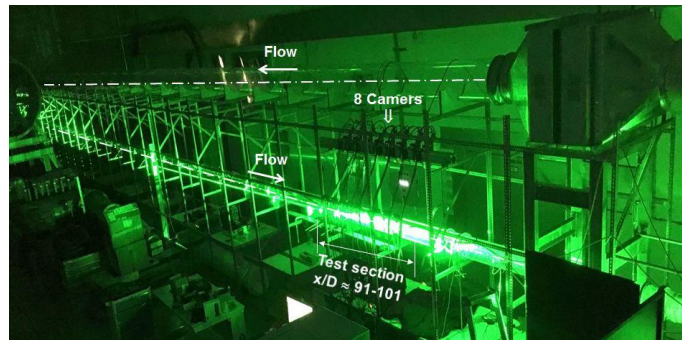
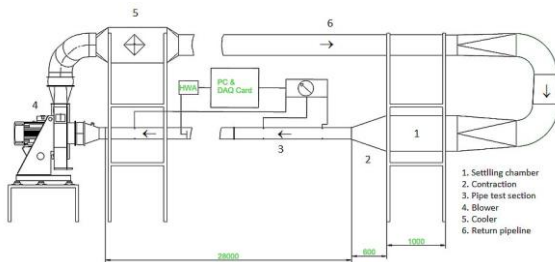


Figure 1: The CoLa-Pipe facility: (left) facility schematic, (right) the facility with a streamwise PIV optical setup.

The facility provides air with 80m/s maximum velocity at the contraction exit with turbulence level less than 0.5%, for more details see Ref. [4]. The facility has full transparent test sections that allow optical measuring techniques to be utilized. HWA, LDV and PIV are representing the major instrumentations used to carry out measurements in the facility.

Results

This section focuses on scaling of the streamwise mean velocity component, the Reynolds normal stress, and size estimation of the large and very large scale motions. Figure 2 illustrates the inner scaling of the streamwise mean and Reynolds normal stress profiles from experiments Ref. [5], and simulations Ref. [6]. The scaling of the local mean velocity, and wall normal distance were carried out using the wall friction flow velocity (u_τ), and the viscous length scale ($\ell_c = \nu/u_\tau$), respectively. The experimental and numerical mean velocity profiles in Fig. 2 show good collapse, and a satisfactory agreement with the logarithmic line, $U^+ = 1/\kappa \ln y^+ + B$, where $\kappa=0.384$ and $B=4.43$, proposed by Ref. [7]. The figure also presents selected experimental data sets for the Reynolds normal stress at $Re_\tau \approx 2675$ & 11000.

Aktuelle Forschungsschwerpunkte / Current research topics

Plausible agreement between experiments for $R^+ \approx 2675$ with the DNS data from Ref. [6] is observable. For high enough R^+ , back to 1976, Townsend showed that the streamwise turbulence intensity behave logarithmically, $u^{+2} = B_2 - A_2 \ln(y^+/Re_\tau)$, in the interior part of the inertial region. In-line with Townsend's observation, a clear logarithmic behavior for u^{+2} is being obtained in Fig. 2 for $R^+ = 11000$ with $A_2 = 1.25$, and $B_2 = 1.61$. Focusing on the region close to the wall, the data presented showed an inner peak, located at $y^+ \approx 15$ in good agreement with predictions utilizing an empirical formula proposed by Ref. [8], as well in reasonable agreement with peak resulted from DNS Ref. [6], and experimentally with Ref. [9]. *However the dependence/in-dependence of the inner peak in pipe flow with Reynolds number is still under debate.* On the other hand, an outer peak is hardly observable in Fig. 2 which might be attributed either to insufficient spatial resolution or to low Reynolds number effect, however, a plateau is being clear for $R^+ \approx 11000$ along the overlap region. The plateau observed for high Reynolds number might represents structural changes which to be considered a sing of presence of new outer phenomena; claim made by Ref. [9]. These observations motivate further cooperation with Bologna University, utilizing the CICLOPE facility Ref. [10] to extend the working range of friction Reynolds number to $R^+ \approx 4 \times 10^4$ as well as utilizing the NSTAPs probes at CoLa-Pipe in co-operation with Alex Smits (Princeton University).

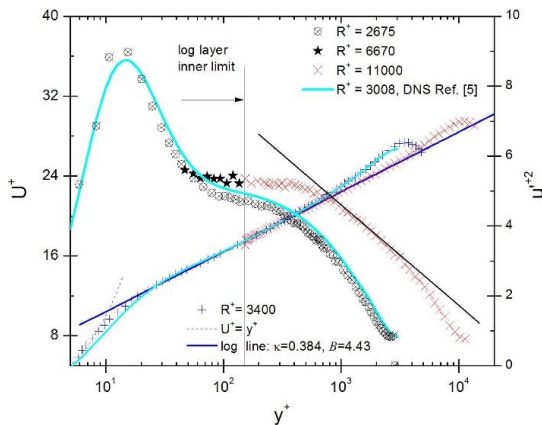


Figure 2: Inner scaling of the streamwise mean velocity and Reynolds normal stress profiles from experiments Ref. [5], and simulations, Ref. [6].

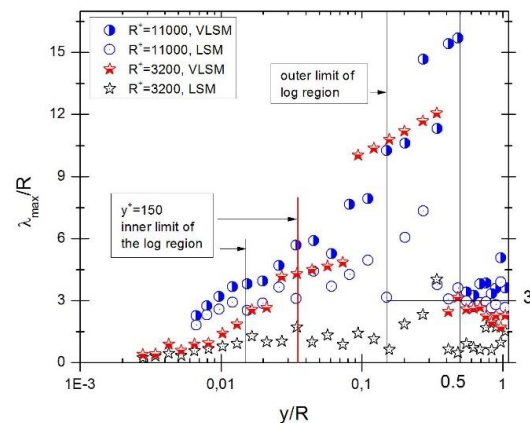


Figure 3 Semi-log representation of dimensionless wavelength of the large scale and very large scale motions for two Reynolds numbers.

Based on streamwise spectral analysis, see Ref. [5], sizes of the large-scale structures were estimated and presented in Fig. 3. Figure 3 is a semi-log representation of the large scale motions, showing that the LSMs start within the buffer layer and grows through the inertial sublayer, reaching maximum wavelength of $\lambda_x \approx 12$ radii for $R^+ \approx 3200$, and $\lambda_x \approx 16$ radii for $R^+ \approx 11000$ at half of the pipe radius, i.e. outside the logarithmic layer. A sudden drop in the normalized wavelength of the VLSM is obtained at $y \approx R/2$ due to merging of the VLSM and the LSM forming one flow structure beyond $y/R \approx 0.5$ in agreement with Ref. [2].

Bibliography

- [1] Townsend AA, "The Structure of turbulent shear flow," Cambridge University Press. (1976).
- [2] Kim KC, and Adrian RJ, Phys. Fluids 11, p. 417422, (1999).
- [3] Jiménez J, J. Fluid Mech., 842, pp. 1–100, doi:10.1017/jfm, (2018).
- [4] König F, Zanoun E-S, Öngüner E, and Egbers C, Review of Scientific Instruments, Vol: 85(7), (2014).
- [5] Zanoun E-S, Öngüner E, Egbers C, Bellani G, and Talamelli A, Progress in Turbulence (in press), (2019).
- [6] Ahn J, Lee JH, Lee J, Kang J, and Sung HJ, Phy. Fluids 27, 065110; doi: 10.1063/1.4922612, (2015).
- [7] Zanoun E-S, Durst F, Saleh O, and Al-Salaymeh A, J. Exp. Therm. Fluid Sci. 32(1), 249-261, (2007).
- [8] Hutchins N, Nickels TB, Marusic I, and Chong MS, J. Fluid Mech. 632:431–42, (2009).
- [9] Morrison JF, McKeon BJ, Jiang WJ, and Smits AJ, J. Fluid Mech., Vol. 508, pp.99 .131, (2004).
- [10] Örlü R, Fiorini T, Segalini A, Bellani G, Talamelli A, and Alfredsson PH, Phil. Trans. R. Soc. A., 375, (2017).

Aktuelle Forschungsschwerpunkte / Current research topics

A Aerodynamics

A2 Large scale coherent structures in turbulent wall-bounded flows

M. Sc. Amir Shahirpour, Christoph Egbers (inside the framework of DFG SPP 1881 “Turbulence & Superstructures”, EG100/24-1)

Large-scale coherent structures dominate the nature of wall bounded turbulent flows and contribute prominently to the turbulent kinetic energy and Reynolds shear stress, while affecting the global transport of mass, heat and momentum. In spite of large range of experimental and numerical investigations carried out during the last decade, many of the fundamental questions regarding their origin, regeneration mechanism, evolution and their interactions are yet to be answered.

Spectral analysis has been extensively used to investigate the energy distribution of the flow in the wavenumber space. The footprints of the structures can be followed by observing the peaks in premultiplied velocity spectra which are associated with large and very large-scale structures known as LSM and VLSM respectively. This analysis is one of the very few methods that have been widely used to determine length scales, energy content and wall normal location of the structures. While this information is valuable, it is not sufficient to gain insight about the evolution and interactions of structures.

This main goal of this project is to find answers to the above-mentioned uncertainties, by applying Characteristic DMD (Sesterhenn and Shahirpour 2019) to time-resolved experimental and numerical data. For this purpose, direct numerical simulations are being performed at intermediate to high Reynolds numbers using a hybrid parallel DNS code (Shi et al. 2015), where Navier-Stokes equations are solved in cylindrical coordinates for an incompressible pipe flow fulfilling mass and momentum conservations.

Premultiplied energy spectra of streamwise velocity component is plotted in figure 1 for simulations at shear Reynolds numbers of $Re_\tau = 180$ and 360. A prominent peak is observed at $y^+ = 15$ in both figures, with the wavelength of the corresponding peaks reducing as Reynolds number increases. A similar trend is detectable in the carpet plots of streamwise velocity component taken at $r/R = 0.85$, as the patterns grow smaller and show a more meandering behavior. Spectral foot prints of the structures will play an important role in validating the results gained by CDMD.

To assess the capability of CDMD in capturing the coherent structures in wall-bounded flows, it has been applied to a Minimal Flow Unit (MFU) in a turbulent channel flow at $Re_\tau = 200$. The minimal flow accommodates only one group of structures and therefore serves as an ideal starting point to capture turbulent coherent structures. Applying a DMD in the spatio-temporal space, the structure could be detected using a few modes only. This is while a DMD in a shifted frame of reference and a traditional DMD, both fail to represent an acceptable description of the structure (figure 2).

The study is carried out in the frame work of DFG-SPP 1881 “Turbulent Superstructures”, (EG100/24-1), and in collaboration with our SPP partners, Technical University of Berlin (J. Sesterhenn) and Karlsruhe Institute of Technology, KIT (D Gatti and B. Frohnepfel). Results of this collaborative study will be compared with the experimental data measured in CoLa-Pipe at BTU Cottbus within the bulk Reynolds number range of $8 \times 10^4 \leq Re_b \leq 1 \times 10^6$. Simulations run on HLRN-Berlin with project number bbi00011.

Aktuelle Forschungsschwerpunkte / Current research topics

Figure 1. Premultiplied energy spectra of streamwise velocity component for turbulent pipe flow at $Re_\tau = 180$ (a) and $Re_\tau = 360$ (b). Carpet plots of streamwise velocity component normalized by bulk velocity at radial location of $r/R = 0.85$ at $Re_\tau = 180$ (c) and $Re_\tau = 360$ (d).

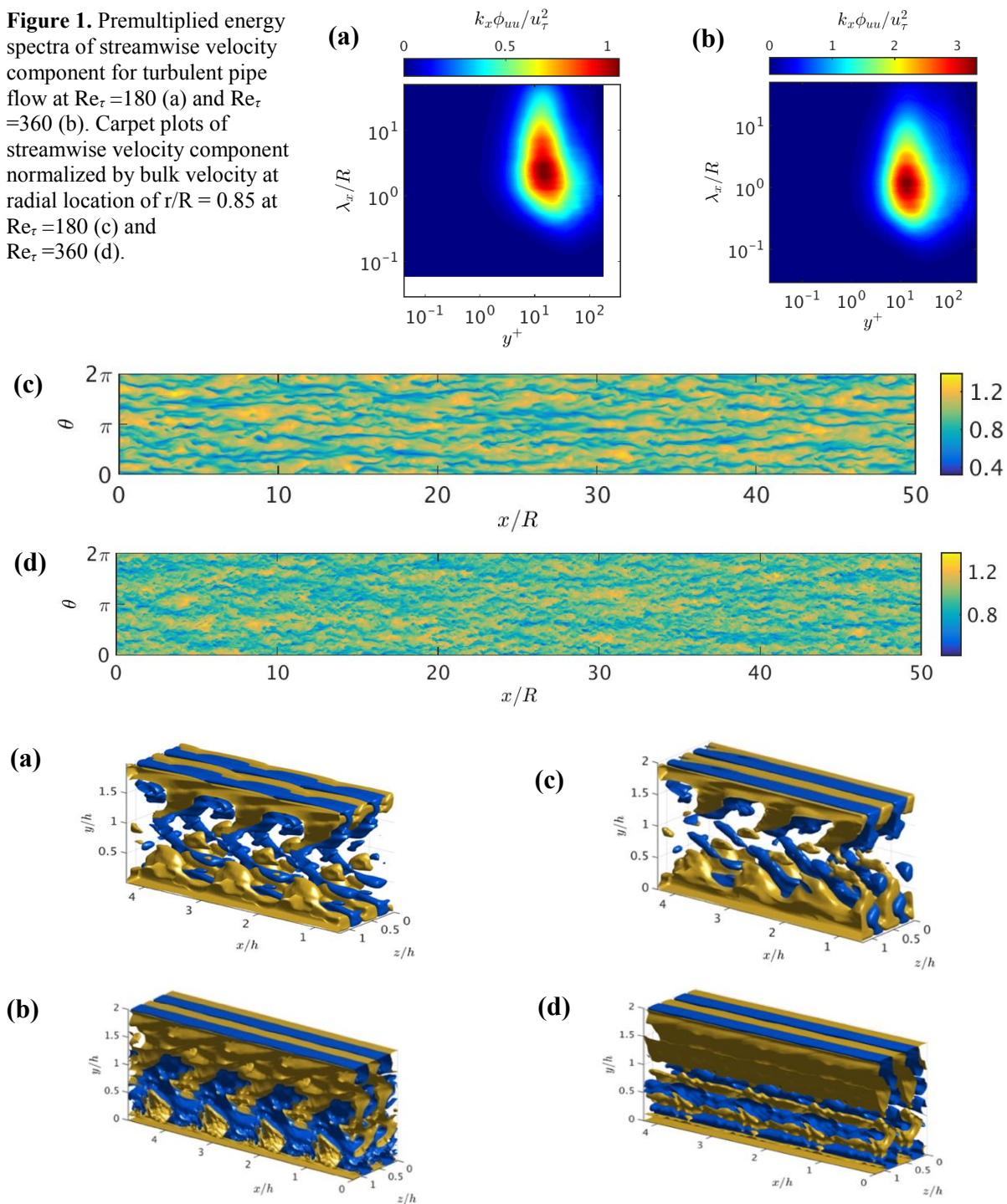


Figure 2. Iso surfaces of stream wise velocity component in a minimal flow unit, full-field (a), 1st CDMD mode (b), 1st ShDMD mode (c) and 1st DMD mode (d). Yellow and blue Iso-surfaces correspond respectively to $\langle U \rangle \pm 0.9 U_{\tau_{au}}$ (DNS by Gatti and Frohnappfel, KIT)

Bibliography:

Sesterhenn, J., Shahirpour, A., "A characteristic Dynamic Mode Decomposition", Theor. Comput. Fluid Dyn., <https://doi.org/10.1007/s00162-019-00494-y>, (2019)

She, L., Rampp, M., Hof, B., Avila, M., "A hybrid MPI-OpenMP parallel implementation for pseudospectral simulations with application to Taylor-Couette flow", Computer and Fluids, 106, 1-11, 2015

Aktuelle Forschungsschwerpunkte / Current research topics

A Aerodynamics

A3 A Characteristic dynamic mode decomposition

M. Sc. Amir Shahirpour, Jörn Sesterhenn (TU Berlin)

Transport-dominated turbulent coherent structures in wall bounded turbulent flows, pose a major problem to standard decomposition methods such as Dynamic Mode Decomposition (DMD). These methods will fail to reconstruct a reduced-order model of the flow with a minimal number of modes. The same fact will lead to inaccurate estimation of decay rates and frequencies for such motions.

We have addressed and resolved this issue by introducing a Characteristic DMD (CDMD) (Sesterhenn and Shahirpour 2019). To test and calibrate the method it has been applied to DNS of a vortex head in a starting jet (Fernandez and Sesterhenn 2017). In this approach, the structures are followed in a properly chosen frame of reference along the characteristics representing their convective velocity. The latter takes place using a coordinate transformation from physical space into spatiotemporal space. The transformation is in form of a rotation in space and time with the rotation angle θ corresponding to the most dominant group velocity u_g in the flow, determined by the maximum drop of the singular values. This transformation is illustrated in figure 1a, where space-time diagram has been plotted with the horizontal and vertical axes corresponding to advection direction and time respectively. The plot shows contours of vorticity magnitude and is taken on the center of the vortex head propagating downstream.

To detect the direction of characteristics, the transformation is carried out for a range of rotation angles. A singular value decomposition is performed for each angle on the snapshots matrix. In figure 1b the first 15 singular values are plotted for each transformation. It is clear that for a certain angle, corresponding to a certain group velocity, an optimal drop is resulted. Having detected the optimal frame of reference, the data is transformed to the spatiotemporal space. The transformed snapshots matrix is decomposed via the standard DMD algorithm (Schmid & Sesterhenn 2008) along the characteristics, therefore seeking the structures in planes normal to the direction of characteristics. Faster drop of singular values and mode amplitudes along the characteristics is obvious in figure 2.

Modes with smallest decay rates and largest amplitudes are selected and reconstructed along τ and then transformed back to physical space. The latter will represent a reduced order model of the flow using only a few modes accommodating the structure with the dominant group velocity. Reconstruction of the first 4 CDMD modes in physical space is compared with the full field in figure 3. The same number of modes have been implemented to reconstruct the first DMD modes. While the DMD modes give a smeared representation of the vortex head, the CDMD modes have clearly captured the structure.

The main aim of this study is to detect transport-dominated coherent structures on a moving frame of reference along their characteristics, to shed light on their physical properties which have remained unanswered so far. This study is carried out in the frame work of DFG-SPP 1881 “Turbulent Superstructures”, (EG100/24-1), and in collaboration with our SPP partner, Technical University of Berlin (J. Sesterhenn).

Aktuelle Forschungsschwerpunkte / Current research topics

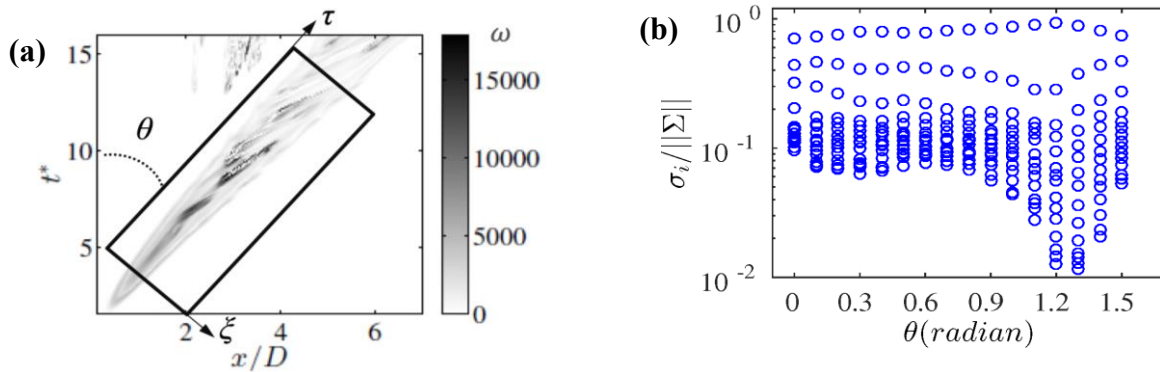


Figure 1. Characteristic diagram along the vortex center line (a) and drop of the first 15 singular values for a range of rotation angles (b), (Figures taken from Sesterhenn and Shahirpour).

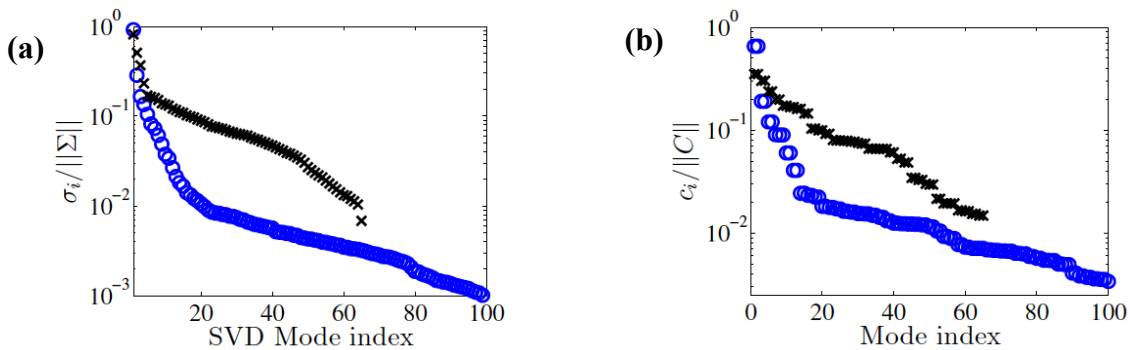


Figure 2. Normalized singular values and modal decays for CDMD (o) and DMD (x), (Figures taken from Sesterhenn and Shahirpour).

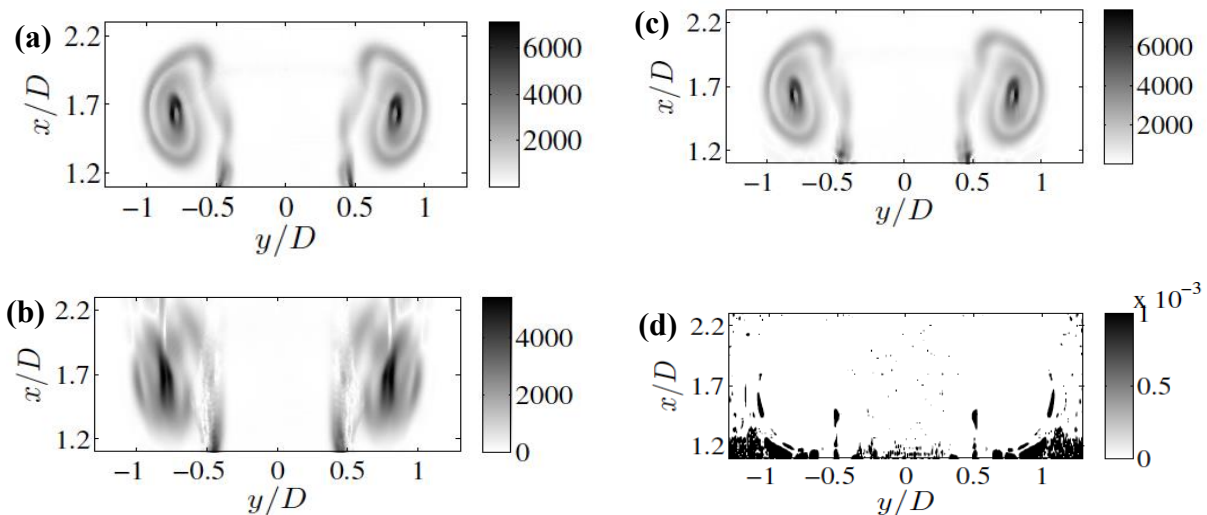


Figure 3. The fullfield vortex head (a), reconstruction of 4 CDMD (b) and DMD (c) modes, and the relative error for CDMD modes (d), (Figures taken from Sesterhenn and Shahirpour).

Bibliography:

- Sesterhenn, J., Shahirpour, A., “A characteristic Dynamic Mode Decomposition”, *Theor. Comput. Fluid Dyn.*, <https://doi.org/10.1007/s00162-019-00494-y>, (2019)
 Peña Fernández, J., Sesterhenn, J., “Compressible starting jet: pinch-off and vortex ring-trailing jet interaction“, *J. Fluid Mech.* **817**, 560–589 (2017).
 Schmid, P.J., Sesterhenn, J. “Dynamic Mode Decomposition of Numerical and Experimental Data“, 61st APS Meeting, p. 208. American Physical Society (2008)

Aktuelle Forschungsschwerpunkte / Current research topics

A Aerodynamics

A4 Single and Multi-Point Velocity Measurements in CoLa-Pipe at High Reynolds Number Zeinab Hallol*, Yasser Dewidar, E.-S. Zanoun, Christoph Egbers (*BTU- PhD Scholarship)

Introduction

Large-scale motion (LSM) in the turbulent pipe flow are still not clear till now. For that investigation of LSM as $\lambda_{LSM} = 2R-3R$ structure in fully turbulent pipe flow got an important concern to clarify and understand the behavior of this turbulent structure to identify it in a quantitative manner. The measurement techniques used in the present investigation are hot wire anemometry (HWA). Our study is going to be conducted in pipe facility called the CoLaPipe built at the Department of Aerodynamics and Fluid Mechanics (LAS) at the Brandenburg University of Technology (BTU-Cottbus-Senftenberg). The LAS CoLaPipe (Cottbus Large Pipe) is a closed-return facility with the suction side made of high-precision smooth acrylic glass, having an inner pipe diameter (d) of 190 ± 0.23 mm and total length (L) of 28 m, i.e., $L/d = 148$. The facility has a return pipe section made also of smooth Acrylic glass with an inner diameter of 342 ± 0.32 mm, and having $L/d = 79$. The facility is equipped with water cooler to keep the air temperature constant inside the pipe. The air temperature was measured within an accuracy of $\pm 1^\circ\text{C}$. At the exit of the contraction section, the flow has uniform velocity profile with low turbulence intensity level, always less than 0.5%. Further details about Cola Pipe test facility can be found in König et al. 2014.

Relevant experiment in Colapipe

The main aim of this study is to distinguish between azimuthal and streamwise velocity components/structures of the pipe flow using hot-wire anemometry. Hence, velocity measurements utilizing multiple hot-wire probes will be performed to provide time resolved velocity data. All measurements are to be carried out using the new Dantec Streamline 9091N0102 CTA with Dantec commercial hot-wire probes to facilitate measuring the overheat ratio, ambient temperature and velocity. For this study, a new acryl-glass pipe section is to be designed with an appropriate traverse mechanism.

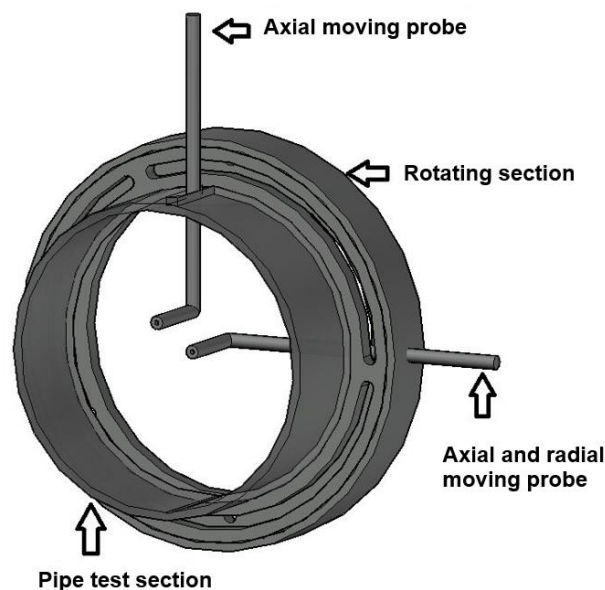


Figure 1: Schematic design used to measure the azimuthal structures

Aktuelle Forschungsschwerpunkte / Current research topics

To distinguish between azimuthal and streamwise structures of the pipe flow, the traverse system that is going to use for holding and moving hot wire anemometer inside and outside the pipe designed such that a single probe can be positioned at a fixed wall-normal location, while a second probe at the same distance from the wall could be rotated to an arbitrary angular separation θ . The second probe was driven at a 1:1 gear ratio by a high-resolution (0.45° per step) stepper motor, located outside the test pipe and operated in half-step mode, resulting in an angular resolution of $\pm 0.23^\circ$. The traverse geometry is illustrated in figure 1. The measurements will be carried out within Reynolds number range of $6 \times 10^4 \leq Re_b \leq 5 \times 10^5$.

The second part of the study is to investigate experimentally the pipe flow scaling and structure using PIV in double 2D domain flow field as depicted in figure 2, to study the proper inner and outer scaling of the mean and higher order statistics of flow field for relatively wide range of Reynolds number, $6 \times 10^4 \leq Re_b \leq 5 \times 10^5$, and compare between PIV and HWA results. Keeping in our consideration High-speed PIV measurements with higher acquisition frequency and larger number of snapshots are essential to have more precise analysis for determining the length of the structures in fully developed pipe flow as well as contributions of the large-scale structures to various turbulence properties, one dimensional energy spectrum, cross-spectral analysis, proper orthogonal decomposition (POD) of multi-point velocity data are to be studied.

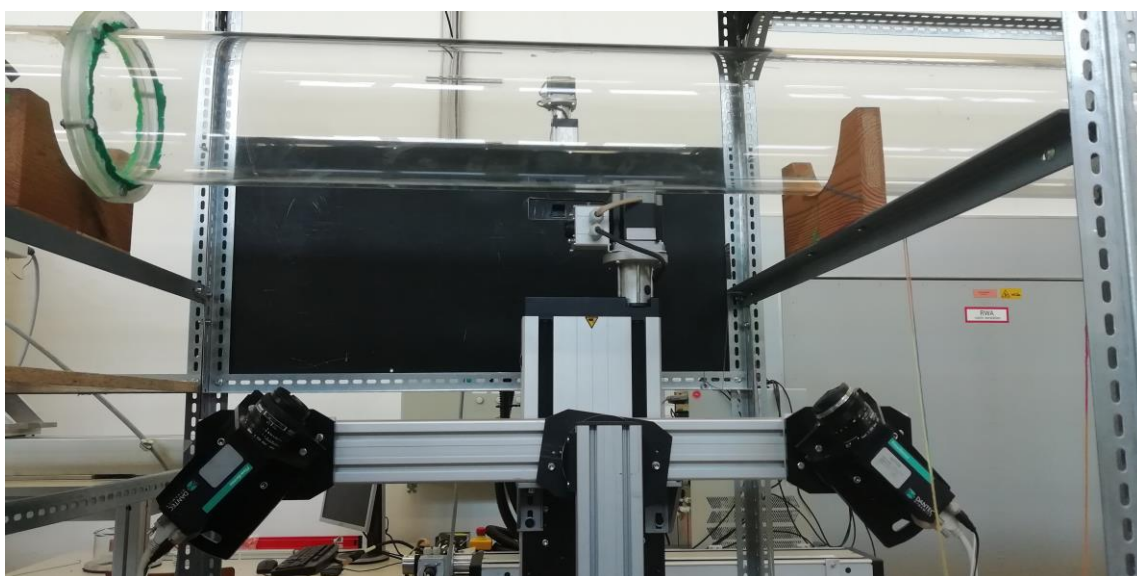


Figure 2: PIV setup for cross-sectional measurements.

Bibliography:

- [1] Sean C. C. Bailey, Marcus Hultmark, Alexander J. Smits and Michael P. Schultz, " Azimuthal structure of turbulence in high Reynolds number pipe flow ", J. Fluid Mech., vol. 615, pp. 121–138, (2008).
- [2] B. J. McKeon, K. R. Sreenivasan, " Introduction: scaling and structure in high Reynolds number wall bounded flows ", Phil. Trans. R. Soc. A vol. 365, 635–646, (2007).
- [3] König F., Zanoun E.S., Öngüner E., and Egbers C., " The CoLaPipe - the new Cottbus Large Pipe test facility at BTU Cottbus", Review Scientific Inst., 85, No. 7, 075115-1075115-9, (2014).

A Aerodynamics

A5 Cottbus Small Pipe: New Facility

S. Richter, E.-S. Zanoun, Ch. Egbers (DFG-SPP 1881, EG 100/24-1,2)

Introduction

Over decades pipe flow is a subject of extensive research and is most likely to remain of vital interest. Pipe flow structure, i.e. large and very large scale motions, and scaling are still under debate, see e.g. Refs. [1-2]. Hence, the new pipe facility (CoSma-Pipe) at the Department of Aerodynamics and Fluid Mechanics (LAS) aims at complementing the ongoing research work at LAS, however, for low range of Reynolds number, see Ref. [2]. In addition, there is a shortage of high quality pipe flow data comparable to the most recent numerical results, see Refs. [3-4]. The current phase of the facility, see Fig.1, is an open return to carry out measurements for shear Reynolds number in the range $4 \times 10^2 \leq R^+ \leq 6 \times 10^3$ ($15 \times 10^3 \leq Re_b \leq 2.8 \times 10^5$), where R^+ is defined as $R^+ = R u_\tau / \nu$, R is the pipe radius, u_τ is the wall friction velocity, and ν is fluid kinematic viscosity, while Re_b is defined based on the bulk velocity, U_b , and the pipe diameter, D . It is worth noting that the ongoing research work at LAS focuses currently on high Reynolds numbers (Re), i.e. $Re_b \leq 10^6$, utilizing the so-called CoLa-Pipe facility. However, a common working Reynolds number range, $6 \times 10^4 \leq Re_b \leq 2.8 \times 10^5$, between the two facilities exists, allowing for comparisons as well as validating each other, using the same measuring techniques such as PIV, HWA and pressure measurements.

The Experimental Setup

In the contrary to the closed-return CoLa-Pipe with two different test sections, the CoSma-Pipe is an open return facility and has one test section, having an inner diameter of 60mm. A schematic drawing of **Cottbus Small Pipe** (CoSmaPipe) is depicted in Figure 1.

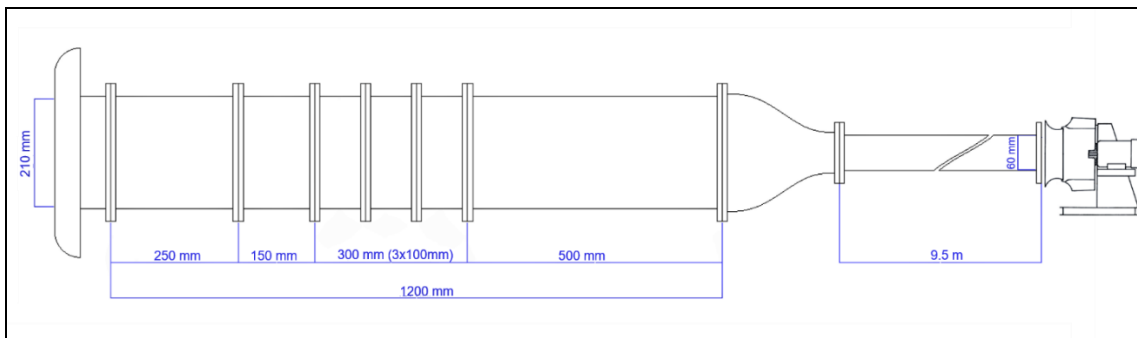


Figure 1 – Schematic drawing CoSmaPipe

Component	d [mm]	M [mm]	Type	Distance from bell mouth [m]
1	-	-	Bell Mouth	
2	9.5	2.4	Perforated plate	
3	5.00	-	Honeycomb	
4.1	1.00	4.00	Screen	
4.2	0.71	2.50	Screen	
4.3	0.45	1.40	Screen	
4.4	0.016	0.70	Screen	
4.5	0.016	0.70	Screen	
5	-	-	Relaxation chamber	

Table 1 – Settling chamber properties

Settling chamber:

The working medium, i.e. air, is uniformly sucked through the symmetrically shaped bell mouth into the settling chamber. Thereafter, it passes through honeycombs straightening the air flow before crossing the next passive control devices, i.e. screens of different mesh sizes (M), see Table 1. Table 1 shows the properties of the different components of the settling chamber. Figure 2 illustrates the settling chamber itself as well as the inlet contraction.

Aktuelle Forschungsschwerpunkte / Current research topics

Inlet Contraction and Test Section:

The contraction has a contraction ratio of 12.25, accelerating the laminar flow into the pipe. Its main functions are to produce a uniform velocity distribution at the contraction exit with very thin boundary layer and low turbulence intensity level and a separation free flow at the inlet of the pipe. With an inner diameter of 60mm the test section consists of 1.5m long borosilicate glass and the rest is made out of acrylic glass sections, each is 2m long. Hence, the total length of the pipe section is approximately 7.5m, providing a length-to-diameter ratio (L/D) of ~ 125 , however, the test section is extendable up to 350 for future plans. To carry out PIV measurements, the 60mm in diameter high precision smooth borosilicate glass tube provides high-quality optical access is located between $L/D=100$ and 125. It is worth noting that careful installation of the pipe test section with the plenum chamber and the contraction using laser alignment was able to limit misalignment in the pipe facility.

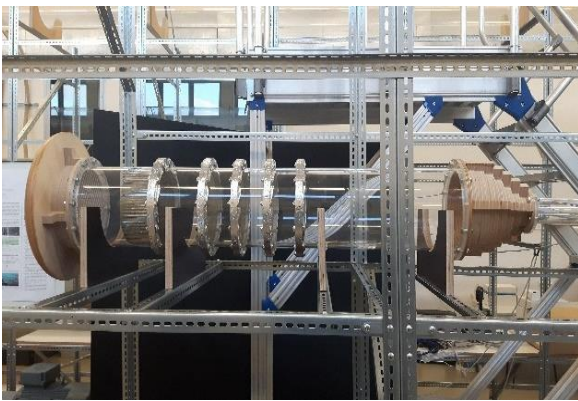


Figure 2 – Settling chamber

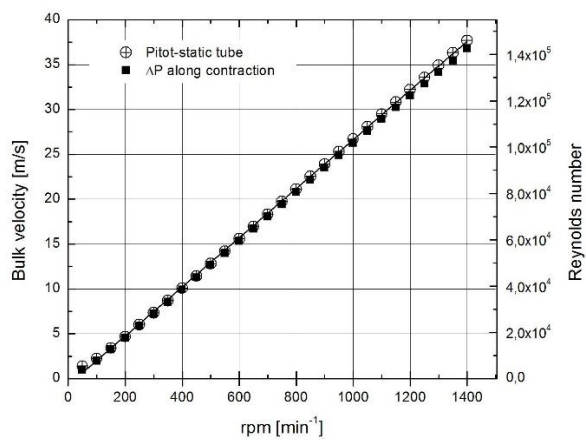


Figure 3: Calibration data of the CoSmaPipe

Preliminary Measurements:

The pipe flow rate for each investigated case was controlled by changing the rotational speed of the blower via a frequency converter unit. The bulk flow velocity, U_b , is measured using a 2mm pitot-static probe directly located at the contraction exit, i.e. close to the pipe inlet, where a uniform velocity distribution exists Ref. [5]. In addition, the bulk velocity is also obtained utilizing pressure drop along the contraction section to ensure a good assessment of the bulk flow velocity for each running speed. Good agreement within $\pm 1\%$ is achieved for estimating the bulk velocity from both methods, see Fig. 3, and it was then used to compute the bulk-based Reynolds number of the flow, $Re_b = D U_b / \nu$. A high range of Reynolds number $Re_b \leq 1.5 \times 10^5$ is set up in this way. It is note mentioning that only half of the rotational speed of the blower had been used to produce Fig. 3. The wall pressure along the pipe test section is measured using wall pinhole and static pressure taps. The pinhole diameter is of 500 μ m and its depth is ~ 2 mm. Pressure taps are available along the pipe test section on 20 locations. At each location, three pressure taps are installed 120 degree around the pipe circumference. The pressure is measured using a pressure scanner with a range of 7 kPa (Net Scanner System Model 9116), connected through an Ethernet cable, 16 channels are simultaneously measured while the acquisition is performed using LabView. Each pressure signal is 1000 samples at a frequency of 100 Hz.

Bibliography

- [1] Jiménez J, J. Fluid Mech., 842, pp. 1–100, doi:10.1017/jfm, (2018).
- [2] Zanoun E-S, Öngüner E, Egbers C, Bellani G, and Talamelli A, Progress in Turbulence (in press), (2019).
- [3] Ahn J, Lee JH, Lee J, Kang J, and Sung HJ, Phy. Fluids 27, 065110; doi: 10.1063/1.4922612, (2015).
- [4] Feldmann D, Bauer C, Wagner C, J. Turbulence, Vol. 19, No. 3, 274-295, (2018).
- [5] Zanoun, E.-S., and C. Egbers, J. Eng. and Applied Science, Cairo University, Vol. 63, No. 2, pp. 141-159, (2016).

Aktuelle Forschungsschwerpunkte / Current research topics

A Aerodynamics

A6 Flow control of a flat plate turbulent boundary layer flow through micro-blowing under stochastic forcing.

G. Hasanuzzaman*, S. Merbold, V. Motuz, Ch. Egbers (*BTU-GRS PhD Scholarship)

Introduction

Large subsonic jet aircraft's are operated within chord Reynolds number ($Re_x = u \cdot L/v$) range up to and beyond 10^7 . In order to improve the drag reduction of aircraft surfaces, present experiment was intended to evaluate experimentally a novel flow control technique e.g micro-blowing/uniform blowing in turbulent boundary layer (TBL). Flow control experiments have more engineering importance and particularly challenging due to the presence of different interacting scales which are increasingly becoming significant as the flow initial conditions keeps growing. Therefore, energy content of the coherent structures in outer layer becomes stronger and necessitates measurements in relatively large Reynolds number. Hence, a set of measurements using Laser Doppler Anemometry (LDA) and Particle Image Velocimetry (PIV) have been performed in the range of momentum thickness Reynolds number within $7495 \leq Re_\theta \leq 19763$. In order to achieve uniform blowing upstream a flat plate, the solid wall is replaced with a perforated surface, therefore, it is possible to use uniform blowing coming vertically from the wall located in the turbulent regime of the boundary layer. Albeit uniform, a controlled volume air was supplied to through hermetically sealed device attached to the TBL wall. Hence, pre-emptive air flow rate was applied and can be expressed as blowing ratio e.g a percentage of the free stream velocity ($F = U_{blowing}/U_\infty \times 100$), here, magnitude of blowing ratio was varied between 0% ~ 6%.

Present measurements have two principal aspects, drag reduction as a quantitative measure of the reduction of friction drag and study of the superstructure (particularly Large Scale Motions) morphology. In order to realize the importance of these structures one needs to look into the Turbulent Kinetic Energy of the measurements. In traditional viewpoint, energy contribution is maximum in the near wall region. Therefore, focus was to obtain near wall data in order to determine the changes observed in the output variable. However, recent advances in the research of TBL suggests that energy contribution from the large scales are increasing as Reynolds number increases.

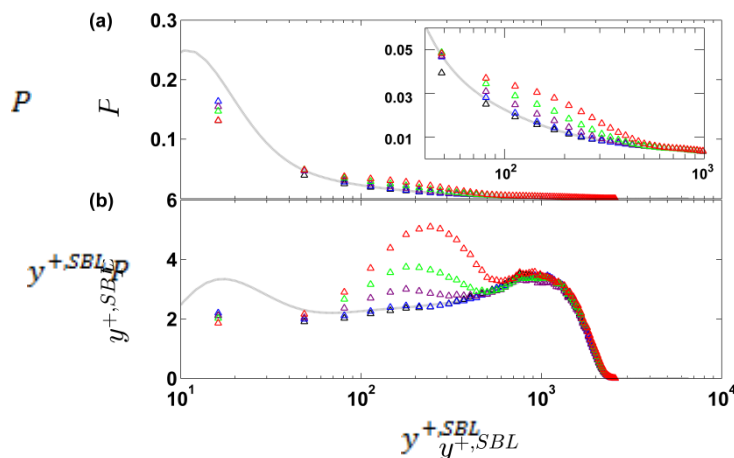


Figure 1. $Re_{\theta,SBL} = 7495$, (a) Production of the TKE along wall normal direction, inset figure magnifies the effect of blowing at different rate and exhibit the change of TKE in the log region. (b) Pre-multiplied P with non-dimensional wall locations.

Aktuelle Forschungsschwerpunkte / Current research topics

High energy containing region is observed in logarithmic and outer layer when plotted in pre-multiplied form to the respective wall normal distance. It is observed that inner and outer region is mostly unaffected while production is maximum within logarithmic region.

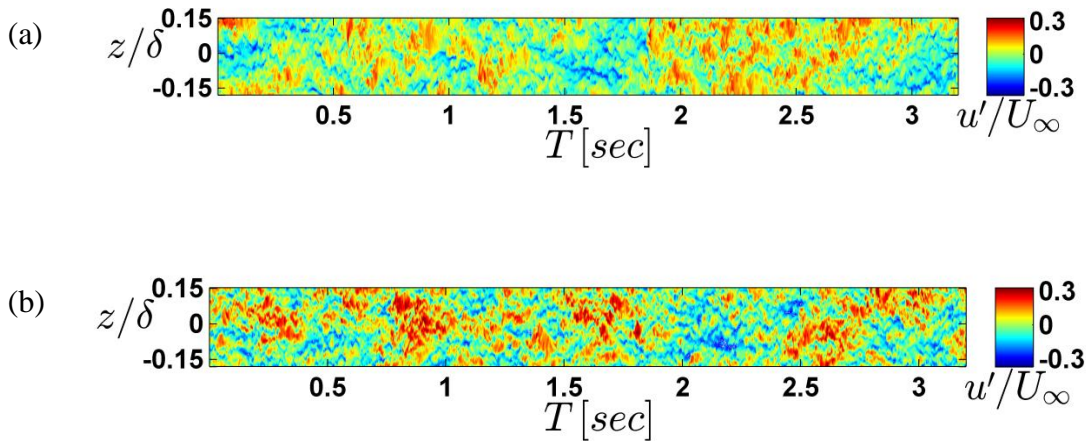


Figure 2. Contour plots of streamwise velocity fluctuations normalized with U_∞ over perforated surface (a) at blowing ratio, $F = 0$; (b) $F = 6\%$. Flow is coming from left to right with the reader's reference point.

The analysis of the second aspect e.g morphology of the LSMs under stochastic blowing is displayed in Figure-2. These figures presents contour plots of streamwise velocity fluctuations measured with the high temporal resolution SPIV in YZ plane at $Re_{\theta, SBL} = 7495$. The streamwise velocity has been scaled with the free stream velocity, U_∞ . (a) $F = 0$; (b) $F = 6\%$. exhibit the streamwise fluctuation. Taylor's frozen turbulence hypothesis was inferred in order to obtain the contour plots at $y/\delta = 1.62e-06$ ($y^{+, SBL} \sim 36$). Here, regions indicated by blue flanked by red is the signature of coherent structures, which forms a larger packet as the blowing increases. Gradually, their occurrence grows while blowing rate increases. Therefore, large regions with stronger energy is observed in Figure-2 (b). Contour plots of streamwise velocity based on Taylor's frozen hypothesis exhibit small pockets of high velocity region which increases with blowing. On the contrary, low velocity pockets are in dominant number for wall normal velocity. Therefore, blowing air affects streamwise velocity in adding momentum whereas it prevents the wall normal component.

For further information on the measured data please visit:

https://turbase.cineca.it/init/routes/#/logging/view_dataset/82/tabfile

Bibliography:

[1] Hasanuzzaman, G., Merbold, S., Motuz, V., Egbers, Ch., (2016)., Experimental Investigation of Turbulent Structures and their Control in Boundary Layer Flow. Experimentelle Strömungsmechanik, German Association for Laser Anemometry GALA e.V., Karlsruhe, Germany, (ISBN 978-3-9816764-2-6).

Aktuelle Forschungsschwerpunkte / Current research topics

A Aerodynamics

A7 On the influence of flow behaviour passes through structured surface

Mohamed Yousry*, Sebastian Merbold, Christoph Egbers (*BTU-LAS PhD Scholarship)

Introduction

Lightweight construction blocks is a multidisciplinary engineering science with great growth dynamics, which requires a holistic technological approach covering the whole system “design-material-manufacturing- application”. For that reason a state financed Graduate class named ‘Destruct’ was established from 9 different disciplines at the BTU Cottbus-Senftenberg to investigate the various aspects of structured sheets. The sheet material used to produce the hexagonal structured sheets was DC04 steel with an initial sheet thickness of 0.5 mm, developed at the Chair for Mechanical Design and Manufacturing of BTU using indirect hydroforming process. The developed process allows for producing structured sheets in the size of 585 mm x 585 mm, height of the structure (k) to diameter of the structure (D) ratio is 86%

Preliminary results from experiments with the structured sheets.

1. Channel flow:

The experimental investigation for the channel flow is conducted for Reynolds number, based on bulk velocity and half channel length, ranging from 7.84×10^3 to 3.8×10^4 . The experiments are taken within the wind tunnel of the Department of Aerodynamics and Fluid Mechanics of the BTU Cottbus-Senftenberg. The Göttingen-type wind tunnel was designed for good performance up to bulk velocity 50 m/s with background turbulence intensity less than 0.5% of the incident flow. Different measurement techniques were used to investigate the flow over the hexagonal structured surface such as LDA, PIV and pressure gradient.

LDA measurements were carried out with a relatively coarse measurement grid spacing with $\Delta x \approx 0.07D$ and $\Delta z \approx 0.07D$ above the hexagonal structured cavity to reveal the flow behaviour around a single hexagonal structured cavity. The investigation showed that the hexagonal structures have the effect of introducing streamwise vorticity into the base flow as shown in fig.(1). The flow scaling changes from those of the base flow parameters to parameters related to the hexagonal structures geometry. The streamwise vorticity acts to reduce skin friction drag. The spanwise flow components disrupt the normal cascading of the turbulent energy to the smaller scales for dissipation. Instead, the energy is being retained at the larger scales, implying greater streamwise coherence and stability of the flow. The reduced turbulent energy production of this stabilized flow results in the skin friction drag reduction observed with the negative structures. Further details can be found in Yousry et al. 2017 & 2019.

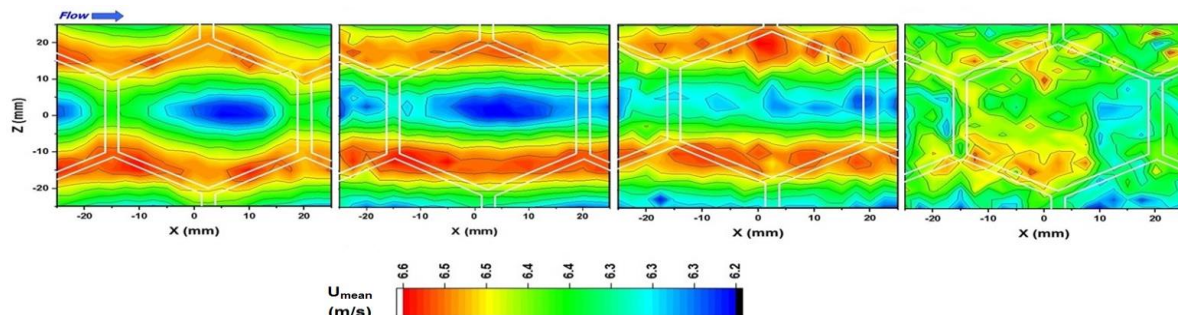


Figure 1: Mean streamwise velocity contours at $Re = 10900$ for $y/h = 0.05, 0.125, 0.25,$ and 0.5 .

Particle Image Velocimetry (PIV) measurements have been carried out rear the tested sheets. A standard Nd: YLF double-pulse laser, having 527nm/pulse was utilized. The measurements were

Aktuelle Forschungsschwerpunkte / Current research topics

carried out using CMOS camera, having 2560×1600 pixels, was installed with sampling frequency of 250 Hz, i.e. 4715 snap shots have been acquired. The size of the images was chosen to be 1686×1227 pixels and the sampling frequency was set at 250 Hz. A selected sample of the instantaneous velocity field is presented in fig.(2) for $Re_b = 10900$ and channel heights 50 for the smooth and hexagonal structures. The hexagonal structures shows regions of streamwise velocity fluctuations are observable in the core region of flow field that might be considered as a sign of the large-scale motion in the structured channel flow.

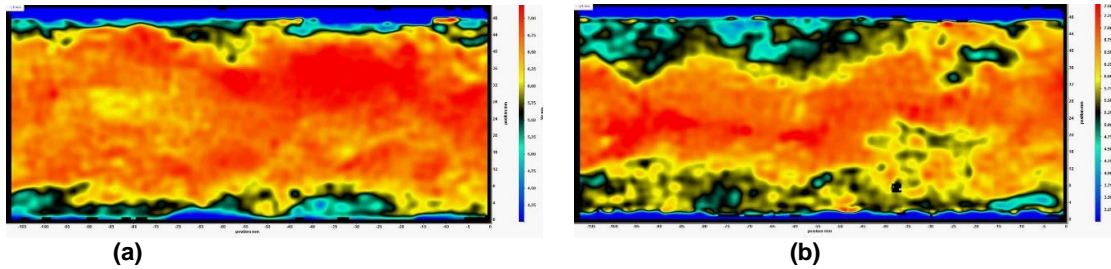


Figure 2: PIV instantaneous velocity field $Re_b = 10900$ and $H = 50$ mm (a) Smooth surface (b) Convex surface.

2. Pipe flow:

The experimental investigation for the pipe flow is conducted for Reynolds number ranging from 1.12×10^5 to 8.4×10^5 in pipe facility called the CoLaPipe built at the Department of Aerodynamics and Fluid Mechanics (LAS) at the BTU Cottbus-Senftenberg. Two pipe segments (190 mm diameter and 2 meter long) were constructed from DC04 steel with hexagonal structured patterns and equipped with flanges at its 2 ends to facilitate their installation in the Cola pipe fig.(3). Each pipe segment was investigated at $L/D = 113$, as König et al. 2014, reported that the flow in the ColaPipe is fully developed turbulent starting from $L/D = 75 - 80$. The pressure gradient measured upstream and downstream the structured pipe segments. It showed as shown in fig.(3) that the pressure losses increased for the concave and convex structured pipe segments by 50% and 41% respectively than the smooth pipe segments.

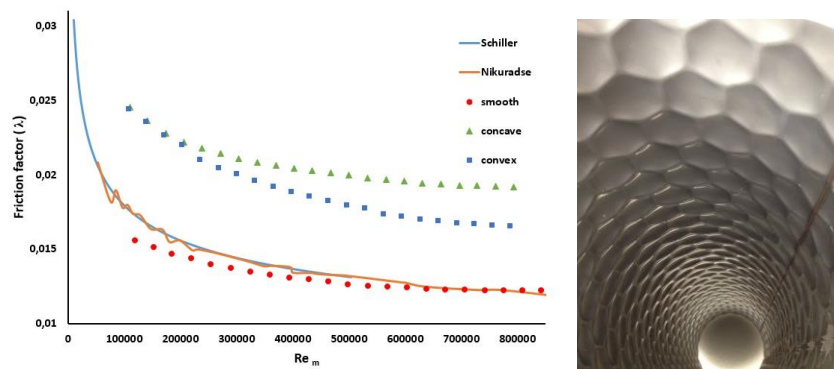


Figure 3: friction factor vs. Reynolds number based on diameter of the pipe for range $1.12 \times 10^5 \leq Re_m \leq 8.4 \times 10^5$ compared other studies and the structure segment from inside.

Bibliography:

- [1] M.Yousry, S. Merbold, and C. Egbers , " LDA measurements over hexagonal structured cavity inside turbulent channel flow" 25. GALA - Fachtagung Experimentelle Strömungsmechanik, 5. - 7. September 2017, Karlsruhe-Ettlingen (2017).
- [2] F.König,. E.S. Zanoun, E.Öngüner, and C. Egbers, " The CoLaPipe - the new Cottbus Large Pipe test facility at BTU Cottbus ", Review Scientific Inst, Vol. 85, No. 7, P. 075115-1-075115-9,(2014).
- [3] M.Yousry, S. Merbold, and C. Egbers , " Influence of convex structured surfaces on turbulent channel flow at different channel heights " 27. GALA - Fachtagung Experimentelle Strömungsmechanik, 3. - 5. September 2019, Erlangen (2019).
- [4] M.Yousry, S. Merbold, and C. Egbers , " Influence of hexagonal structured pattern on the flow behaviour inside a turbulent pipe flow " under preparation.



A Aerodynamics

A8 Building Integrated Wind Turbines

Stefan Richter, Sebastian Merbold, Christoph Egbers (EFRE-FKZ.:85008526)

Introduction

The importance of Green energy generation is not neglectable concerning current global environment protection discussions. It is a present topic in the political agenda of various countries and plays a vital role in German policy and economics creating a growing sector of renewable energy corporations. This is underlined by the attempt to find new ways to exploit renewable energy resources, such as small scale energy production within an urban environment. With its successful accomplishment general production costs could sink what leads to decreasing electricity costs and increasing security of supply with a simultaneous load relieve of the transmission grid.

Small wind turbines are one way to achieve these goals due to the fact that they can generate electricity close to the consumer. Different application fields of this turbines are researched widely over the last decades. The "Building Integrated Wind Turbines" project targets a new application of small wind turbines by using already existing but abandoned infrastructure such as buildings made with precast concrete slaps. Those buildings like the one depicted in Figure 1(a) were widely spread in the former GDR and Eastern European countries. Nowadays, people tend to avoid those domiciles leaving them uninhabited and unused. This has led to different reconstruction projects with tens of thousands teared down apartments over the last three decades. Still, a lot of those buildings exist and are assumed to be available for several years of power generation in the future. Therefore, this project is concentrated on the conversion of the symmetrical apartments with the so called P2 layout into a wind channel with a small wind turbine in its center. The attempted modification can be seen in Figure 2 by the red lines.

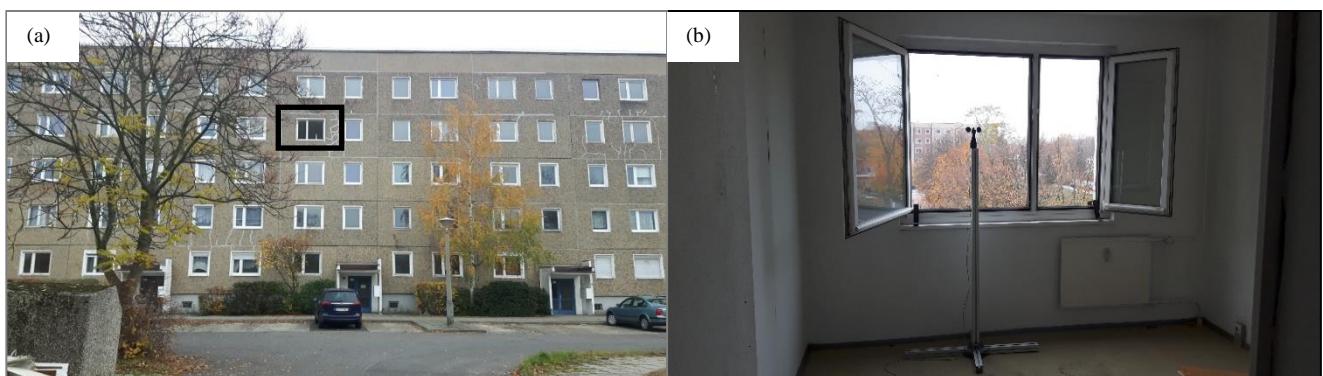


Figure 3: Precast concrete slaps building with (a) apartment position and (b) anemometer behind wind-entering window

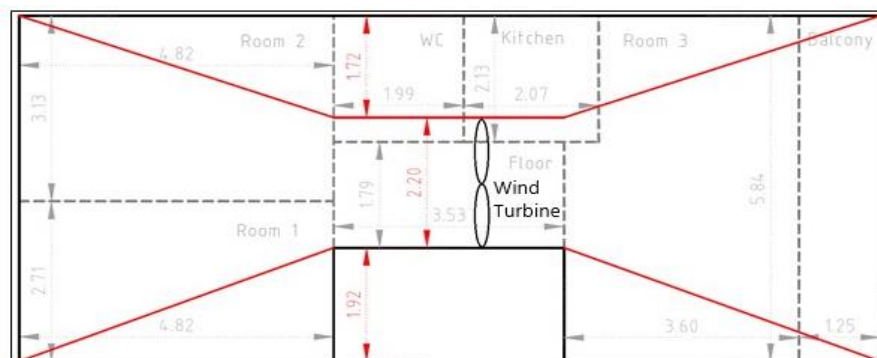


Figure 4: P2 apartment ground plan (grey) with planned modification (red)

Aktuelle Forschungsschwerpunkte / Current research topics

Experimental Results

In the first step experiments were done in a wind tunnel using a model building with a down scaled ratio of 1:125. The occurring wind velocities and velocity fields in front and behind the model were measured by Laser Doppler Anemometry (LDA) and Particle Image Velocimetry (PIV). A selection of the most promising type of turbine, duct shape and most efficient duct size compared to the area of the building has been done. The findings obtained that no specific size offers the highest acceleration increase for all free stream velocities. Thus, the most effective duct size depends on the incoming wind speed level. The highest velocity acceleration effect found so far is 60 % for a duct size which is represented by two apartments. Consequently, the effect of a modified apartment was investigated. Doing so, a plastic model shaped like an ideal wind tunnel was installed within the model building. The findings have obtained an average wind acceleration effect of in average 56 %.

After this basic small scale modeling was done field measurements were carried out which took place for over seven weeks from September to early November 2018 inside an actual apartment. The position of that apartment with a P2 layout inside the building can be seen in the black frame in Figure 1(a). Anemometer measurements were done in the middle of the apartment where the smallest cross-sectional area was situated with the estimated highest wind speeds. During the measurements all windows and doors were completely open. The purpose of this measurements was to test the already existing potential for wind energy production of a not yet modified apartment. However, the measured wind speeds were averaging between 0.9 m/s and a maximum speed of up to 4.3 m/s, which could be measured only four times. So the suspicion was that the turbulence effects within the premises upstream of the anemometer were so high that the inflowing wind was slowed down so much in the first third of the unmodified dwelling that during that selected windy measurement period the loss was too high for an efficient energy production. To avoid this effect the anemometer was positioned behind the wind-entering window as depicted in Figure 1(b). The knowledge gained from this confirmed the necessity of a modification of the apartment. Furthermore, other location options of the wind turbine have been considered such as the use of the flow around the roof edges. However, the LDA measurement results for this purpose had only a minor effect on the flow behavior, so that no usable wind speeds could be measured, which would be comparable with the flow around the building.

The next step is to model a whole precast concrete slabs building such as depicted in Figure 1(a) in a scale of 1:12. The model will have 50 apartments including 3 modified apartments according to the example of an ideal wind tunnel. The exact positioning of this 3 apartments inside the building is going to be variable in order to be able to detect the optimal distribution of the model apartments among each other. Within each of these modified apartments a small wind turbine with a diameter of 5 cm is going to be installed and its generation of electrical power measured. The model turbine is the limiting factor of the model building. The entire model is then fixed to the roof of the LG 3d of the chair and thus brought to a suitable height.

Since this project aims to bring those findings to economical use also Germany's statutory framework and electricity market had to be taken into account. An evaluation of a potential small wind power plant towards its economic feasibility implied that the so far obtained wind acceleration properties were not sufficient to run such a plant in an effective manner. This has been done for an assumed site in Cottbus using performance data of different turbine types. The estimated costs to modify an apartment in order to meet legal requirements are for now too high compared to the revenues made by a wind turbine given the obtained wind acceleration effects. Besides, research is done under which circumstances the acceleration factor can be further enhanced.

A Aerodynamics

A9 Numerical Study and Experimental Validation of Thermal Coupling Phenomena of Assembled Flip-Chip Test Dies on a typical Printed Circuit Board

T. Nowak*, R. Schacht*, S. Merbold, Ch. Egbers

* BTU Cottbus-Senftenberg, Fakultät 3, Fachgebiet Elektronische Schaltungstechnik

Introduction

The amount and concentration of active electronic components and passive objects on board level increase rapidly. Furthermore, the complexity between conductive heat spreading and the use of forced thermo-fluidic coupling effects with application-near-behavior will become a challenge to prevent thermal bottlenecks and guarantee thermal cooling performance during the early design state of the PCB layout process. A typical test board setup was chosen to address new experimental and numerical studies of assembled test dies (thermal test chips, TTC) on a typical printed circuit board (PCB) substrate [1]. In addition to the presented work of Hwang et al. [2] the approach was taken into account to represent thermal models of complex micro-technologic parts and assemblies as an equivalent resistor circuit (Fig. 1a). The equations of thermal conductivity are well known and with them are calculate thermal interactions between chips nearby. Otherwise, the convective initiated fluid flow over the chips and possible interactions with obstacles are more difficult to calculate, often only with the help of numerical software tools (CFD). Research investigations often use JEDEC standards with defined conditions and common electronic packages [3, 4]. The investigation studies in this paper forcing the analytic methods to analyse thermal convective and conductive driven heat flows experimentally and numerically.

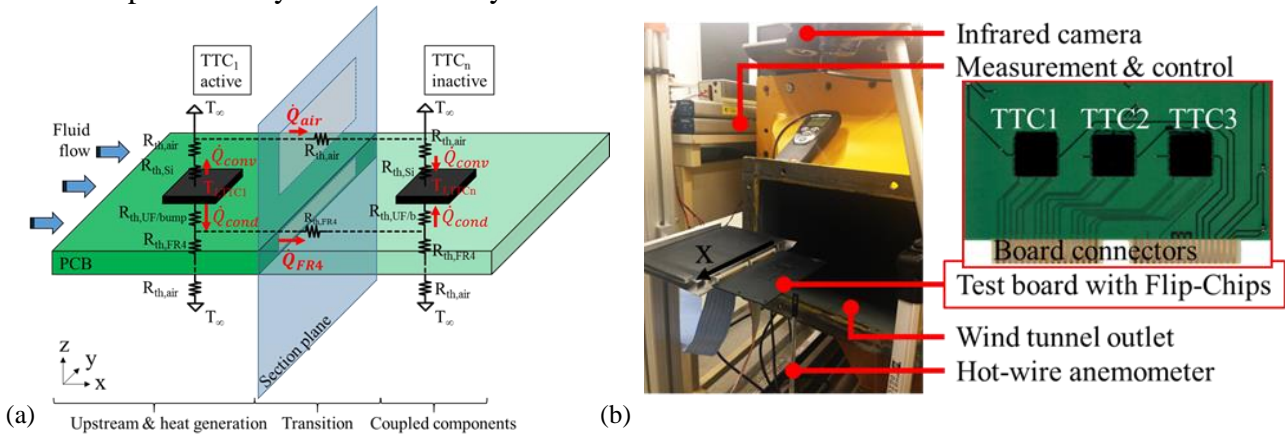


Figure 1: Sketch of a simplified thermal equivalent circuit (a) of a test board with thermal test chip (TTC) on top, heat flow and thermal resistances of solid and fluid materials of the area of interest to obtain conductive and convective heat coupling theory, (b) test scenario with wind tunnel outlet at the LAS CB, test PCB with three TTC, infrared camera (Optris PI160) and hot-wire anemometer (Testo 425).

Fig. 1b, the experimental setup at laboratory facilities of the LAS consists of the wind tunnel as ‘Göttinger’ type (closed loop) to provide laminar fluid flow at the outlet, different meshes (honey comb/rectangles) with decreasing openings are integrated. The test chips are covered with black paint ($\epsilon = 0.92$) to observe absolute surface temperatures by an infrared (IR) imager. The test PCB ($130 \times 80 \times 1.5 \text{ mm}^3$) consists of FR4 substrate laminates with copper layers on top and bottom side. The three TTCs ($16 \times 16 \times 0.67 \text{ mm}^3$) on top of the board has been assembled in Flip-Chip-technology with underfilling and has a pitch distance $d=24 \text{ mm}$. One chip consists of a cell 5×5 array and allows accurate single cell temperature measurements along the chip area. Low electrical resistance lanes in parallel can heat up every single cell unit. The measurements are run with active and inactive fluid

Aktuelle Forschungsschwerpunkte / Current research topics

flow (air, normal pressure, at 27 °C) with the variation of fluid velocity (0...5 m/s), power loss of TTC1 (0...3 W) and additional inner copper layers for the PCB test board to increase effective thermal conductivity of the substrate. To evaluate local temperature distributions on chip level at laminar fluid flow, a numerical simulation attend the experiments of the test scenario.

Experimental and Numerical Results

Within Fig. 2a, infrared images indicates thermal heat spreading of the activated test die TTC1 and the FR4-substrate according to different of power losses (1...3 W), fluid flow velocities (1...5 m/s) and two additional inner copper layers of the PCB. With higher flow rates, the temperature decreases and heating performance can multiplied by the factor of two. The heat transportation theory of involved chips in direct neighborhood are affected by forced air cooling systems and strictly depends on velocity, power loss, pitch distance and the heat transfer coefficients.

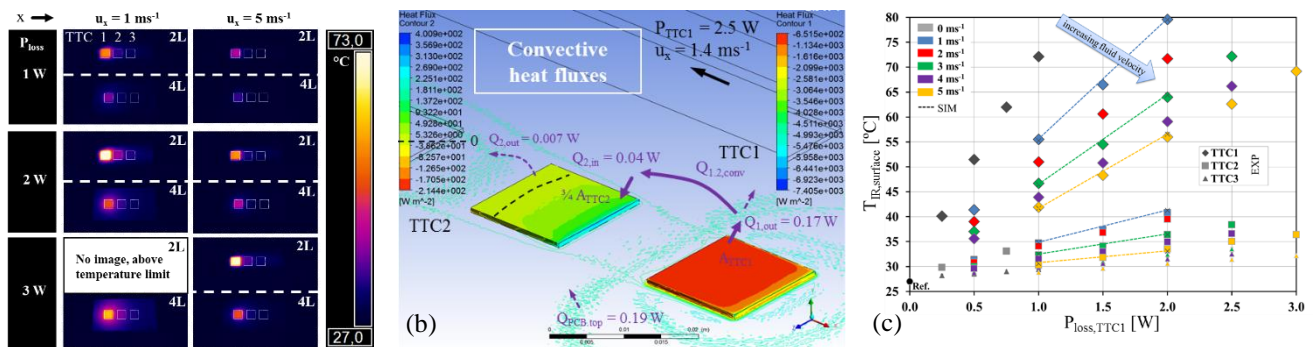


Figure 2: IR images (a) of the test board with active TTC1 and passive TTC2/3 according to increase of power loss, fluid velocity and variation of copper layers of the PCB (2 or 4 layers), simulation results of an active TTC1 and passive TTC2 to analyze heat flow distribution for convective heat transportation (b). Comparison of experimental and CFD results (c)

The results of numerical analysis following the separation into convective und conductive heat flow pathways. The main driven heat flow (over 90 %) is covered up by conductive thermal spreading through solid materials. Therefrom $Q_{2,\text{in}} = 0.09 \text{ W}$ (TTC2) of $Q_{1,\text{out}} = 2.33 \text{ W}$ (TTC1) is transferred to by heat conduction through the substrate. In Fig. 2b, the convective heat flow of TTC1 is calculated by the given parameters with $Q_{1,\text{out}} = 0.17 \text{ W}$ and coupled to TTC2 by air. The influenced area of TTC2 belongs to approximately three-fourths of the entire chip area. Up to $Q_{2,\text{in}} = 0.04 \text{ W}$ coupled thermal energy of TTC2 by convective transportation (24 % of $Q_{1,\text{out}}$). A comparison of experimental data and CFD-based numerical study shows a good agreement to expected linear behavior of the temperature. Thermal driven micro-electronic systems in combination of active cooling shows a valid data set to improve the ongoing research for convective initiated coupling effects. The influences of thermal conductive spreading have to be considered due to increasing velocity and power losses. The ongoing research focused an analytic approach in a corresponding simplified thermal equivalent circuits with the help of electronic *SPICE* simulations to reduce computationally intensive time.

Bibliography

- [1] R. Schacht, J. Punch, E. Merten, S. Rzepka and B. Michel, "Thermo-Fluidic Coupled Analysis of Flip-Chip Mounted Thermal Test Chips on a PCB – a Numerical and Experimental Study", 21th International Workshop on Thermal Investigations of ICs and Systems, THERMINIC, 2015
- [2] Ching-Bai Hwang, "Thermal Design for Flip Chip on Board in Natural Convection", 15th IEEE SEMITHERM Symposium, 1999
- [3] Tara Dalton, Jeff Punch, Mark R. Davies, Ronan Grimes, "Forced Convection Board Level Thermal Design Methodology for Electronic Systems", Electronics Packaging, Transactions of the ASME, Vol. 123, p. 120-126, 2001
- [4] Valérie C. Evely, Peter J. Rodgers, John M. Lohan, "Numerical Heat Transfer Predictive Accuracy for an In-Line Array of Board-Mounted PQFP Components in Forced Convection", IPACK'01, Pacific Rim/ASME International Electronic Packaging Technical Conference and Exhibition, 2001, Kauai, USA

Aktuelle Forschungsschwerpunkte / Current research topics

B Fluid Mechanics

B1 The DFG Core Facility Center “Physics of Rotating Fluids Lab” at BTU

Sebastian Merbold, Uwe Harlander & Christoph Egbers (DFG EG100/23-1, HA 2932/9-1)

The present proposal aims to establish a new international research center in form of a core facility center for “Physics of Rotating Fluids (PRF)” with geo-/astrophysical, meteorological and technical applications located at BTU. The main goal is to integrate cutting-edge rotating and stratified fluid flow experiments across national boundaries in order to foster internationally competitive experimental research in the research field of rotating and stratified fluids by providing an easy access to outstanding experimental facilities (Fig. 1, left) equipped with state-of-the-art instrumentation. The research areas covered by the experimental facilities inside the new center are (Fig. 1, right):

- Planetary and astrophysical flows (with focus on disk formation, instabilities and mixing)
- Geophysical fluid dynamics (with focus on strato-rotational turbulence, mean flow generation and wave interaction)
- Rotating flows with technical applications (centrifuges, turbines, journal bearings and rotor/stator cavities)

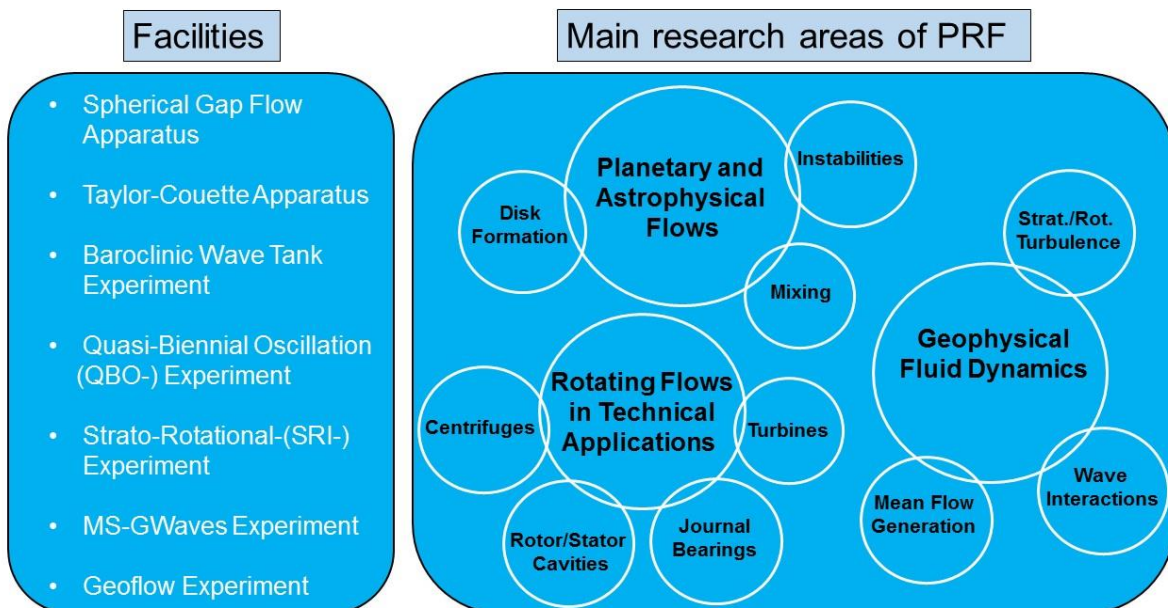


Figure 1: Summary of provided facilities and related and intended research areas of PRF

Thus, the main goals of this proposal are to:

- advertise and enforce the different research activities on rotating and stratified fluid flow experiments at BTU
- provide these outstanding research facilities at BTU to a larger national and international research community

Aktuelle Forschungsschwerpunkte / Current research topics

- bring together the recognized expertise of national and international working groups in the field of rotating and stratified fluids at BTU
- interconnect and help interested users by a networking program and joint research activities
- establish training groups for young researchers (Ph.D. students, Postdocs) in the field of rotating and stratified fluids
- organize exchange of scientific staff between the different research groups
- develop new experiments and models for a better insight into the dynamics and the role of these mean flows in geophysical, astrophysical, meteorological and technical flows at BTU
- deliver experimental data (including the use of modern experimental techniques like Thermography, Laser-Doppler-Anemometry, Particle Image Velocimetry (PIV), Laser Induced Fluorescence (LIF) techniques and Liquid Chrystal Tracer techniques, while the research approach as a whole is experimental, numerical and theoretical for the “PRF”
- organize and prepare collaborative applications to national and international calls for proposals (ANR, DFG, EU_FP8).
- collaborative data analysis of experimental, theoretical and numerical simulations.

These goals will be achieved by

- maintaining a suitable and safe physical environment with access to the required research services
- establishing a transparent and short review process for the external user community
- providing easy application forms for external scientific users, that ensures that proposals fit into the scientific frame of PRF research topics and are also compatible with the experiment facilities available
- sustaining a critical mass of scientific and technical expertise
- training and advising researchers as required
- providing appropriate and timely assistance
- enabling, advising and training on safe working practices
- ongoing research on new developments in instrumentation and responding to changes of experimental research; e.g. by designing, implementing or procuring appropriate mechanical, optical and electronic solutions to meet new experimental and diagnostic requirements
- documentation (user guides, safety-/laboratory manuals, annual reports, publications)
- public relations/ outreach (web-site, flyer, poster, presentations etc.)
- training / education (summer schools, workshops, young researcher meetings)
- continuation of core facility center activities after 3 years DFG funding through succeeding funding by BTU

Organization and interfaces of the core facility center “Physics of Rotating Fluids (PRF)”:

The new core facility center for “Physics of Rotating Fluids (PRF)” will cover and focus all previous single research and guest scientist exchange activities like EuHIT, CNRS French/German-cooperation and ESA Topical Team with BTU/CFTM² in the field of rotating and stratified fluid flows as illustrated in Fig. 2. After funding from DFG via the present proposal, the core facility center for “Physics of Rotating Fluids (PRF) will be continued and financed sustainably by BTU.

Aktuelle Forschungsschwerpunkte / Current research topics

Services and joint research activities of the core facility center “Physics of Rotating Fluids (PRF)”:
 The actual status of the core facility center for “Physics of Rotating Fluids (PRF)” comprises all experimental facilities and measurement techniques located in the Fluid-Center-Building in different rooms next to each other.

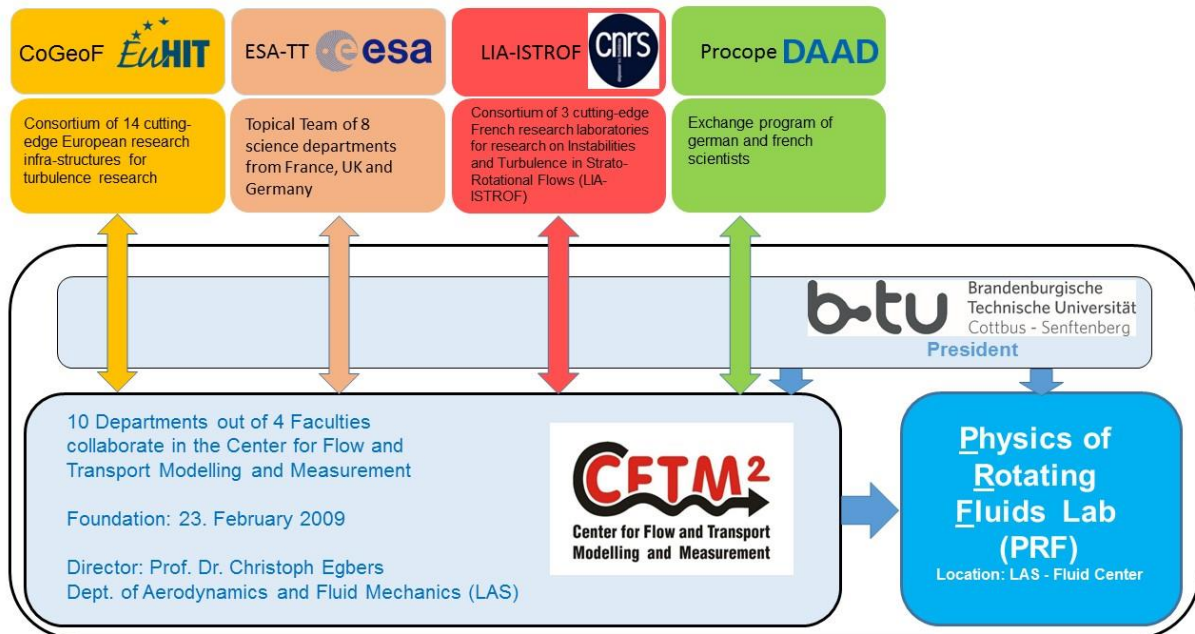


Figure 2: Organization structure and interfaces of core facility “Physics of Rotating Fluids (PRF)” Lab

The PRF is located in the Fluid-Center-building, on the campus of the Brandenburg University of Technology, Siemens-Halske-Ring 14, 03046 Cottbus, Germany. Responsible for the experiments is the Department of Aerodynamics and Fluid Mechanics. In this department about 30 technical & scientific employees work on experimental, theoretical and numerical questions of fluid mechanics. Generally we offer two types of services: i) in situ research with a direct access to the facility, and ii) commissioned research. In the first case i), the user in person will be conducting the research at our facility. To these researchers we offer practical guidance as well as technical assistance on the part of our scientific and/or technical staff, which is necessary due to the high complexity of the experimental installations. In preparation of such joint research project, the user will work with the facility lead scientist and the facility technician. The guesthouse of the BTU will minimize the organizational effort required for arranging the visits to the different facilities. In the second case ii), the commissioned research, the user can demand for certain measurements to be performed at our facility without being actually present in Cottbus. In this case our personnel will carry out the requested measurements and transmit the results to the user. This type of research is particularly appealing to users from the computational fluid dynamics community who are interested in validating their numerical data using experimental data.

Aktuelle Forschungsschwerpunkte / Current research topics

Scientific experimental equipment:

- Spherical gap flow apparatus (DFG EG 100/1-1, 1-2)
- Taylor-Couette apparatus (DFG EG 100/2, EG 100/7; EG 100/15-1, 15-2; FOR1182)
- Baroclinic wave tank experiment (DFG EG 100/3; EG 100/13-1, 13-2, 13-3; SPP 1276 “Metström”)
- Quasi-Biennial Oscillation (QBO-) experiment (DFG EG 100/14-1; HA2932/6-1)
- Strato-Rotational-experiment (DFG EG 100/18-1; HA2932/7-1)
- MS-GWaves experiment (HA2932/8-1,2; FOR 1898)
- Geoflow experiments (DLR, ESA)

Measurement equipment

- 2D-Particle Image Velocimetry (PIV) System, 15mJ Nd:YAG LASER, monochromatic CCD camera, resolution 1 megapixel (New Wave Research, TSI)
- Stereo-PIV system, 100mJ Nd:YAG LASER, 2 cameras with 2 MP resolution (Dantec Dynamics)
- Dantec Dyn. Laser Induced Fluorescence (LIF) system to measure concentration and temperature
- Volumetric Velocimetry, 100mJ Nd:YAG LASER, 3 cameras with a resolution of 2 megapixel, telecentric lenses for a measurement volume of 10 x 10 x 10 cm³ (Dantec Dynamics)
- Particle Tracking (2D, 3D) with the dantec system mentioned above
- 2x 1D (He-Ne LASER) and 2D Laser Doppler Anemometry (LDA), Ar-Ion-LASER
- Infrared-Thermography system

Bibliography:

1. Egbers, Ch., Pfister, G., (Eds), 2000, Physics of Rotating Fluids, **Lecture Notes in Physics 549**, Springer
2. Harlander, U., v. Larcher, T., Wang, Y., Egbers, Ch., 2011, PIV- and LDV-measurements of baroclinic wave interactions in a thermally driven rotating annulus, **Exp. Fluids**, 51, 37-49, DOI 10.1007/s00348-009-0792-5
3. Feudel, F., Bergemann, K., Tuckerman, L., Egbers, Ch., Futterer, B., Gellert, M., Hollerbach, R., 2011, Convection patterns in a spherical fluid shell, **Phys. Rev. E**, 83 (2011), 046304
4. Harlander, U., Wenzel, J., Alexandrov, K., Wang, Y., Egbers, C., 2012, Simultaneous PIV- and thermography-measurements of partially blocked flow in a heated rotating annulus, **Exp. Fluids**, 52, 1077-1085
5. Koch, S., Harlander, U., Egbers, Ch., Hollerbach, R., 2013, Inertial waves in a spherical shell induced by librations of the inner sphere: experimental and numerical results, **Fluid Dyn. Res.** **45**, **Best paper 2013 Jap. Soc. Fluid Mech.**
6. Merbold, S., Brauckmann, H.J., Egbers, Ch., 2013, Torque measurements and numerical determination in differentially rotating wide gap Taylor-Couette flow, **Phys. Rev. E** 87, 023014
7. Futterer, B., Krebs, A., Plesa, A.-C., Zaussinger, F., Hollerbach, R., Breuer, D., Egbers, Ch., 2013, Sheet-like and plume-like thermal flow in a spherical convection experiment performed under microgravity, **J. Fluid Mech.**, vol. **735**, 647-683, Cambridge University Press 2013, doi:10.1017/jfm.2013.507,
8. Klein, M., Seelig, T., Kurgansky, M. V., Ghasemi V., A., Borgia, I.-D., Will, A., Schaller, E., Egbers, Ch., Harlander, U., 2014, Inertial wave excitation and focusing in a liquid bounded by a frustum and a cylinder, **J. Fluid Mech.**, vol. **751**, 255-297, doi:10.1017/jfm.2014.304, 2014
9. Vincze, M., Borchert, S., Achatz, U., von Larcher, Th., Baumann, M., Liersch, C., Remmler, S., Beck, T., Alexandrov, K.D., Egbers, Ch., Fröhlich, J., Heuveline, V., Hickel, S., Harlander, U., 2014, Benchmarking in a rotating annulus: a comparative experimental and numerical study of baroclinic wave dynamics, **Meteorolog. Zeitschrift**, 23, 611 - 635
10. Harlander, U., v. Larcher, Th., Wright, G.B., Hoff, M., Egbers, Ch., 2014, Orthogonal decomposition methods to analyze PIV, LDV and thermography data of a thermally driven rotating annulus laboratory experiment. AGU book: **Modelling Atmospheric and Oceanic flows: insights from laboratory experiments and numerical simulations**, Th. v. Larcher and P. Williams (ed.), Wiley

B Fluid Mechanics

B2 Transport processes in the Turbulent Taylor-Couette Cottbus (T²C²) and Top-view Taylor-Couette Cottbus (TvTCC) facilities

Sebastian Merbold, Andreas Froitzheim, Christoph Egbers (DFG FOR 1182, EG100/15-1,2)

The Taylor-Couette (TC) flow, which is the flow between independently rotating cylinders, is a model for general rotating shear flows with technical (turbines or compressors) as

well as geo- and astrophysical applications (accretion discs, star formation). Within this geometry a rich variety of flow states can be adjusted by changing the control parameters, namely the ratio of angular velocities $\mu=\omega_2/\omega_1$, the radius ratio $\eta=r_1/r_2$, the aspect ratio $\Gamma=L/d$ with the gap width $d=r_2-r_1$ and the shear rate inside the gap in terms of the shear Reynolds number

$Re_S=2r_1r_2d|\omega_2-\omega_1|/((r_1+r_2)\nu)$ with the kinematic viscosity ν of the fluid and the indices 1 for the inner and 2 for the outer cylinder. When only the inner cylinder is rotating, the flow is linearly unstable as the Rayleigh-Benard flow (flow heated from below and cooled from above), while for pure outer cylinder rotation, the flow is linearly stable as the pipe flow. Further, a close analogy between all three systems exists for the global transport properties, which shows the importance of understanding the Taylor-Couette flow.

A very important quantity for transport processes in Taylor-Couette flows is the angular momentum current $J_\omega=r^3\langle(u_r\omega)_{t,\varphi,z}-v\partial_r\langle\omega\rangle_{t,\varphi,z}\rangle$, which can be directly measured by the torque T at the inner or outer cylinder. When J_ω is normalized by its corresponding laminar value $J_{\omega,lam}$, a quasi Nusselt number Nu_ω can be defined in analogy to heat transport problems [2].

For investigations of the TC flow, we have two facilities at the Department of Aerodynamics and Fluid Mechanics at the BTU-Cottbus, the Turbulent Taylor-Couette Cottbus (T²C²) facility and the Top-view-Taylor-Couette Cottbus (TvTCC) facility. The T²C² facility has a transparent outer cylinder, a precise torque measurement unit based on strain gauges inside the inner cylinder and is capable of controlling the angular velocities of the end plates. The TvTCC facility features a transparent outer cylinder and top plate, a shaft to shaft rotary torque sensor connected to the inner cylinder and an exchangeable inner cylinder to realize different radius ratios. The key parameters are summarized in table 1:

Table 1: Parameter for T²C² and TvTCC facilities

	Gap width d (mm)	Radius ratio η	Aspect ratio Γ	Re_S
T ² C ²	35	0.5	20	10^3-10^6
TvTCC	35, 45, 56, 63	0.5, 0.357, 0.2, 0.1	20, 15.5, 12.5, 11.1	$10^3-3\cdot 10^5$

In [2], the essential results of torque measurements in the T²C² facility ($\eta=0.5$) are discussed. For pure inner cylinder rotation, the dimensionless torque scales as $G\sim Res^\alpha$ with two different regimes. For $3\cdot 10^3\leq Res\leq 8\cdot 10^4$, the scaling is $\alpha=1.62\pm 0.04$ and for $10^5\leq Res\leq 10^6$, $\alpha=1.78\pm 0.06$. In case of $Res>6\cdot 10^5$, the scaling exponent approaches against a constant value of $\alpha=1.75\pm 0.03$. For small Reynolds numbers ($10^3\leq Res\leq 2\cdot 10^4$), the measured torques could be compared to direct numerical simulations with the same η and $\Gamma=2$, showing an excellent agreement with a relative deviation smaller than 4%.

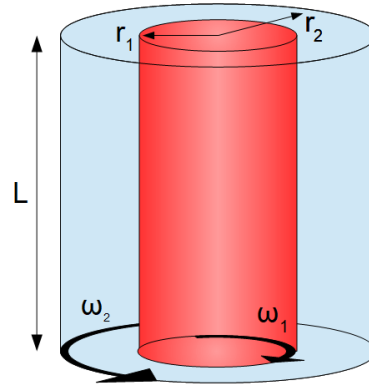


Figure 1: Sketch of Taylor-Couette geometry.

Aktuelle Forschungsschwerpunkte / Current research topics

Further, in both studies the torque exhibits a maximum for $\mu=-0.2$ independent of the shear Reynolds number for $Re_S < 7 \cdot 10^5$.

These studies have been continued for very wide gaps ($\eta=0.357$) in the TvTCC experiment, depicted in Figure 2. For pure inner cylinder rotation we can again identify a power law scaling of the Nusselt number with the shear Reynolds number and the local exponent α shows a prominent change around $Re_S=1.3 \cdot 10^4$ much earlier than for $\eta=0.5$. Further, the torque maximum has been shifted to $\mu=-0.12$ in good agreement with the predicted one ($\mu_{pred.}=-0.106$). These results are discussed in a manuscript under review at Phys. Rev. Fluids.

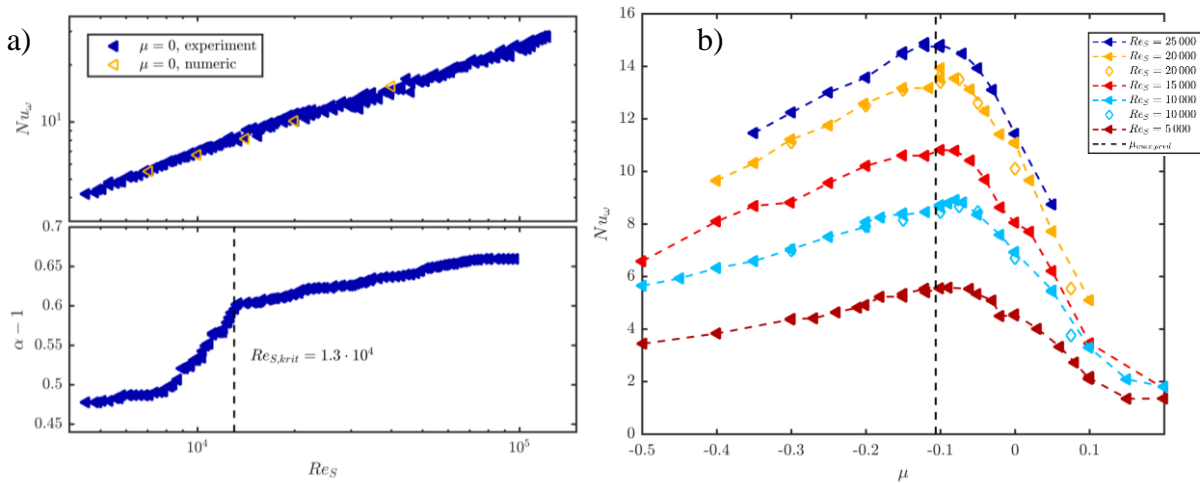


Figure 2: a) Torque data and local scaling exponent for pure inner cylinder rotation as function of the shear Reynolds number for $\eta=0.357$. b) Torque data for co- and counter rotation for various shear Reynolds numbers. The maximum of the Nu_ω curves is located at $\mu=-0.12$.

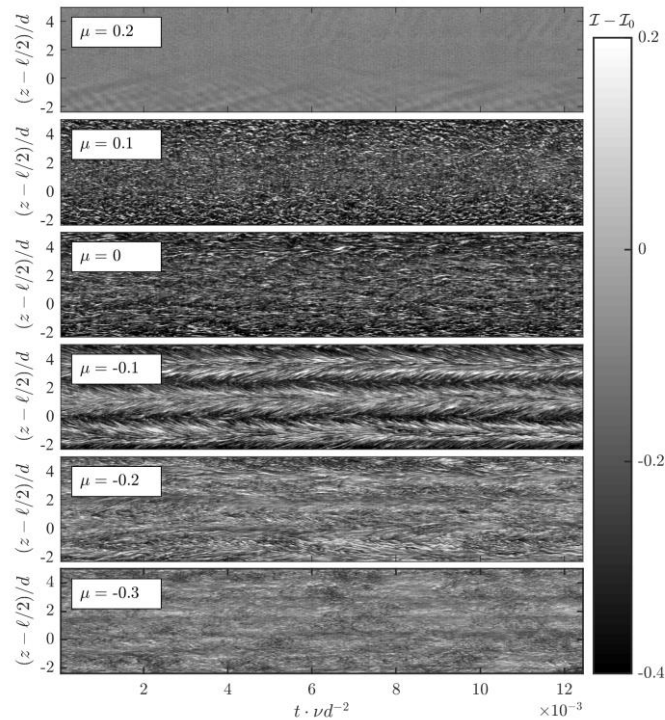


Figure 3: Space-time diagrams of the intensity distribution along an axial, central line over time for the shear Reynolds number $Re_S=2.5 \cdot 10^5$ and different μ . The time coordinate is normalized by the viscous time scale and the axial coordinate by the gap width d . All videos have been acquired at 60Hz.

Aktuelle Forschungsschwerpunkte / Current research topics

To investigate further the physical mechanism underlying the phenomenon of the torque maximum, we performed flow visualization measurements and discussed in [3]. Therefore, aluminum flitter or Kaliroscope particles are added to the working fluid and the scattered light of these tracers has been recorded. The light intensity information for one axial line as function of time for is depicted in Figure 3 for the radius ratio $\eta=0.357$. The flow behavior for radius ratio $\eta=0.5$ is discussed in [3]. To overcome the limitations of flow visualizations, where we can only analyze the flow close to the outer cylinder, we further performed Particle Image Velocimetry in horizontal planes at different cylinder heights at $\eta=0.5$ and $Re_s=10^5$.

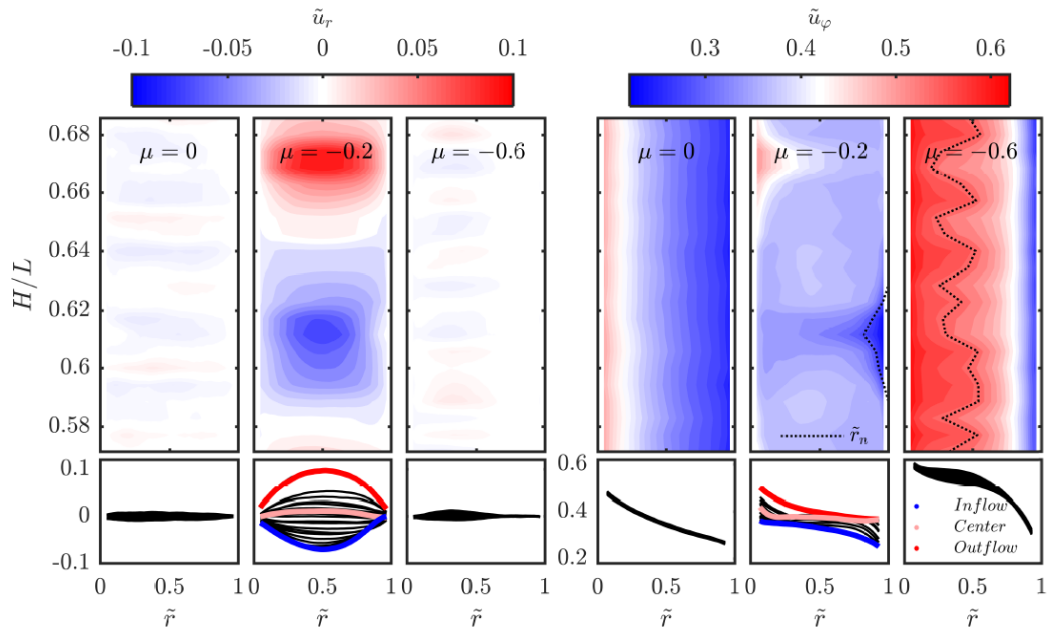


Figure 4: Contour plots and velocity profiles of the temporal and azimuthally averaged, normalized radial u_r and azimuthal velocity component u_ϕ at 21 different heights for $Re_s=10^5$ and the rotation ratios $\mu=0$; -0.2 ; -0.6 . Profiles at the axial position of the inflow, outflow and center of a turbulent Taylor vortex for $\mu=-0.2$ are highlighted in blue, red and light red respectively. The dotted lines indicate the position of the neutral surface r_n . The representation of the colormaps of the contour plots is based on a bilinear interpolation. Figure taken from [1].

For pure inner cylinder rotation, the temporal and azimuthally averaged radial velocity component is nearly zero at all radial locations and the azimuthal velocity component does not show an axial dependence. Obviously, no roll structures are evident inside the flow. At the rotation ratio of the torque maximum ($\mu=-0.2$), dominant vortices appear in the flow filling the whole gap and causing the maximum transport. Especially in the in- and outflow regions of these vortices, angular velocity is transported strongly in the radial (wall-normal) direction. The radial as well as the azimuthal velocity profiles vary significantly with the axial coordinate. For stronger counter rotation ($\mu=-0.6$), the increased outer cylinder rotation stabilizes the flow in the outer gap region and the axial dependence of the velocity components is restricted to the inner region.

Aktuelle Forschungsschwerpunkte / Current research topics

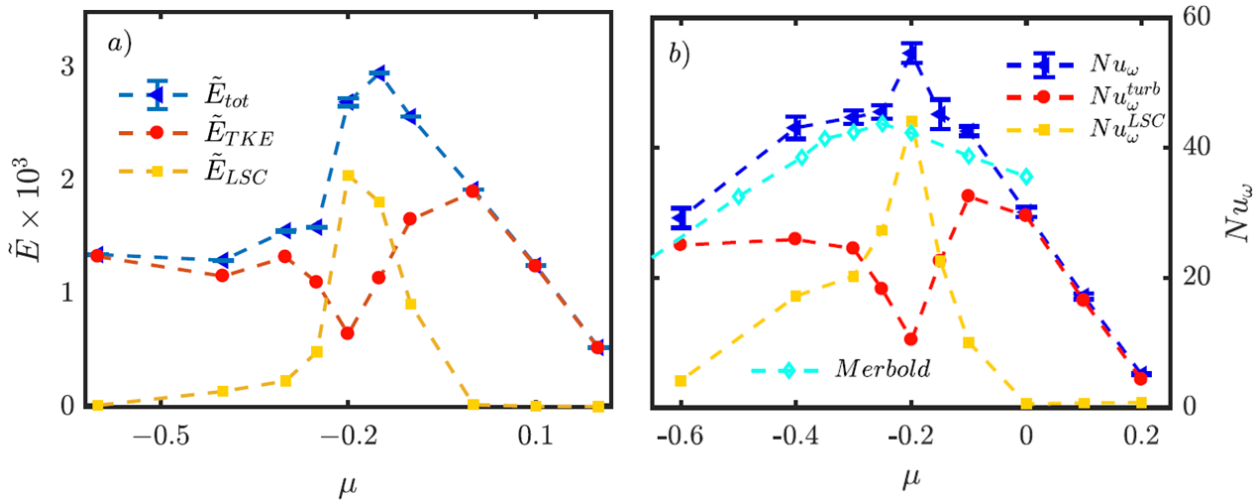


Figure 5: Distribution of kinetic energy and angular momentum transport for $Re_s=10^5$ and different μ . Figure taken from [1].

Based on the velocity field, we can further calculate the energy and angular momentum fractions $Re_s=10^5$ by decomposing the flow into its large scale and turbulent contribution: $\mathbf{u} = \langle \mathbf{u} \rangle_{\phi,t} + \mathbf{u}'' = \bar{\mathbf{u}} + \mathbf{u}''$. Neglecting the axial velocity component concerning the kinetic energy, the flow contributions are defined as:

- Turbulent kinetic energy $E_{TKE} = \frac{1}{2} \langle \mathbf{u}_r''^2 + \mathbf{u}_\phi''^2 \rangle_{t,\phi,z,r}$
- Large scale circulation energy $E_{LSC} = \frac{1}{2} \langle \bar{\mathbf{u}}_r^2 \rangle_{t,\phi,z,r}$
- Turbulent momentum transport $Nu_\omega^{turb} = J_{lam}^{-1} \langle r^3 \langle \mathbf{u}_r'' \omega'' \rangle_{t,\phi,z} \rangle_r$
- Large scale circulation transport $Nu_\omega^{LSC} = J_{lam}^{-1} \langle r^3 \langle \bar{\mathbf{u}}_r \bar{\omega} \rangle_{t,\phi,z} - \nu \partial_r \langle \bar{\omega} \rangle_{t,\phi,z} \rangle_r$

The large scale circulation energy becomes maximal at the rotation ratio of the torque maximum, while the turbulent fraction exhibits a local minimum. For co- and strong counter rotation, E_{LSC} vanishes and E_{TKE} seems to converge in the high counter-rotating regime to a constant non-zero value. However, the total kinetic energy maximizes at a slightly smaller μ than μ_{max} . In terms of the Nusselt number, a similar behavior can be seen, but the total Nusselt number maximizes in good agreement with the previous investigations at μ_{max} and the peak in the large scale circulation energy is more pronounced than for the energy calculations. Summarizing, the combination of direct torque measurements, flow visualizations and PIV measurements revealed the physical mechanism of maximal transport of angular momentum.

Bibliography:

- [1] A. Froitzheim, S. Merbold, C. Egbers, Velocity profiles, Flow structures and scaling in a wide-gap turbulent Taylor-Couette flow, J. Fluid Mech., 831, 330-357, 2017
- [2] S. Merbold, H. J. Brauckmann, C. Egbers, Torque measurements and numerical determination in differentially rotating wide gap Taylor-Couette flow, Phys. Rev. E, 87, 023014, 2013
- [3] S. Merbold, A. Froitzheim, C. Egbers, Flow pattern and angular motion transport in a wide gap Taylor-Couette flow, TU Dresden, Strömungstechnische Tagung 2014, Schriftenreihe aus dem Institut für Strömungsmechanik Band 10, 2014

Aktuelle Forschungsschwerpunkte / Current research topics

B Fluid Mechanics

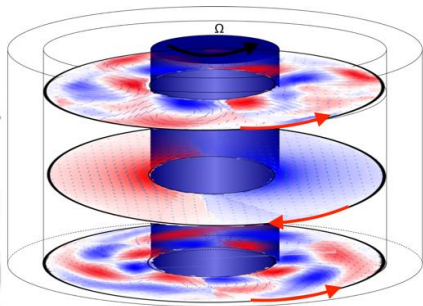
B3 Experimental study of inertia-gravity wave in a differentially heated rotating annulus Costanza Rodda, Ion D. Borcia, Uwe Harlander (DFG HA2932/8-2; FOR1898, MSgWaves)

Introduction

In the atmosphere, Inertia-Gravity Waves (IGWs) are short-wavelength, high-frequency waves that are increasingly recognized as a significant source of uncertainty in weather forecasting, and may play a major role in the dissipation of energy in the oceans as well. While flow-dependent parameterizations for the radiation of inertia-gravity waves from orographic and convective sources do exist, the situation is less developed for spontaneously emitted inertia-gravity waves. This research project focuses on the studies of spontaneous imbalance of IGWs via laboratory experiments. Two differentially heated rotating annulus experiments are used for this purpose at the BTU laboratories.

Pure *gravity waves* are driven by perturbations of density stratification, and therefore their characteristic frequency scale is that of the Brunt-Väisälä (or buoyancy-) frequency N . This can be estimated from $N^2 \approx g \cdot \alpha \cdot \Delta T / D$, where g is the gravitational acceleration, α is the volumetric thermal expansion coefficient of the medium and ΔT is the total vertical temperature change in fluid depth D . Pure *inertial waves*, on the other hand, are excited by the Coriolis force, and thus have a characteristic frequency of around $f = 2\Omega$, where Ω is the angular velocity of the rotating system. IGWs are “hybrid” combinations of these wave types, and their frequencies are expected to lie in the range of $f < \omega < N$ in the atmosphere. The configuration of the differentially heated rotating annulus typically used in the laboratory has a ratio $N/f < 1$, which is very different from that occurring in the real atmosphere and, hence, is not suitable for the investigation of IGWs. For this reason, two modified experiments are used in our laboratories, both allowing to reach $N/f > 1$.

Small tank baroclinic annulus with additional salt stratification

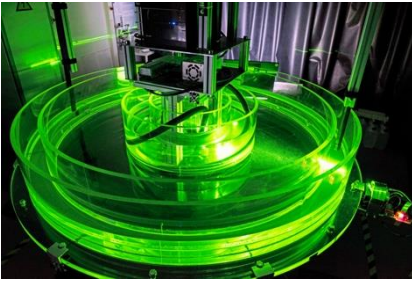


The first modified set-up is a thermohaline version of the classical baroclinic experiment—the so-called barostrat experiment—in which a juxtaposition of convective and motionless stratified layers can be created by introducing a vertical salt stratification. The thermal convective motions are suppressed in a central region at the mid-depth of the rotating tank. Hence, baroclinic waves can only arise in thin layers located at top and bottom, where the salt stratification is weakest. This new experimental set-up allows to study the exchange of momentum and energy between the layers, especially by the

propagation of IGWs, and first experimental results have been published in [2]. Moreover, contrarily to the small tank without salt stratification, the barostrat experiment has layers where $N > f$. In these layers, gravity waves are observed in the divergence field, and we speculated about the emission of IGWs into the stable middle layer. Subsequent experiments [3] offered a fascinating new insight of wave coupling in baroclinic jet flows: i) two decoupled baroclinic waves in the top and bottom layer have been found; ii) a Kelvin wave that has the strongest signal in the stable stratified middle layer has been detected (these two types of waves are shown in the figure on the left); iii) Poincaré-type waves in the high-frequency part of the spectrum have been observed; vi) finally, local IGW packets along the jets in the surface and bottom layers have been observed for local Rossby numbers larger than 1, suggesting that spontaneous imbalance is one of the possible generating mechanisms.

Aktuelle Forschungsschwerpunkte / Current research topics

MSGWaves tank



The second experiment is a wider and shallower tank (see figure on the left), especially designed and built following the numerical investigations by [1] to study the inertia-gravity wave radiation from jet streams. The large-scale flow regimes have been extensively investigated for different choices of ΔT and Ω , and compared with the ones obtained for numerical simulations (performed at the Goethe University in Frankfurt [4]). Fig.1 shows a comparison of large-scale features between experiment and simulation. The large-scale flow agrees qualitatively and quantitatively well, as it is reported in [5]. Furthermore, the complex horizontal structure of N showing most significant values along the baroclinic jet axis lends credence to the trapped inertia-gravity waves already observed in [3] and well visible also in the MSGWs tank (see figure1 plot on the right).

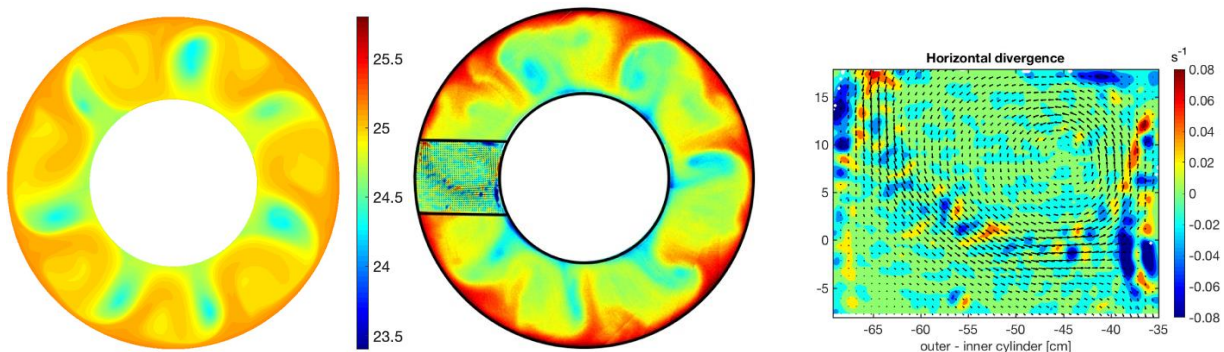


Figure1: Comparison of the surface temperature of simulation (left) and experiment (centre) for $\Delta T = 5K$ and 0.7rpm. The plot on the right shows the gravity waves (in colour) trapped along the jet (black arrows).

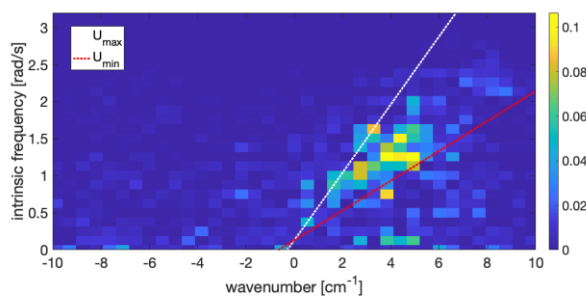


Figure2: Plot of gravity wave frequencies and horizontal wavenumbers.

Bibliography:

- [1] Borchert, Sebastian, Ulrich Achatz, and Mark D. Fruman. "Gravity wave emission in an atmosphere-like configuration of the differentially heated rotating annulus experiment." *J. Fluid Mech.* 758 (2014): 287-311.
- [2] M. Vincze, I.D. Borcia, U. Harlander, and P. Le Gal, "Double-diffusive convection and baroclinic instability in a differentially heated and initially stratified rotating system: the barostrat instability." *Fluid Dyn. Res.*, 48, 061414 (19pp), 2016.
- [3] C. Rodda, I. Borcia, P. Le Gal, M. Vincze and U. Harlander, "Baroclinic, Kelvin and inertia-gravity waves in the barostrat instability experiment," submitted to *Geophysical and Astrophysical Fluid Dynamics (GAFD)*, 2017.
- [4] S. Hien, J. Rolland, S. Borchert, L. Schoon, C. Zülicke and U. Achatz, "Spontaneous gravity wave emission in the differentially heated rotating annulus experiment," *J. Fluid Mech.*, 838 (2018): 5-41.
- [5] C. Rodda, S. Hien, U. Achatz and U. Harlander "A new atmospheric-like differentially heated rotating annulus configuration to study gravity wave emission from jets and fronts." Under review in *Experiments in Fluids*.

B Fluid Mechanics

B4 Numerical and experimental investigations on Stratified Rotational Instabilities

Gabriel Meletti, Torsten Seelig, Andreas Krebs, Stephane Abide, Stephane Viazzo, Uwe Harlander (DFG EG 100/18-1; HA2932/7-1)

Introduction

Understanding the mechanisms that can result in an outward transport of angular momentum is of the most interest for the theory of planets formation, particularly in accretion disks. When a planet forms in a disk, angular momentum has to be carried away from the planet otherwise its rotation speed would be far too large. Only turbulence can achieve such a large angular momentum transport (Lyra & Umurhan (2018)). For disks coupled to a magnetic field, Magneto Rotational Instability (MRI) can occur and, regardless of other angular momentum transport processes, one expects the fluid to sustain Magneto Hydrodynamic Turbulence. However, accretion disks can be turbulent even in the absence of a magnetic field, e.g. in regions where the ionization fraction is low. In such regions, the disk cannot be unstable due to MRI and it is an important question to ask whether other instabilities can excite turbulence there (Armitage (2010)). Among other candidates, the Stratified Rotational Instability (SRI) has attracted attention in recent years. The SRI is a purely hydrodynamic instability and much insight can be obtained from particularly designed laboratory experiments and numerical simulations in an axially-stratified Taylor-Couette setup.

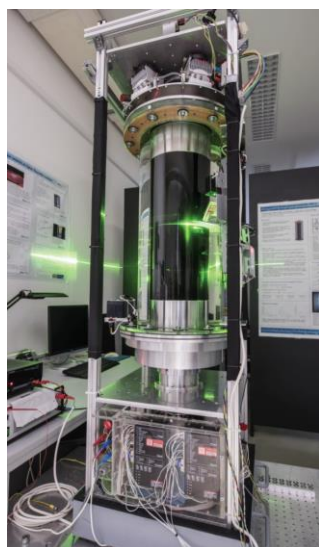
Experimental and Numerical Approaches

For studying the SRI phenomena and better investigate the still many open questions to be studied, an experimental setup was designed, constructed and built at the Department of Aerodynamics and Fluid Mechanics of the Brandenburg University of Technology Cottbus-Senftenberg (BTU) for studying temperature-stratified rotating flows with Reynolds numbers $300 < Re < 32000$. The configuration used to study the SRI phenomena is shown in **Figure 1**. The experimental velocity profiles are obtained using *Particle Image Velocimetry* techniques (PIV). A series of experiments with different rotation ratios between inner and outer cylinders (μ) and different Reynolds numbers (Re) were performed at BTU to inspect the transitions to SRI, to construct stability diagrams, and to compare the results with fully nonlinear numerical results.

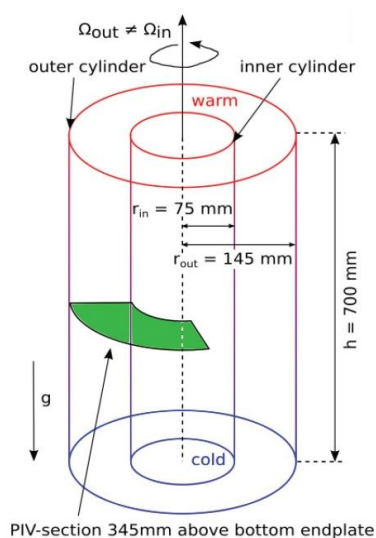
The numerical simulations regarding the SRI phenomena have also been explored considering the same configuration and geometry of the experimental setup as shown in **Figure 1**. The numerical results are obtained with a non-linear high performance parallel code that solves the Navier-Stokes equations under the Boussinesq approximation. This numerical simulations have been developed in tight collaboration with French researchers from the *Aix-Marseille University* and the *University of Perpignan*.

Comparisons of the numerical and experimental results have been showing good agreements, and did already show interesting results, as that the mode with azimuthal wave number $m=1$ is unstable beyond the Rayleigh limit (see **Figure 2**).

Aktuelle Forschungsschwerpunkte / Current research topics

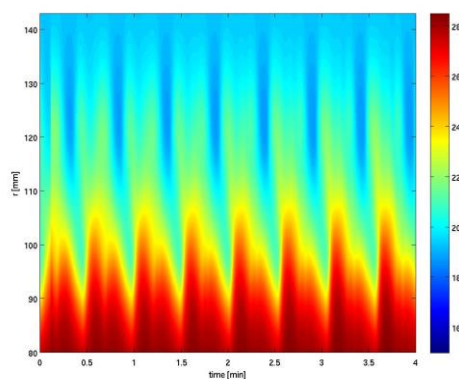


(a)

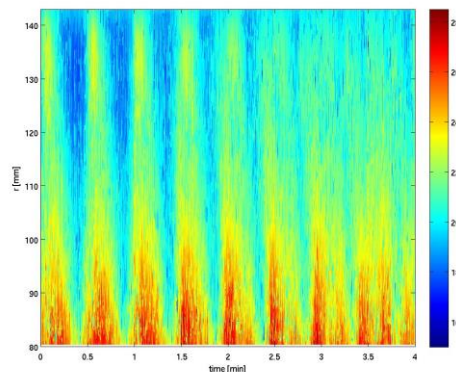


(b)

Figure 1: (a) The SRI experiment at BTU Cottbus-Senftenberg. (b) Definition of the geometrical parameters and orientation of the PIV laser sheet for experimental investigation. The system is cooled at the bottom and heated at top. Both cylinders can rotate independently



(a)



(b)

Figure 2: Time space (Hovmöller) diagrams for the azimuthal velocity with Reynolds numbers $Re=400$ and rotation ratio between inner and outer cylinders of $\mu=0.35$ obtained with (a) numerical simulation (b) experiment (PIV). For $\mu=0.35$, the flow would be Taylor-Couette stable, but it is SRI unstable.

Flows with larger Re can rather easily be studied with the SRI experiment at the BTU laboratory (**Figure 1**) but can be more difficult to be investigated numerically. This did underpin the necessity to do more laboratory experiments, although new numerical techniques are under development for continuing these investigations, and having a greater numerical spectrum of higher Reynolds numbers at different rotation ratios, that is still a non-investigated SRI region, allowing a better understanding of the angular momentum transport in accretion disks.

Bibliography

- [1] W Lyra, O Umurhan, arXiv preprint arXiv:1808.08681 (2018)
- [2] G Rüdiger, T Seelig, M Schultz, M Gellert, Ch Egbers, and U Harlander. Geophysical & Astrophysical Fluid Dynamics, 111(6):429–447 (2017).

B Fluid Mechanics

B5 Mean flow generation and inertial mode interaction in rotating annulus with stochastic methods

Wenchao Xu*, Uwe Harlander (*BTU-GRS „Stochastic Methods for flow and transport processes”)

Introduction

In fluid mechanics, the term “energy cascade” refers to the energy transfers from large-scale motion to small-scale motion, which is also called direct energy cascade. An inverse energy cascade, where the energy transfers upscale from small-scale motion to large-scale motion, can also exist. The theory of inverse energy cascade is used to explain of the jet flows on gas planets, such as Jupiter. One model proposed that the jet flows extend into the planetary molecular envelope and is formed due to the deep-seated small-scale motion. The possibility of this model is experimentally and numerically investigated by Cabanes et al. [1]. This research project focuses on investigating the influence of deep-seated stochastic shear force on Taylor-Couette flow.

Experimental set-up

The laboratory experiments were carried out with the QBO (Quasi Biennial Oscillation) tank. The QBO tank has an annulus form and consists of two independent rotating cylinders. The radius of the outer cylinder (OC) is 20 cm and the inner cylinder (IC) radius is 7.5 cm. The tank is partially filled with deionized water. A truncated cone can be mounted at the bottom of the annulus with small obstacles generating stochastic motions. This sloping bottom rotates simultaneously with the OC. A schematic sketch is shown in figure 1. Aluminum alloy racks are installed on the OC and rotate with the OC. A camera and a laser device are installed on the rack so that the Particle Image Velocimetry (PIV) can be applied for quantitative measurement.

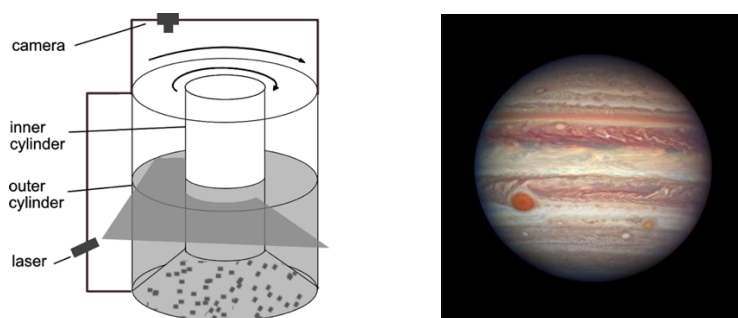


Figure 1: Left: schematic sketch of the experiment configuration. Right: jet flows on Jupiter. (image credits: NASA, ESA, and A. Simon (NASA Goddard))

Preliminary results from experiments with co-rotation

Mean flow generation is firstly investigated in a slightly tilted co-rotating annulus with free surface. Instead of the conic annuli, the experiments apply a flat bottom. The IC and OC co-rotate with the same angular velocity Ω . The PIV results of time averaged azimuthal velocity in figure 2 show that a mean flow is generated by nonlinear self-interaction of the oscillating boundary layers produced by the tank inclination. Its magnitude is influenced by the inclination angle. With larger tilt angle, a

Aktuelle Forschungsschwerpunkte / Current research topics

stronger mean flow can be observed.

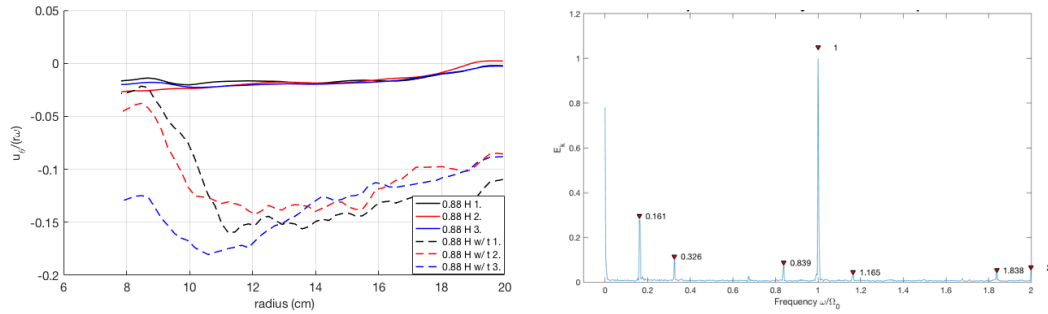


Figure 2: Left: time averaged azimuthal velocity in radial direction. Solid lines: tank with a small tilt angle of 3 experimental attempts; dashed lines: tank with an increased tilt angle of 3 experimental attempts. Right: spectrum of absolute velocity $|U|$ with increased tilt angle, IC/OC rotates with 20 rpm.

Due to the inclination of the tank, a forced Kelvin mode is generated with frequency $\omega/\Omega = 1$ together with a number of free Kelvin modes with frequency $0 < \omega/\Omega < 2$, see figure 2. Using harmonic analysis, we can identify and reconstruct the forced and free modes, e.g. the vorticity field of the mode with $\omega/\Omega = 0.172$ is shown on the left hand side of figure 3.

The bicoherence, which gives a statistical measure of the quadratic phase coupling, is also used to analysis the mode coupling [2]. The diagram plotted in figure 3 shows the application of this tool, where the value 1 means perfect coupling and 0 means no coupling. E.g. the strong peaks on the line starting at $\omega_1 = 0$ and $\omega_2 = 1$ with slope -1 can be identified as triads formed by the free modes with the forced mode with $\omega/\Omega = 1$. Thus, a number of triads in frequency can be find such as (0.838, 0.162, 1), (0.676, 0.327, 1), (0.838, 0.327, 1.162), (1, 0.162, 1.162) as well as the triplet (0.162, 0.676, 0.838). The triads we identified from the bicoherence diagram prove the existence of the triadic resonance and further emphasize that the triads are formed not only by one forced mode and two free modes but also by three free modes. The latter points to a cascading process that, for smaller Ekman number, will lead to wave turbulence driving a complicated mean flow as shown in figure 1 (right).

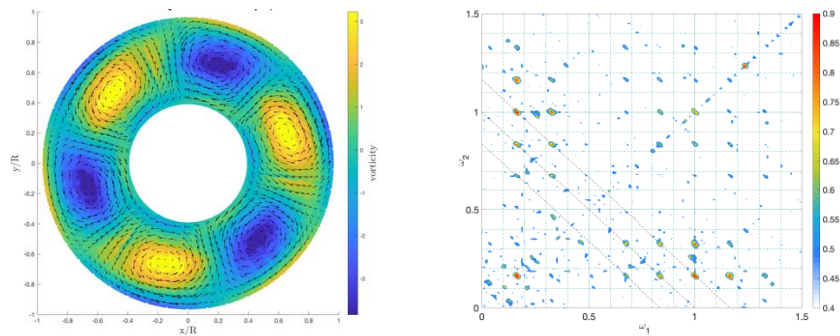


Figure 3: Left: Reconstruction of the vorticity field of mode $\omega/\Omega = 0.172$ using harmonic analysis. Right: bicoherence spectral of azimuthal velocity. Measured with increased tilt angle and angular velocity 20 rpm.

Bibliography

- [1] S. Cabanes, J. Aurnou, B. Favier, and M. Le Bars. A laboratory model for deep-seated jets on the gas giants. *Nature Physics*, 13(4), 387–390 (2017)
- [2] C. Brouzet, E. V. Ermanyuk, S. Joubaud, I. Sibgatullin, and T. Dauxois. Energy cascade in internal-wave attractors, *EPL (Europhysics Letters)* 113, 44001-7 (2016)

B Fluid Mechanics

B6 TEHD in a cylindrical annulus: laboratory experiments

Torsten Seelig, Antoine Meyer, Martin Meier, Christoph Egbers (DFG EG 100/20-1)

The effect of the dielectrophoretic force on a dielectric fluid confined in a vertical cylindrical annulus is considered through laboratory experiments. In that case the Earth's gravity acts on the radial density stratification, which leads to a base convective unicellular flow. For sufficiently large aspect ratio $\Gamma = l/d$ (l is the cylinders length and d is the gap size) and temperature gradient, this base flow can destabilize to an oscillatory axisymmetric instability, known as hydrodynamic or thermal modes, depending on the diffusion properties of the fluid [1]. Chandra and Smylie [2] performed an experiment where they applied an alternative high voltage between the two cylinders and showed a significant increase of the heat transfer when the voltage reached a critical value. Futterer et al. [3] also reported this increase of the Nusselt number, as well as the perturbation of the velocity field which has been measured by Particle Image Velocimetry (PIV) technique. Recently [4, 5], linear stability analysis and numerical simulations showed that, under Earth's gravity environment, the base flow destabilize to stationary columnar vortices. For the present experiment, the shadowgraph method is used to visualize the density variation in the radial-azimuthal directions, and the PIV technique is used to visualize the flow in the radial-axial directions. In addition, numerical simulations have been performed by Gerstner in our cooperative project [7]. The columnar structure of the flow has been validated by the accurate matching of the flow patterns observed experimentally and numerically (figure 1). The stationary columnar vortices are trapped between the top and bottom recirculation zone. This effect is accompanied by the increase of the heat transfer.

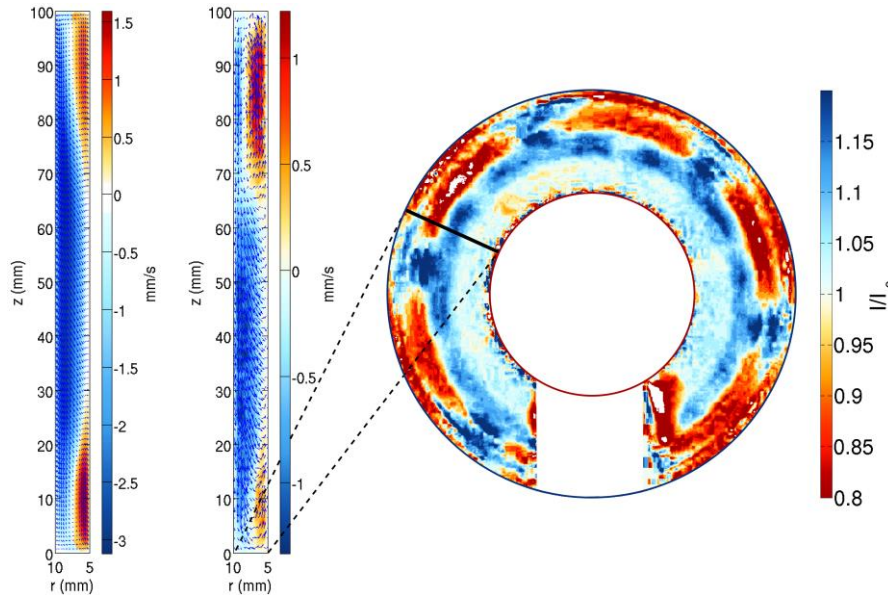


Figure 1: Composition of (a) PIV (left - numerical simulation, middle - experiment) and shadowgraph measurement (right - experiment) of the flow in the cavity with aspect ratio $\Gamma = 20$ caused by a temperature gradient $\Delta T = 7$ K ($Ra = 23946$) and electric potential $V_0 = 7$ kV ($L = 15220$). The black solid line refers to the plane used for the PIV measurement. (b) Shadowgraph measurement (left) and 3D temperature distribution from numerical simulation (right) of the flow with $\Delta T = 2$ K ($Ra = 6842$), electric potential $V_0 = 6$ kV ($L = 3173$).

A stability diagram has been built using the latest experimental ($\Gamma = [20, 60]$) and theoretical ($\Gamma \rightarrow \infty$) results (figure 2). A good agreement between both stability thresholds is found until a certain temperature gradient.

Aktuelle Forschungsschwerpunkte / Current research topics

Above this limit the experimental threshold exhibits a larger critical electric potential. This stabilizing effect is related to the top and bottom thermal boundary layers. This phenomenon is identified by the criterion given by Lopez et al. [6] which indicates if the base temperature profile cannot be identified as the one from the conductive state anymore. For large temperature gradients and electric potentials, the columnar columns become oscillatory, and could be compared with the vacillation observed in [5].

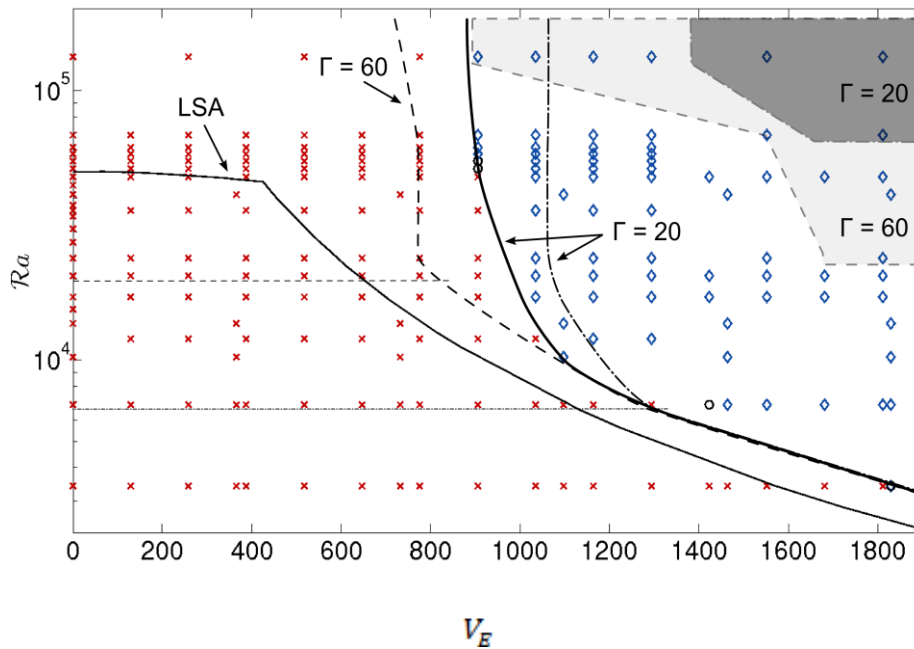


Figure 2: Regime diagram spanned by V_E and Ra . The symbols indicate Shadowgraph experiments with $\Gamma = 20$. Red crosses, blue diamonds and black circles stand for unicellular flow, stationary or oscillatory columnar vortices and indifferent flow, respectively. The thin solid line shows the stability diagram obtained by linear stability analysis ($\Gamma = \infty$, Meyer et al. 2017). The thick solid line and the dash-dot line are the experimental transition line for $\Gamma = 20$ and for the Shadowgraph and PIV measurements, respectively. The dashed line is the experimental transition line for $\Gamma = 60$ (PIV). The light and dark gray regions indicate regions where oscillatory modes have been observed for $\Gamma = 60$ and $\Gamma = 20$, respectively. The two horizontal lines indicate the Lopez et al. criterion for the transition from conductive to convective regime of the unicellular flow for $\Gamma = 20$ (dash-dotted line: $Ra=6587$) and for $\Gamma = 60$ (dashed line: $Ra = 19630$).

Bibliography:

- [1] Bahloul, A., Mutabazi, I., Ambari, A. (2000). *Codimension 2 points in the flow inside a cylindrical annulus with a radial temperature gradient*. Eur. Phys. J. AP, 9, 253- 264.
- [2] Chandra, B. and Smylie, D. E. (1972). *A laboratory model of thermal convection under a central force field*. Geophysical Fluid Dynamics, 3, 211- 224.
- [3] Futterer, B., Dahley, B., Egbers, C. (2016). *Thermal electro-hydrodynamic heat transfer augmentation in vertical annuli by the use of dielectrophoretic forces through a.c. electric field*. Int. J. Heat Mass Trans.
- [4] Meyer, A., Jongmanns, M., Meier, M., Egbers, C., Mutabazi, I. (2017). *Thermal convection in a cylindrical annulus under a combined effect of the radial and vertical gravity*. C. R. Mec., 345, 11-20.
- [5] Kang, C., Mutabazi, I. (2019). *Dielectrophoretic buoyancy and heat transfer in a dielectric liquid contained in a cylindrical annular cavity*. J. Appl. Phys., 125, 184902.
- [6] Lopez, J., Marquez, F., Avila, M. (2015). *Conductive and convective heat transfer in fluid flows between differentially heated and rotating cylinders*. Int. J. Heat Mass Transfer, 90, 959-967
- [7] Seelig, T., Meyer, A., Gerstner, P., Meier, M., Jongmanns, M., Baumann, M., Heuveline, V., Egbers, C., (2019). *Dielectrophoretic force-driven convection in annular geometry under Earth's gravity*, International Journal of Heat and Mass Transfer, 139, 386-398.

Aktuelle Forschungsschwerpunkte / Current research topics

B Fluid Mechanics

B7 Einfluss grundlegender Parameter eines Sprühstrahles auf die Beschichtungsqualität Vasyl Motuz, Christoph Egbers (AiF Projekt ZF4479201LT7)

Einführung

Der Ausgangspunkt des laufenden AiF Projektes ZF4479201LT7 ist die Entwicklung eines neuen innovativen Beschichtungssystemes für Lötstopplack auf Leiterplatten. Die vordergründigen Ziele des Projektes sind höhere Produktionskapazität sowie eine wesentliche Verbesserung des Lacknutzungsgrades im Vergleich zu den von Kooperationspartner I.T.C. Intercircuit Production GmbH früher entwickelten Beschichtungsanlagen.

Je gleichmäßiger die Größe der Lacktropfen in einem Sprühstrahl und je bessere deren Verteilung über den zur Strahlrichtung senkrechten Querschnitt ist, desto besser wird die Beschichtungsqualität bei der Lackierung von Leiterplatten. In einem Lacksprühstrahl befinden sich Lacktropfen verschiedener Größe. Das Vorhanden der großer Partikel im Strahl beeinflusst die die Qualität der Beschichtung sehr stark. Durch das Variieren verschiedener Parameter der experimentellen Anlage ist es möglich, nicht nur die Verteilung der Tropfen nach deren Größe zu steuern, sondern auch die Form und Querschnittgröße des Sprühstrahles zu kontrollieren.

Zu diesem Thema wird am Lehrstuhl für Aerodynamik und Strömungslehre (LAS) mit Hilfe vorhandener optischen Strömungsmessverfahren die Strömung von Lackpartikeln sowie eine optimale Tropfengröße in einem Sprühstrahl direkt nach der Zerstäubung ermittelt. Die Erkenntnisse über die Strömung von Lackpartikeln des Sprühstrahles und mögliche Strukturen in der Strömung lassen die Parameter des Lacks und der Beschichtungsanlage so optimieren, dass die Qualität der Plattenbeschichtung bestmöglich wird.

Experimentelle Ergebnisse

Um die Strömung von Lacktropfen in einem Sprühstrahl zu untersuchen wurde zunächst am LAS die von unserem Kooperationspartner I.T.C. Intercircuit Production GmbH entwickelte und gefertigte experimentelle Beschichtungsanlage so nachgerüstet, dass sie den Einsatz aller geplanten Strömungsmesstechniken ermöglicht. Die Nachrüstung betraf sowohl den inneren als auch den äußeren Teil der Beschichtungsanlage (Siehe Abbildung 1, links).

Die Eigenschaften der Lackpartikelströmung und infolgedessen die Beschichtungsqualität hängen stark von Eigenschaften des Lacks ab, nämlich von deren Viskosität und der Temperatur als auch von den Parameter der Beschichtungsanlage wie Lack-, Atom- und Fandruck. Darüber hinaus sollten geometrische Parameter und Einstellungen des Sprühkopfes berücksichtigt werden.

Zur Untersuchung der Lackpartikelströmung wurde ein PIV-Messsystem mit einer Hochgeschwindigkeitskamera eingesetzt. In Abbildung 1 ist auf der rechten Seite ein 2D-Strömungsfeld des Sprühstrahls eines kommerziellen Sprühstrahl-Kopfes für X-Komponente der Strömungsgeschwindigkeit dargestellt.

In Abbildung 2 sind die Entstehung und die Entwicklung eines Sprühstrahles bzw. eine typische Strömung von Lackpartikeln während eines 500 μ s dauerndes „Lackschusses“ in dem Raum zwischen Sprühkopf und der beschichtenden Oberfläche zu sehen. Da die Auswahl der Aufnahmen aus Messdaten des Hochgeschwindigkeit-PIV-Messsystems – zwar chronologisch - jedoch zufällig war, geht es hierbei nicht um regelmäßige Aufnahmen.

Aktuelle Forschungsschwerpunkte / Current research topics

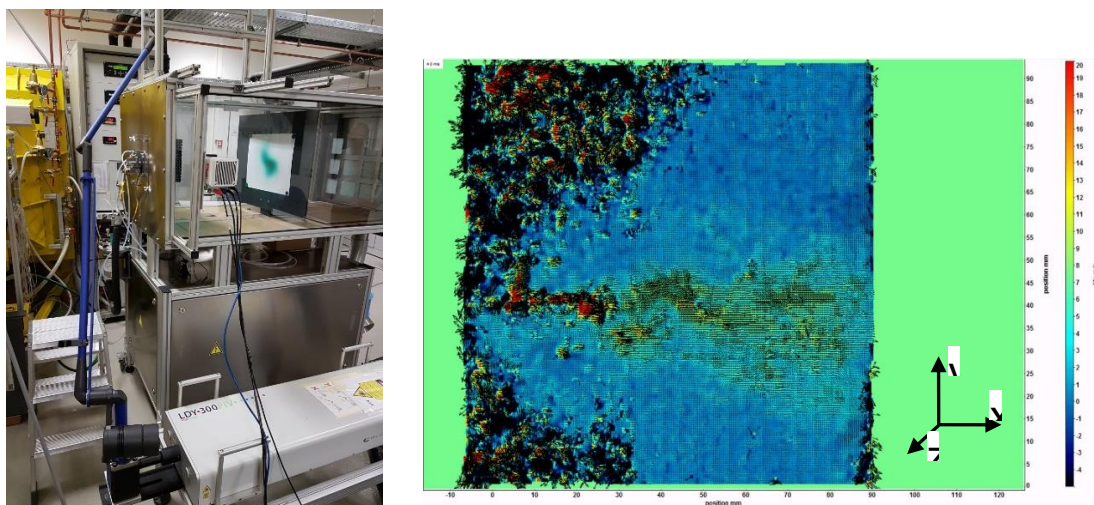


Abbildung 1. Links: Beschichtungsanlage mit gekoppeltem Hochgeschwindigkeits-PIV-Strömungsmesssystem für einen Experiment zur Untersuchung der Partikelströmung eines Sprühstrahls. Rechts: 2D-Strömungsfeld des Sprühstrahls (X-Komponente der Strömungsgeschwindigkeit) eines kommerziellen Sprühstrahl-Kopfes.

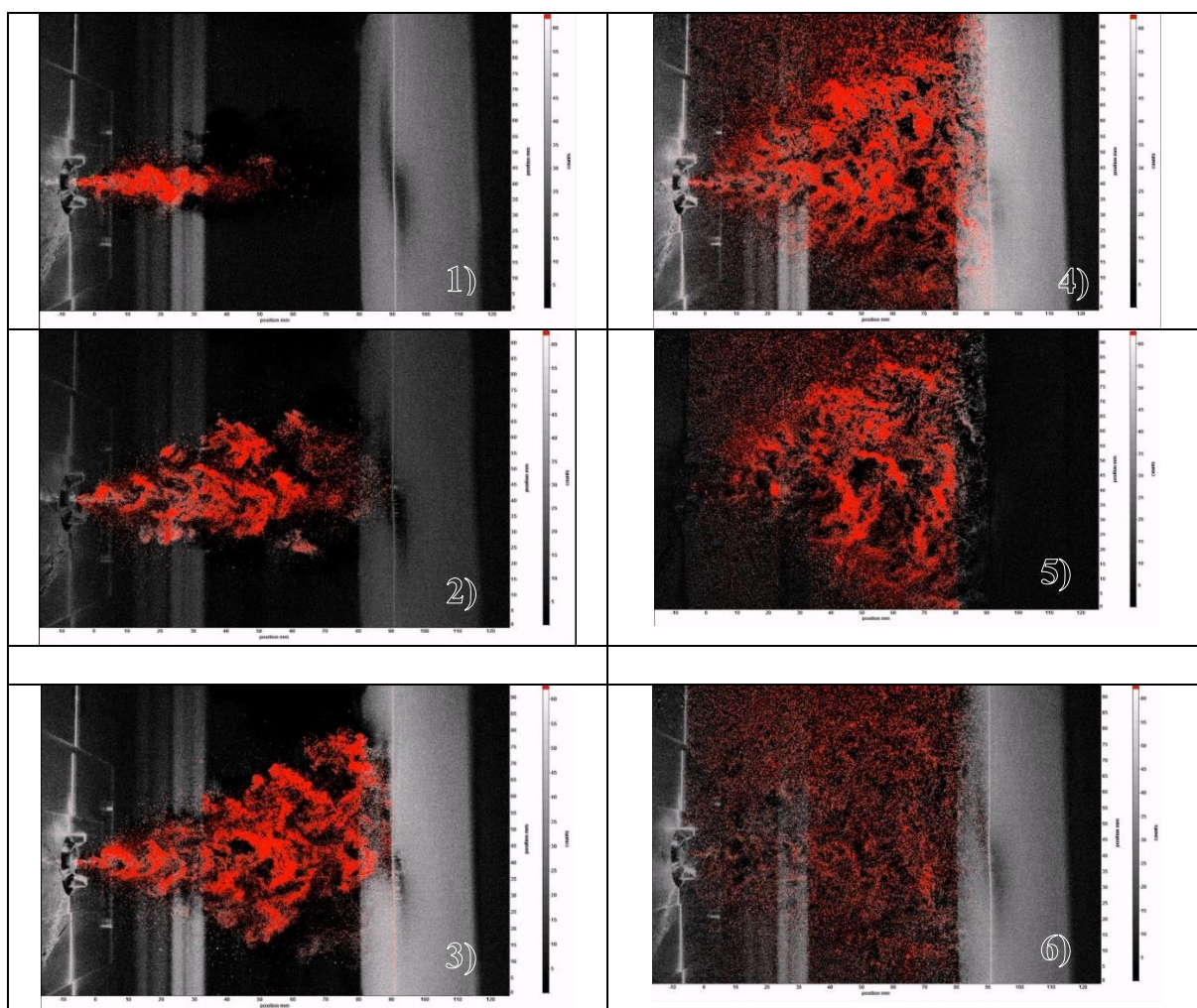


Abbildung 2. Eine typische Strömung von Partikeln im Lackstrahl während und kurz nach einem 500 ms „Lackschuss“ in dem Raum zwischen Sprühkopf und der beschichteten Wand. Hier sind in der Zeit nicht regelmäßige Aufnahmen abgebildet.

Aktuelle Forschungsschwerpunkte / Current research topics

B Fluid Mechanics

B8 Numerische und experimentelle Untersuchungen der Strömung in hydrostatischen Gleitlagern

M. Böhle, TU Kaiserslautern, Lehrstuhl für Strömungsmechanik und Strömungsmaschinen,
J. Hussong, Ruhr-Universität Bochum, AG Lasermesstechnik der Mehrphasenströmungen,
P. Reinke, HAWK, Fakultät Naturwissenschaften und Technik, Lehrgebiet Fluidtechnik,
Ch. Egbers & F. Zaussinger, BTU, Lehrstuhl Aerodynamik & Strömungslehre

Die hydrostatische Gleitlagerung ist für moderne Maschinenkonzepte wie z.B. für Wärmepumpen und Turbinen, die mit CO₂ oder Wasser als Arbeitsmedium sowie bei hohen Drehzahlen arbeiten, von bedeutender Wichtigkeit für die Weiterentwicklung der Technologie, z.B. im Hinblick auf die Energiewende. Insbesondere ist die Gleitlagerströmung mit erhöhtem Kavitationsrisiko bei hohen Drehzahlen und hohen Schmiermitteldurchsätzen noch nicht ausreichend erforscht, so dass eine Dimensionierung solcher Lager nur unzureichend möglich ist. Offene Fragestellungen sind hier die Kavitationsdynamik zwischen eng benachbarten Wänden, der Einfluss verstärkter auftretender Kavitation bei hohen Drehzahlen, sowie das Potential für den Einsatz poröser Lagerschalenmaterialien bei kavitierenden Gleitlagerströmungen.

Für diesen Gruppenantrag haben vier Forschungsstellen ihre jeweiligen Kompetenzen gebündelt, um die nicht kavitierende und kavitierende Spaltströmung in einem laminare und turbulente Strömungen umfassenden Reynoldszahlenbereich experimentell und numerisch auf skalenübergreifenden Detaillierungsgraden zu untersuchen. Ziel ist es, durch detaillierte Versuche und eine erweiterte 3D-Modellierung der Mehrphasenströmung ein tieferes Verständnis der Strömung in hydrostatischen Gleitlagern zu gewinnen und die numerisch und experimentell ermittelten Datensätze zur Verbesserung bestehender Auslegungswerkzeuge einzusetzen.

Ziel der Untersuchungen der Kavitation in Wandnähe ist die detaillierte Betrachtung des Blasenzerfalls zwischen eng benachbarten Wänden bei verschiedenen Wandabständen, Drücken, Temperaturen, Fluiden und unter dem Einfluss von Gaskeimen. Hierfür steht der AG Lasermesstechnik der Mehrphasenströmungen in Bochum eine Blasenkommer zur Verfügung, welche die experimentelle Analyse des Zerfalls von Einzelblasen unter kontrollierten Bedingungen ermöglicht. Dieser Prozess wird an der BTU (LAS) mit einer numerischen Simulation begleitet, die auf dem HLRN Berlin umgesetzt werden soll. Die berechneten lokalen Größen werden auf globale Kavitationsgebiete extrapoliert und für eine bedarfsgerechtere Auslegung von Gleitlagern verwendet. Ziel detaillierter experimenteller und numerischer Untersuchungen der Kavitation bei hohen Drehzahlen und Schmiermitteldurchsätzen ist es, durch zeitliche Kopplung des Reynolds-Modells (TU Kaiserslautern, SAM) und des 3D-Substrukturmodells (HAWK Göttingen, LFT) ein neues effizientes Berechnungswerkzeug bereitzustellen, mit welchem Kavitation in kritischen Lagerbereichen mit hoher Auflösung simuliert werden kann. Experimente am LFT validieren der berechneten Werte für Strömungsfeld und Dampfphase unter verschiedenen Betriebsbedingungen. Die Ergebnisse umfassen Position und Größenverteilung der Kavitationsblasen in der Gleitlagerströmung.

Ziel detaillierter experimenteller und numerischer Untersuchungen ist die Verbesserung des am SAM entwickelten Reynolds-Modells zur Auslegung von hydrostatischen Gleitlagern. Dieses Modell soll um eine Berechnung der Temperaturverteilung im Schmierstoff erweitert und dabei die Interaktion zwischen Temperaturverteilung und Viskosität bei der Modellierung berücksichtigt werden. Es sollen dynamische Steifigkeiten und Dämpfungen berechnet und das Modell für poröse Gleitlager verfeinert werden. Messungen am Modell-Gleitlager auf dem SAM-Gleitlagerprüfstand und im Gleitlager-Modellexperiment validieren die theoretischen Modellierungsergebnisse.

B Fluid Mechanics

B9 Investigation on particle banding and segregation of suspensions in laminar and centrifugally stable Taylor-Couette flows

J. Hussong, Ruhr-Universität Bochum, AG Lasermesstechnik der Mehrphasenströmungen,
Ch. Egbers & S. Merbold, BTU, Lehrstuhl Aerodynamik & Strömungslehre

Particle banding of suspensions refers to the formation of band-shaped particle clouds along horizontally aligned rotating drum or annular gap flows. Particle banding is not imposed by the flow field, but is a self-induced mechanism that takes place in laminar and centrifugally stable flows. Even though the phenomenon is well-known, its origin and the role of gravity, particle and flow characteristics inducing stationary or alternating particle bands is still little understood. It was studied to date mainly in confined parameter ranges for drum flows. In the present study we aim to investigate particle banding and segregation of suspensions in laminar and centrifugally stable Taylor-Couette (TC) flows over a parameter range extending that of previous studies. Compared to drum flows, TC flows cover different flow modes, including drum flow states through co-rotating TC cylinders. To gain a detailed picture of different particle banding modes, the role of different particle and flow characteristics as well as gravity, seeding densities and the effect of polydispersity shall be investigated over a large parameter range in a joint work effort of research group Hussong and Egbers. For this, experiments in dedicated TC set-ups of both research groups will be performed covering together thirteen orders of magnitude in Archimedes number (Ar) and approximately nine orders of magnitude in shear Reynolds number (Re_s). While, Ar will be varied at constant Re_s through different particle sizes or relative particle densities, an increasing Re_s at constant Ar will be verified through changes in rotation rate and radius ratio of the annular TC gap. Result data shall be used to formulate empirical scaling characteristics capable of predicting the occurrence of particle banding and switching between different particle banding modes. In test studies, stationary particle bands could be observed to depart from their initial condition for increasing tilting angles of the TC rotation axis. Furthermore, the particle concentration seems to affect time scales of particle band formation. These effects shall be studied in different TC facilities that allow to conveniently vary gravity orientation and particle concentrations. In test studies, particle segregation effect could be observed for the first time in classical Taylor-Couette flow. Systematic parameter studies aim to explore the parameter range in which both particle banding and particle segregation occur in bi- or tridispers suspensions of either different particle sizes, densities or particle shapes and if both phenomena occur simultaneously or consecutively. In the present study combined A-PTV/Micro-PIV or PTV/PIV measurements will be utilized to reveal both microstructural characteristics of the suspension and details of the flow field such as particle concentration distributions and relative velocities particles-fluid velocities.

Aktuelle Forschungsschwerpunkte / Current research topics

C Space Research

C1 Thermal electrohydrodynamic (TEHD) convection in a cylindrical gap

M. Meier, A. Meyer, M. Jongmanns, T. Seelig, Ch. Egbers (DLR 50WM1644)

Our experiments focus on the investigation of thermal convection in a dielectric liquid inside an annular cavity under the influence of a superimposed electric force field. This dielectrophoretic (DEP) - force is produced by means of a high voltage a.c. electric field directed to the central axis of the inner cylinder. The earth's unidirectional gravity inhibits these experiments under terrestrial conditions. Therefore, the experiment is performed under microgravity conditions where we expect new and different convection patterns. Microgravity experiments allow us to investigate flow fields and to determine characteristic flow patterns. In alternating current (a.c.) electric fields of high frequency $f \gg 1/\tau_e$, with τ_e as the charge relaxation time, the dielectrophoretic force is dominant. In our work, we study the dielectrophoretic effect as heat transfer augmentation force via the performance of an a.c. electric field superposing natural convection in the vertical annulus experimentally [3 -19].

Subsequently, we performed parabolic flight campaigns (PFCs) supported by the German Aerospace Center DLR, "14th DLR PFC" (September 2009; Testflight), "16th DLR PFC" (November 2010), "19th DLR PFC" (February 2012), 22nd DLR PFC (April 2013), 25th DLR PFC (October 2014), 31st DLR PFC (September 2017), 34th DLR PFC (March 2018) and also three PFC (118th, 134th and 139th) supported by Centre Nationale d'Études Spatiales (CNES) as a cooperative project with LOMC, Normandie University, Le Havre, France in October 2015, 2016 and 2018. Generally, we could demonstrate (see e.g. [13, 14]) that the dielectrophoretic force can induce an "electric buoyancy" in microgravity. This is visible through a rapid growth of a thermoelectric instability, analog to the classical Rayleigh-Bénard instability, during microgravity conditions. Beside heat transfer measurements over the gap, Particle Image Velocimetry (PIV), Synthetic Schlieren and Shadowgraph techniques have been the visualization methods in up-to-now 10 PFCs, of which one PFC was dedicated to a new experimental series with a rectangular cavity. The application of the dielectrophoretic force under low-g and 1-g conditions showed that the flow becomes unstable when the electric tension is sufficiently large. The shape of the unstable regimes depends on the aspect ratio of the cylindrical annulus, on the gravitational condition and on the set of control parameters. Under low-g conditions, the preferred critical mode is mainly helical, at least for low to moderate temperature differences between the two cylinders. Both gravitational levels have been studied through a linear stability theory [1, 4] as well as through numerical simulations [2, 9, 18] and exhibit a qualitatively good agreement with our experimental results. However, the threshold for the occurrence of instabilities is at larger electric potential in the experiments. The top and bottom boundaries stabilize the flow, and it is clear that for sufficiently large temperature differences, the Boussinesq approximation is no more valid.

Till 2016 our investigations on TEHD have been a part of the GeoFlow-project, but, since 3 years two dedicated research-projects have been running in our department: "Untersuchungen zur thermischen Konvektion im konzentrischen Spalt mit elektrischem Zentralkraftfeld unter verminderter Schwerkraft (KIKS)" (BMWi/ DLR- Space Administration; FKZ 50WM1644) and a cooperative research project with the University of Heidelberg "Thermo-elektrohydrodynamisch (TEHD) getriebene Wärmetransporterhöhung im vertikalen Zylinderspalt - Experimente und numerische Simulation im Kontext von Messunsicherheiten und optimaler Versuchsplanung" (DFG EG 100/20-1). The KIKS-project has a successor - the project „TEKUS - Thermoelektrische Konvektion unter Schwerelosigkeit“, which started 2019, 1st of April.

Aktuelle Forschungsschwerpunkte / Current research topics

Bibliography:

- [1] Yoshikawa, H., Crumeyrolle, O., Mutabazi, I. (2013). Dielectrophoretic force-driven thermal convection in annular geometry. *Phys. Fluids*, 25, 024106-0214120.
- [2] Travnikov, V. Crumeyrolle, O., Mutabazi, I. (2015). Numerical investigation of the heat transfer in cylindrical annulus with a dielectric fluid under microgravity. *Phys. Fluids*, 27, 054103.
- [3] Futterer, B., Yoshikawa, H., Mutabazi, I., Egbers, C. (2013): *Facilities to alter weight - Electric Fields. In: Generation on Earth an extra-terrestrial environment*, Eds: Daniel Beysens, Jack van Loon, River Publisher.
- [4] Meyer, A., Jongmanns, M., Meier, M., Egbers, C., Mutabazi, I. (2017). Thermal convection in a cylindrical annulus under a combined effect of the radial and vertical gravity, *C. R. Mecanique* 345, 11–20
- [5] Meyer, A., Crumeyrolle, O., Mutabazi, I., Meier, M., Jongmanns, M., Ruoff, V., Seelig, T., Egbers, C. (2017). Flow pattern and heat transfer in a cylindrical annulus under 1g and low-g conditions: Theory and simulation, Joint Conference ISPS-7 and ELGRA-25 October, 2-6 2017, Juan-les-Pins, France
- [6] Meier, M., Jongmanns, M., Ruoff, V., Seelig, T., Egbers, C., Meyer, A., Mutabazi, I. (2017). Flow pattern and heat transfer in a cylindrical annulus under 1g and low-g conditions: Experiments, Joint Conference ISPS-7 and ELGRA-25 October, 2-6 2017, Juan-les-Pins, France
- [7] Mutabazi, I., Kang, C., Meyer, A., Meier, M., Egbers, C. (2017). Thermal convection in dielectric liquids in a cylindrical annulus, 70th Annual Meeting of the APS Division of Fluid Dynamics, November 19–21, 2017, Denver, Colorado,
- [8] Jongmanns, M., Meyer, A., Meier, M., Kang, C., Mutabazi, I., Egbers, C. (2018). Experiments on thermoelectric convection in dielectric liquids in a cylindrical annulus under parabolic flight conditions, International Conference on Rayleigh Bénard Turbulence, May 14-18, 2018, Enschede, NL
- [9] Mutabazi, I., Kang, C., Meyer, A., Jongmanns, M., Meier, M., Egbers, C. Thermoelectric convection in dielectric liquids in a cylindrical annulus under parabolic flight conditions, International Conference on Rayleigh Bénard Turbulence, May 14-18, 2018, Enschede, NL
- [10] Meyer, A., Jongmanns, M., Meier, M., Seelig, T., Kang, C., Mutabazi, I., Egbers, C. (2018). Experiments on thermoelectric convection induced in a cylindrical annulus under microgravity conditions, 20th International Couette-Taylor Workshop, 11-13 July 2018, Marseille, France
- [11] Seelig, T., Jongmanns, M., Meyer, A., Meier, M., Egbers, C. (2018). Onset of dielectrophoretic force-driven convection in annular geometry under Earth's gravity, 20th International Couette-Taylor Workshop, 11-13 July 2018, Marseille, France
- [12] Ostmann, V. (2018). Planning and construction of a modular experimental cell for the investigation of a thermal electro hydrodynamic convection in a rectangular cavity, MSc-Thesis, BTU Cottbus-Senftenberg
- [13] Meyer, A., Crumeyrolle, O., Mutabazi, I., Meier, M., Jongmanns, M., Renoult, M.-C., Seelig, T., Egbers, C. (2018). Flow Patterns and Heat Transfer in a Cylindrical Annulus under 1g and low-g Conditions: Theory and Simulation, *Microgravity Sci. Technol.* 30, 653–662, DOI: 10.1007/s12217-018-9636-3
- [14] Meier, M., Jongmanns, M., Meyer, A., Seelig, T., Egbers, C., Mutabazi, I. (2018). Flow pattern and heat transfer in a cylindrical annulus under 1g and low-g conditions: Experiments, *Microgravity Sci. Technol.* 30, 699-712, DOI 10.1007/s12217-018-9649-y
- [15] Jongmanns, M., Meier, M., Meyer, A., Egbers, C. (2018). Bestimmung von Strömungsmustern in einem Zylinderspalt mit radialem elektrischen Kraftfeld unter Schwerelosigkeit, 26. GALA - Fachtagung Experimentelle Strömungsmechanik, 4. - 6. September 2018, Rostock
- [16] Meier, M., Jongmanns, M., Meyer, A., Seelig, T., Egbers, C., Mutabazi, I. (2018). Enhanced heat transfer in a cylindrical annulus under 1g and low-g conditions, 69th International Astronautical Congress (IAC), Bremen, Germany, 1-5 October 2018.
- [17] Meyer, A., Kang C., Jongmanns, M., Yoshikawa, H., Meier, M., Egbers, C., Mutabazi, I. (2017). Convection thermique dans une liquid diélectrique confine dans un anneau cylindrique chauffé de l'intérieur et sous tension électrique alternative. XIIIème Colloque Interuniversitaire Franco-Québécois sur la Thermique des Systèmes (CIFQ) 22-24 mai 2017, Saint-Lô, France
- [18] Seelig, T., Meyer, A., Gerstner, P., Meier, M., Jongmanns, M., Baumann, M., Heuveline, V., Egbers, C., (2019). “Dielectrophoretic force-driven convection in annular geometry under Earth’s gravity”, *International Journal of Heat and Mass Transfer*, 139, 386-398.
- [19] Jongmanns, M. (2019). Flow control of thermal convection using thermo electro hydrodynamic forces in a cylindrical annulus, Dissertation, BTU Cottbus-Senftenberg

C Space Research

C2 Project KIKS – Thermal convection in parabolic flight conditions

M. Meier, M. Jongmanns, A. Meyer, M. Helbig (DLR FKZ 50WM1644)

Within the KIKS-Project, we study the influence of the dielectrophoretic (DEP) in microgravity conditions. Theoretical and numerical research showed a strong analogy between the effect of the electric gravity resulting from the DEP force and the Earth gravity concerning the occurrence of thermal instability [1-4]. Beside laboratory investigations we performed 4 parabolic flight campaigns (PFC) within the KIKS-project; one of them with a rectangular cavity-experiment set-up. PFCs give the opportunity to perform short-time microgravity experiments at gravity levels of about 10^{-2} g. In Europe, scientific PFCs can be executed with the “Zero-g”- Airbus of Novespace, located at the Airport of Bordeaux/ Mérignac. There exist several other ways to obtain microgravity conditions (e.g. drop tower or suborbital rocket flight), but the main advantage of the parabolic flight is the good balance between the duration of the microgravity phase (about 22s), the quite large allowable size of the experiment module, and the opportunity for investigators to be onboard the aircraft during the flight. For these experiments, the control parameters are the temperature difference ΔT and the alternating high voltage V_0 applied between the two cylinders or plates. The dimensionless form of these parameters are the thermoelectric parameter $\gamma_e = e\Delta T$ and the dimensionless electric potential $V_E = V_0/\sqrt{\rho\nu\kappa/\varepsilon}$, where e is the coefficient of thermal variation of the permittivity ε of a dielectric fluid with density ρ , kinematic viscosity ν and thermal conductivity κ .

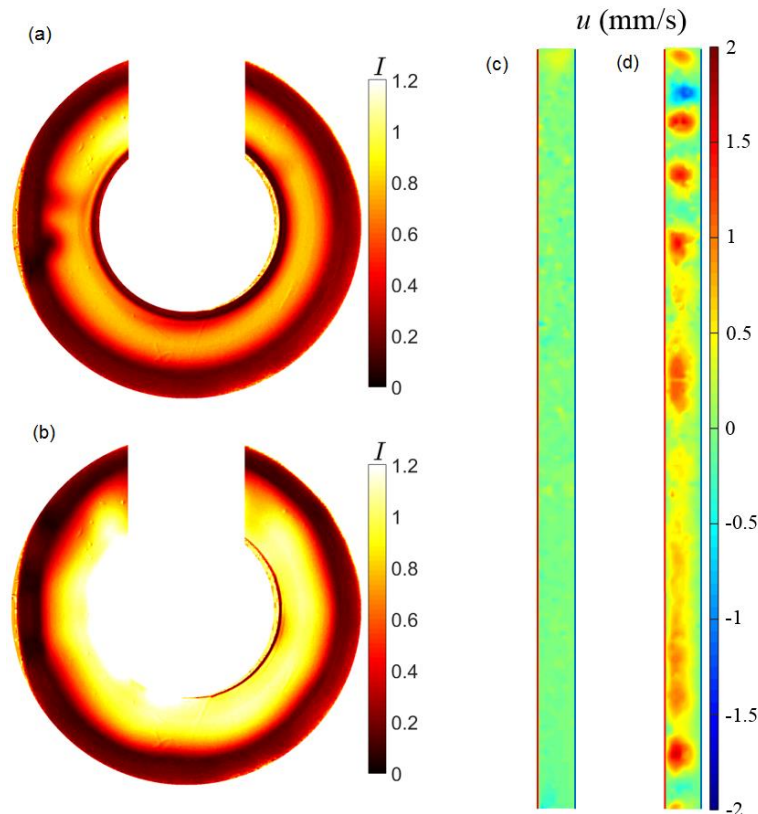


Figure 1: Shadowgraph image at (a) the initial time and (b) the final time of the microgravity phase for $\Delta T = 10$ K and $V_0 = 5$ kV. Radial velocity profiles at (c) the initial time and (d) the final time of the microgravity phase for $\Delta T = 16$ K and $V_0 = 5.7$ kV. For these two parabolas, the voltage was applied only during microgravity conditions.

Aktuelle Forschungsschwerpunkte / Current research topics

During the PF campaign, we use two different methods, which are used separately, to visualize the flow. The first one is the Shadowgraph technique. For that method, the cylindrical annulus is illuminated from the bottom to the top with a source producing light parallel to the cylinder axis. The light intensity, initially homogeneous, is modified because of optical index variation due to temperature perturbations. The light intensity profile at the top of the cell is captured by a camera and compared with a reference profile. The second method is the particle image velocimetry (PIV), performed in a plan parallel to the vertical axis, and which provides the 2-dimensional velocity field. Figure 1 shows the results from these two methods, one picture at the first moment of the microgravity phase, the other at the last moment of the same phase. From these pictures, it is possible to determine the flow stability and to build the stability diagram shown in figure 2. The experimental threshold for convective motion in microgravity conditions qualitatively follows the theoretical one. The difference observed between these studies can be explain by the invalidity of the Boussinesq approximation, or the finite length of the cylinders. But one important reason remains the too short duration of the microgravity phases to obtain an established unstable flow.

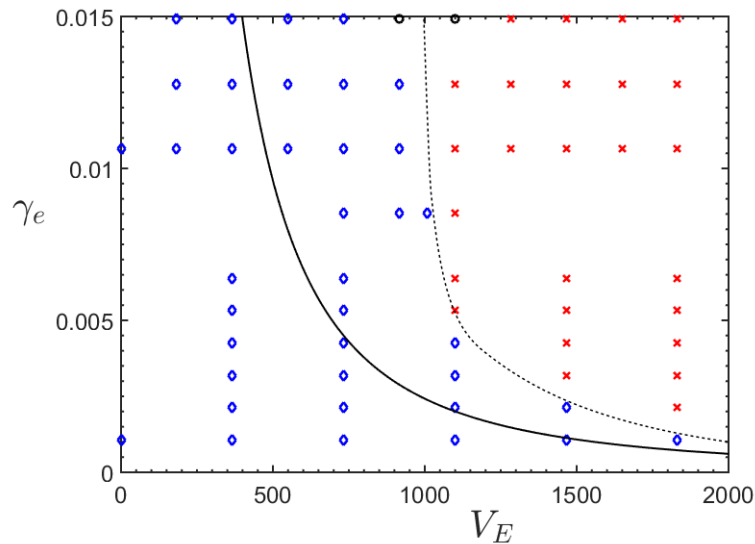


Figure 2: Stability diagram spanned by V_E and γ_e . This stability diagram is concerned with the application of the DEP force on a cylindrical annulus under microgravity conditions. The continuous line shows the threshold between the stable state (bellow) and the unstable state (above) calculated by a linear stability theory [1] for cylinders of infinite length. The blue diamonds and the red crosses correspond to experimental determination of the flow after 22s of microgravity: stable and unstable, respectively. The dashed line represents the experimental threshold between stable and unstable flows.

References

- [1] Yoshikawa, H., Crumeyrolle, O., Mutabazi, I. (2013) Dielectrophoretic force-driven thermal convection in annular geometry. *Phys. Fluids*, 25, 024106-24120.
- [2] Yoshikawa, H. N., Tadie Fogaing, M., Crumeyrolle, O., Mutabazi, I. (2013). Dielectrophoretic Rayleigh-Bénard convection under microgravity conditions. *Phys. Rev. E*, 87, 043003.
- [3] Travnikov, V. Crumeyrolle, O., Mutabazi, I. (2015). Numerical investigation of the heat transfer in cylindrical annulus with a dielectric fluid under microgravity. *Phys. Fluids*, 27, 054103.
- [4] Meyer, A., Jongmanns, M., Meier, M., Egbers, C., Mutabazi, I. (2017) Thermal convection in a cylindrical annulus under a combined effect of the radial and vertical gravity, *C. R. Mecanique* 345, 11–20
- [5] Meyer, A., Crumeyrolle, O., Mutabazi, I., Meier, M., Jongmanns, M., Renoult, M.-C., Seelig, T., Egbers, C. (2018). Flow Patterns and Heat Transfer in a Cylindrical Annulus under 1g and low-g Conditions: Theory and Simulation, *Microgravity Sci. Technol.* 30, 653–662, DOI: 10.1007/s12217-018-9636-3
- [6] Meier, M., Jongmanns, M., Meyer, A., Seelig, T., Egbers, C., Mutabazi, I. (2018). Flow pattern and heat transfer in a cylindrical annulus under 1g and low-g conditions: Experiments, *Microgravity Sci. Technol.* 30, 699-712, DOI 10.1007/s12217-018-9649-y

C Space Research

C3 Project KIKS – Thermal convection in parabolic flight conditions with rectangular cavities

A. Meyer, M. Meier, V. Ostmann, C. Egbers (DLR FKZ 50WM1644)

For our last parabolic flight campaign (CNES, 139th, Sept./ Oct. 2018), we investigated the effect of the dielectrophoretic force in a rectangular cavity. In that case, the considered fluid need a low viscosity and/or a large permittivity. Indeed, the electric gravity in a plane cavity is quiet small compared to that in a cylindrical cavity since the curvature plays an important role for the non-homogeneity of the electric field (figure 1). The selected fluids for this experiment are 1-Nonanol and Novec 7200 (3M). Under microgravity conditions, theoretical and numerical investigations carried out by Yoshikawa et al. [1] and Tadie Fogaing et al. [2] showed the increase of the heat transport in the rectangular cavity, as well as the important feedback effect of the perturbation electric gravity in this configuration. Because of this last point, it is known that the critical electric Rayleigh number is larger than that of the classical Rayleigh-Bénard problem ($Ra = 1708$), i.e. $L = 2128$. Modular experiment cells have been designed and constructed in our department [3]. The gap between the two TCO-coated plates has a length of max. 200 mm, a width of max. 40 mm and a depth of e.g. 3, 5 or 10 mm. The gap depth, width and length can be varied by using different inserts. The Synthetic Schlieren technique is used to visualize the density variations. The gap is illuminated from one side of the rectangular cavity by an LED panel with telecentric light parallel to the gap direction. The lightened area is therefore $(x \times y) = (40 \times 50) \text{ mm}^2$. A surface with black dots randomly distributed is placed directly at the LED panel. A camera is placed on the other side of the rectangular cavity and captures the dot pattern displacement with respect to a reference image, which is taken as the image of the dot pattern when no temperature gradient and no high voltage are applied. The divergence of the displacement field highlight the regions where the light beams have converged (diverged) while passing through a cold (warm) front. In these experiments, the high voltage is applied only during microgravity conditions, but we considered two different configurations in order to change the initial conditions at which the voltage is applied. The first configuration is the Rayleigh-Bénard one with a stable stratification. The horizontal plate is heated from the top and cooled from the bottom. This configuration ensures that there is no flow due to the previous gravity phases of the parabolic flight when the high voltage is applied.

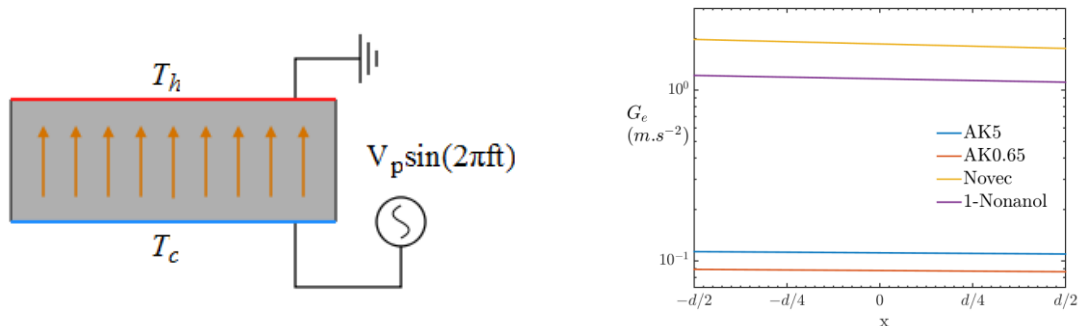


Figure 1: Schematic representation of the rectangular cavity (left) and electric gravity as function of the distance between the two plates for a gap of $d = 5 \text{ mm}$ and for various fluids.

Aktuelle Forschungsschwerpunkte / Current research topics

The second configuration corresponds to a vertical cavity. In that case there is a base convective flow during the previous gravity phase which does not have time to dissipate before the activation of high voltage. The best results has been obtained for the horizontal cavity filled with Novec 7200. In that case the Synthetic Schlieren technique enabled us to observe the occurrence of thermal convection due to the thermo-electric force. In figure 2 are shown different profiles of the divergence of the pattern displacement field captured at the end of the microgravity phase. We can see that no density variation is observed for $V_p < 2$ kV. At $V_p = 2$ kV an instability is visible through the periodic change of sign of the displacement field divergence. This can be directly related to hot and cold jets occurring because of the onset of instability. For $V_p = 3$ and 5 kV, the signal is more turbulent and instationary. It is not yet clear if a real turbulent flow has been captured, or if the algorithm used to post treat the Synthetic Schlieren images failed because of a too large concentration of dots on the background pattern. This last point will be investigated in a near future, in preparation of the next parabolic flight campaign involving the rectangular cavity.

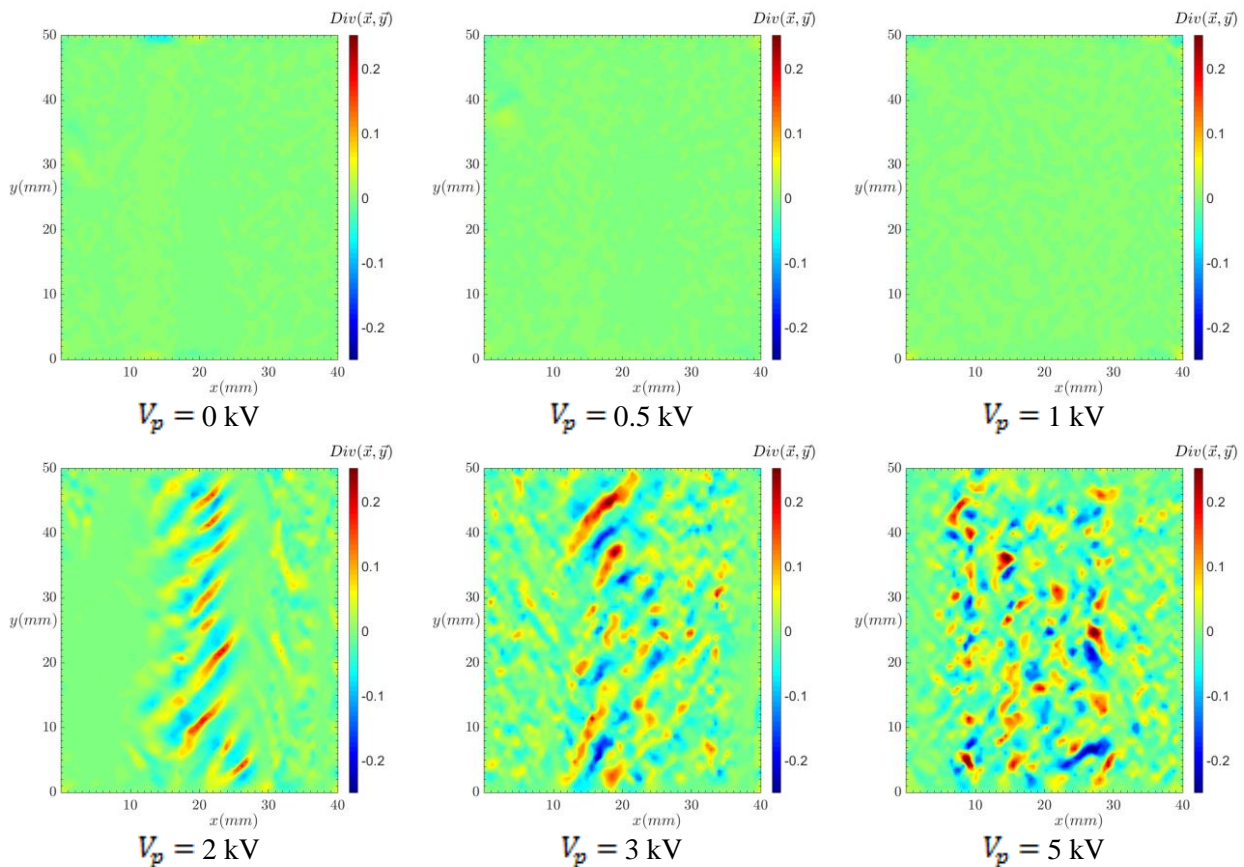


Figure 2: Profile of the divergence of the dot pattern displacement field in the horizontal cell with $\Delta T = 7$ K with a gap size of 5 mm. All the pictures, obtained for different peak voltage V_p are taken at the end of the microgravity phase.

References

- [1] Yoshikawa, H. N., Tadie Fogaing, M., Crumeyrolle, O., Mutabazi, I. (2013). *Dielectrophoretic Rayleigh-Bénard convection under microgravity conditions*. Phys. Rev. E, vol. 87, 043003.
- [2] Tadie Fogaing, M., Yoshikawa, H. N., Crumeyrolle, O., Mutabazi, I. (2014). *Heat transfer in the thermo-electro-hydrodynamic convection under microgravity conditions*. Eur. Phys. J. E, vol. 37, pp. 35-40
- [3] Ostmann, V. (2018). *Planning and construction of a modular experimental cell for the investigation of a thermal electro hydrodynamic convection in a rectangular cavity*, MSc-Thesis, BTU Cottbus-Senftenberg

Aktuelle Forschungsschwerpunkte / Current research topics

C Space Research

C4 Project TEKUS - Thermal convection under weightlessness

Martin Meier, Antoine Meyer, Christoph Egbers (DLR FKZ: 50WM1944)

The application of the dielectrophoretic force under low-g and 1g conditions showed that the flow becomes unstable when the electric tension is sufficiently large. The shape of the unstable regimes depends on the aspect ratio of the cylindrical annulus, on the gravitational condition and on the set of control parameters. Under low-g conditions, the preferred critical mode is mainly helical, at least for low to moderate temperature differences between the two cylinders.

Both gravitational levels have been studied through a linear stability theory [1, 2] as well as through numerical simulations [3] and exhibit a qualitatively good agreement with our experimental results. However, the threshold for the occurrence of instabilities is at larger electric potential in the experiments. The top and bottom boundaries stabilize the flow, and it is clear that for sufficiently large temperature differences, the Boussinesq approximation is no more valid. Theoretical researches have considered microgravity conditions in order to focus on the DEP force, but laboratory experiments have to involve the Earth's gravity effect, which is modifying the stability conditions of the system [4]. Theoretical and numerical research presents an analogy between both convective modes (see 1, 5, 6 and 7)). Sitte [8] verified the DEP-induced buoyancy effect by laboratory and parabolic flight experiments. New 3-D numerical simulations have been performed by Travnikov, Kang, and Gerstner [9, 10, 11]. Using PIV and Shadowgraph methods, it has been found that, under Earth's gravity condition, the first unstable regime takes the form of stationary columnar counter-rotating vortices. A stability diagram spanned by the thermal Rayleigh number and the dimensionless electric potential has been built experimentally and compared to results from a linear stability analysis, see [11]. For a set of given control parameters, the experimental measurements of velocity and temperature have been compared to numerical simulations and showed a good qualitative agreement. Indeed the columnar structure has been confirmed experimentally, numerically and theoretically and could be explained by simultaneous effects of the axial Earth gravity and the radial electric gravity. The low gravity phase provided by the parabolic flights lasts about 22s, which is too short to establish a fully developed thermoelectric instability in our experimental parameter range. But, it has been possible to detect the growth of perturbations which allowed us to build a stability diagram, to characterize the geometry of the flow, and to compare the growth rates of perturbations between Earth's gravity and weightlessness environment (see [12,13]).

Consequently, we are now preparing a sounding rocket flight experiment - foreseen for the TEXUS 57 campaign in 2021. For this experimental set-up, we developed a combination of Shadowgraph and PIV-techniques, which we apply simultaneously for each experiment cell. Figure 1 gives an example for the processed flow field images of the cylindrical gap for natural and DEP-forced convection under earth conditions. The combination of the two measurement techniques allows the simultaneous visualization of the flow pattern in vertical (integrated over the height) and meridional direction.

By using the TEXUS-rocket with 6 minutes of microgravity time we will be able to determine the flow stability, the mode shape and the corresponding heat transfer in our TEHD-experiments with much higher accuracy than in parabolic flights.

Aktuelle Forschungsschwerpunkte / Current research topics

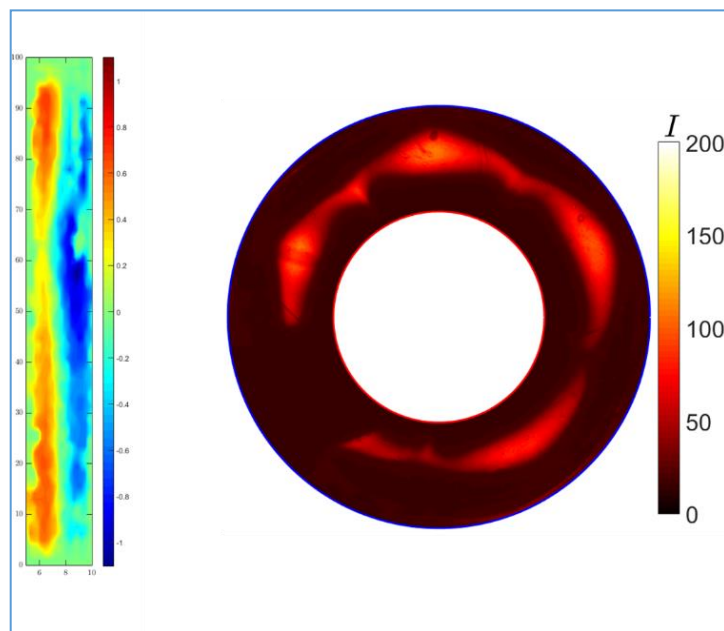


Fig. 1: Simultaneous measurement of the flow field inside the cylindrical gap. Experiment parameters: $\Delta T=2K$, $T_0=25^\circ C$, $1g$. Natural convection with basic flow. Left picture from PIV-analysis; right picture Shadowgraph image.

Bibliography:

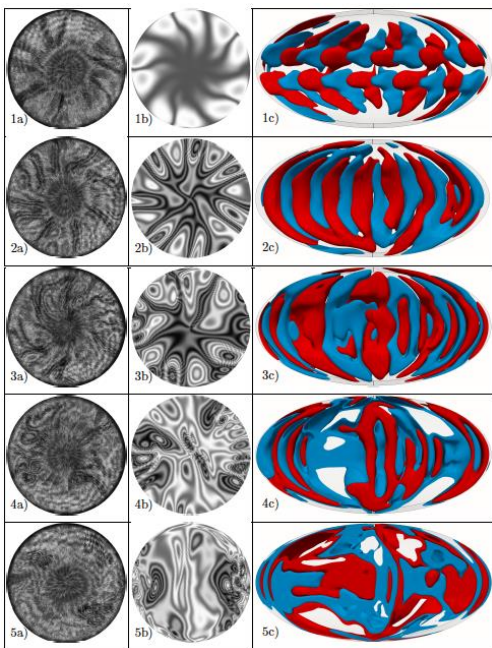
- [1] Yoshikawa, H., Crumeyrolle, O., Mutabazi, I. (2013). Dielectrophoretic force-driven thermal convection in annular geometry. *Phys. Fluids*, 25, 024106-0214120.
- [2] Meyer, A., Jongmanns, M., Meier, M., Egbers, C., Mutabazi, I. (2017). Thermal convection in a cylindrical annulus under a combined effect of the radial and vertical gravity, *C. R. Mec.* 345, 11–20
- [3] Travnikov, V. Crumeyrolle, O., Mutabazi, I. (2015). Numerical investigation of the heat transfer in cylindrical annulus with a dielectric fluid under microgravity. *Phys. Fluids*, vol. 27, 054103.
- [4] Takashima, M. (1979). Electrohydrodynamic instability in a dielectric fluid between two coaxial cylinders, *Mech. appl. Math.* 33, 93-103.
- [5] Chandra, B., Smylie, D. E. (1972). A laboratory model of thermal convection under a central force field. *Geophysical Fluid Dynamics*, 3, 211- 224.
- [6] Malik, S., Yoshikawa, H.N., Crumeyrolle, O., Mutabazi, I. (2012). Thermo-electro-hydrodynamic instabilities in a dielectric liquid under microgravity. *Acta Astronautica* 81, 563-569.
- [7] Yoshikawa, H. N., Tadie Fogaing, M., Crumeyrolle, O., Mutabazi, I. (2013). Dielectrophoretic Rayleigh-Bénard convection under microgravity conditions. *Phys. Rev. E*, 87, 043003.
- [8] Sitte, B., Rath, H. J. (2003). Influence of the dielectrophoretic force on thermal convection. *Exp. Fluids* vol. 34, 24-27
- [9] Travnikov, V., Crumeyrolle, O., Mutabazi, I. (2015). Numerical investigation of the heat transfer in cylindrical annulus with a dielectric fluid under microgravity. *Phys. Fluids*, 27, 054103.
- [10] Kang, C., Mutabazi, I. (2019). Dielectrophoretic buoyancy and heat transfer in a dielectric liquid contained in a cylindrical annular cavity, *J. App. Phys.* 125, doi.10.1063/1.5086980.
- [11] Seelig, T., Meyer, A., Gerstner, P., Meier, M., Jongmanns, M., Baumann, M., Heuveline, V., Egbers, C., (2019). Dielectrophoretic force-driven convection in annular geometry under Earth's gravity", *Intern. J. of Heat and Mass Transfer*, 139, 386-398.
- [12] Meier M., Jongmanns, M. Meyer, A., Seelig, T., Egbers, C., Mutabazi, I. (2018). Flow pattern and heat transfer in a cylindrical annulus under 1g and low-g conditions: Experiments, *Microgravity Sci. Tech.* 30, 699-712.
- [13] Meyer, A., Crumeyrolle, O., Mutabazi, I., Meier, M., Jongmanns, M., Renoult, M.-C., Seelig, T., Egbers, C. (2018). Flow Patterns and Heat Transfer in a Cylindrical Annulus under 1-g and low-g Conditions: Theory and Simulation, *Microgravity Sci. Technol.* 30, 653–662.

C Space Research

C5 Dielectrical heating in the spherical gap geometry (Geoflow IIb,c)
 F. Zaussinger, P. Haun, V. Travnikov, Ch. Egbers (DLR FKZ: 50WM1644)

Introduction

Dielectric heating occurs in situations where an alternating electric field is applied on an insulating dielectric material. This effect can produce thermal convection through the thermo-electric coupling by the dielectrophoretic (DEP) force. The onset and the flow properties of the thermal convection are investigated in a spherical gap geometry. We assume microgravity to highlight the effects of the dielectric heating. The thermo-electro hydrodynamical equations often adopted in the modeling of the DEP-force-driven thermal convection are extended by an additional source term arising from the dielectric heating in the energy equation. Three-dimensional direct numerical simulations are performed, assuming microgravity and without any imposed temperature gradient to highlight the effects of dielectric heating. In the conduction state, dielectric heating creates a parabola-shaped mean temperature profile with a maximum in the interior of the spherical gap. In the convective state, the temperature distribution is more homogeneous with a lower maximum temperature. Numerical results are compared with interferograms from the GeoFlow II experiment on the ISS to validate the model. These interferograms are obtained by a Wollaston shearing interferometry which measures first derivatives of the fluid’s refractive index. These derivatives are identified as temperature derivate through nearly identical slopes. The interferograms show two typical patterns: first, double ring structures which originate from local thermal plumes. Second, parallel lines of fringes which are caused by sheet-like structures. The onset of convection as well as basic spatial properties of the resulting internally heated convective zone are in good agreement with the experiment. The computed velocity field reveals strong downdrafts which lead to recognizable fringe patterns in the interferograms.



Comparison of experiment and simulation

Two scenarios are investigated in the spherical gap geometry, namely the non-rotating case and the rotating case with Ekman numbers of about $Ek=10^{-3}$. Fig. 1 depicts such a comparison, where experimental interferograms are compared with numerical interferograms und full 3D simulations. The center is the north pole and the circle is the equator. Convective structures are highlighted by burning. (middle column) numerical interferograms, (right column) Hammer projection of numerical simulations, where red volumes depict positive temperature variations and blue volumes negative temperature variations with respect to the mean temperature field. The fluid flow shows a strong dependence on internal heating. While Proudman-Taylor theorem is valid for low internal heating, it is assumed that high internal heating processes violates it.

Figure 1: Comparison of experimental interferograms (left), numerical interferograms (middle) and 3D simulation for increasing internal heating. Hereby, 1a-c has low internal heating and 5a-c has strong internal heating.

The governing equations of thermo EHD, incorporating the static electric field, are solved numerically with the finite volume method (FVM) using the open source software suite OpenFOAM. A cubed sphere grid is used for all simulations. The velocity boundary conditions are kept no-slip. The thermal boundaries are of Dirichlet type, say constant temperatures. The code solves the equations dimensionally in 3D with the PISO algorithm. Time integration is performed with an implicit Crank-Nicolson method. The space derivatives are approximated in second order. Numerical simulations are validated on the onset of convection. Fig. 2 depicts selected experimental points near the onset in the Ek-Ra-plane. The temperature is measured with an accuracy of 0.04K, which results in an error of 10% in case of a temperature difference of 0.4K. This gives an error in the Rayleigh number likewise, see error bars Fig. 2. Conduction is separated from convection by the critical Rayleigh number. The top row of Fig. 2a shows a convective unstable case with $Ra=786$. Fig. 2b shows the corresponding conductive case. This coincide well with linear stability analysis, which predicts the critical Rayleigh numbers in between. This holds for all four Ekman numbers and for the slow rotating case of $Ek=1$ (not shown).

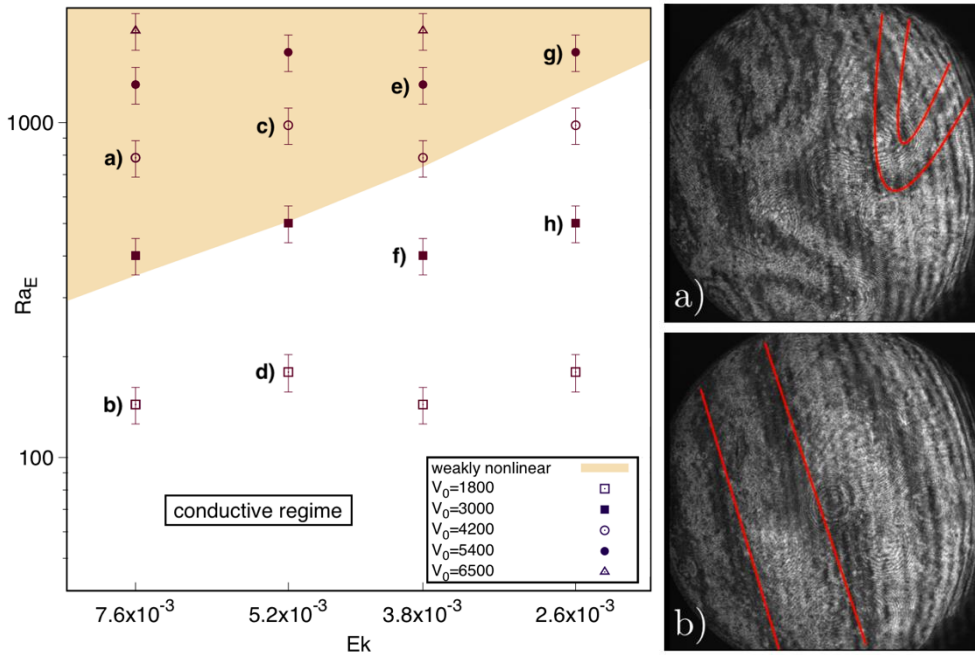


Figure 2: (left) Ekman-Rayleigh phase-space diagram of various experimental points of the GeoFlow experiment. (right) Transition from the conductive to the convective regime visible in the interferograms.

Bibliography:

- [1] F. Zaussinger, P. Haun, M. Neben, T. Seelig, V. Travnikov, Ch. Egbers, H. Yoshikawa, and I. Mutabazi. Dielectrically driven convection in spherical gap geometry. *Phys. Rev. Fluids*, 3:093501 (2018).
- [2] F. Zaussinger, A. Krebs, V. Travnikov, and C. Egbers. Recognition and tracking of convective flow patterns using Wollaston shearing interferometry. *Advances in Space Research*, 60(6):1327 – 1344 (2017).
- [3] V. Travnikov, F. Zaussinger, P. Beltrame, and C. Egbers. Influence of the temperature-dependent viscosity on convective flow in the radial force field. *Physical Review E*, 96(2), (2017).
- [4] F. Zaussinger, P. Haun, V. Travnikov, M. Al Kawwas, Ch. Egbers, Experimental investigation of convection in the internally and boundary heated rotating spherical gap, submitted to *Phys Rev. Fluids* (2019)

C Space Research

C6 AtmoFlow - Numerical investigation of the convective flows in the atmosphere

F. Zaussinger, P. Haun, A. Froitzheim, V. Travnikov, M. Meier, A. Meyer, Ch. Egbers
(DLR-FKZ: 50WM1841)

Introduction

In a first approximation planetary atmospheres are confined fluid layers between two spherical shells. Hence, the fluid flow is determined by the boundaries of the system, which are the inner and outer shell. The inner shell represents the planetary surface or deep, blocking atmospheric layers of e.g. gas giants. The outer shell represents the upper boundary of the climate-relevant atmosphere or, in case of the gas giant, a region, where the gas concentration decreases significantly. This simplified setup makes it possible to break some generic cases to test models, which can be investigated in laboratory experiments and numerical simulations. The main advantage of such an experiment is the reproducibility and the ability to resolve scales, which are parameterized by semi-empirical closure models.

Motivation

The proposed experiment AtmoFlow aims to observe flows in a thin spherical gap that are subjected to a central force-field. The inner and the outer boundaries will both be heated/cooled locally. Additionally, a differential rotating unit is foreseen, to simulate deep shells, as they occur in giant planets. Fig. 1a depicts such a simplified atmosphere, where incoming radiation and rotation lead to global cell formation. These cells (Hadley cell, Ferrel cell or mid-latitude cell, polar cell) are well known from the Earth and co-responsible for global atmospheric dynamics.

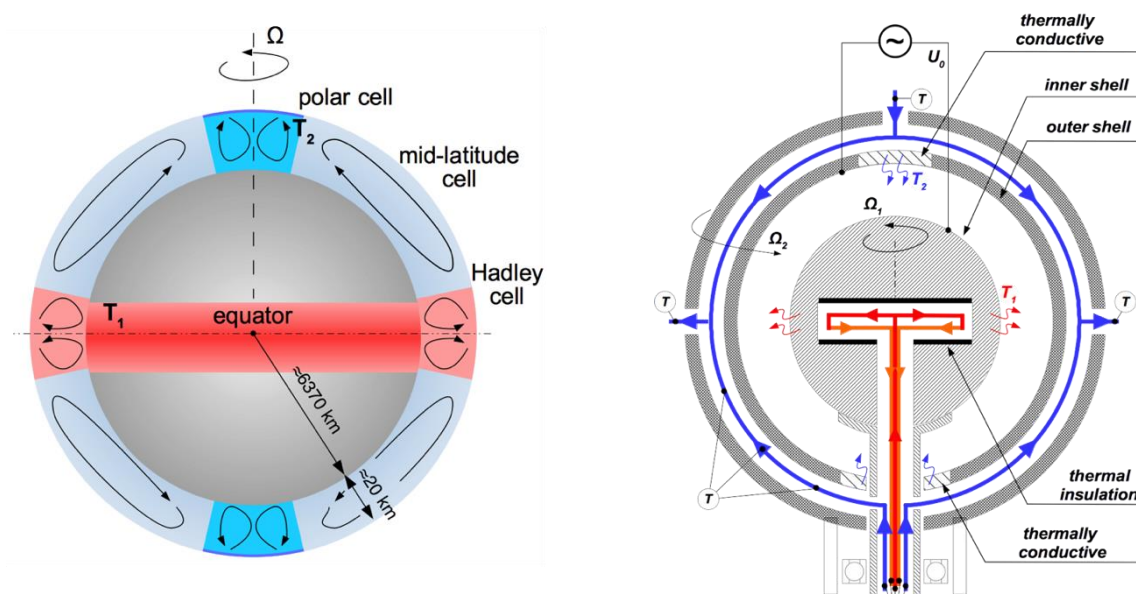


Fig. 1: (left) simplified planetary atmosphere as found on the Earth. Not to scale. (right) vertical cut through the AtmoFlow experiment. Blue lines depict the cooling loop, red lines show the heating circuit. Inner and outer rotation is labeled by Ω_1 and Ω_2 , respectively. The maximum temperature is found at the equator, the minimum temperature at the poles.

Aktuelle Forschungsschwerpunkte / Current research topics

Construction and description

The gap between the inner sphere and the outer sphere is filled with the test liquid 3M Novec 7200 and represents the region of interest for the acquisition of science data. Local temperature boundary conditions are imposed on the poles by cooling plates in the outer shell and at the equator of the inner shell. The mean temperature in the intermediate regions is obtained by a thermalization circuit. Fig. 1b depicts the temperature distribution at both shells in the sketch. Sensors are located throughout the fluid cell to monitor the temperatures of the thermalization zones and within the gap between the cooling shell and the outer sphere. The inner sphere and the outer sphere also function as the electrodes for alternating high voltage electrical field, which generates the dielectrophoretic force on the liquid in the spherical gap to simulate a planet's gravity.

Accompanying numerical simulations are performed for the AtmoFlow experiment. They are used to reconstruct the velocity field, which is not accessible by measurement techniques used in AtmoFlow. The reconstruction is based on a comparison of experimental and numerical interferograms. Matching structures in both interferograms correlate with similar temperature and velocity fields. Based on this assumption, the three-dimensional fluid flow gets accessible.

Fig. 2 shows a representative case of solid body rotation. The overall temperature distribution is dominated by broad up-welling and down-welling regions at the equator and the poles, respectively. However, in contrast to the non-rotating case only a few large vortices are visible. Local plumes are not found, except in the polar region. The equatorial region reveals a dominant planetary wave with mode $m=9$. This wave is visible in the velocity field, the Hammer-Aitoff projection and in the interferogram, too. Hence, this specific simulation can be used as benchmark test for the comparison between the numerical model and the experiment. The poles are characterized by cold fronts reaching deep into the mid-latitudes. These 'fingers' are not symmetrically arranged over both hemispheres, which emphasize the time-dependent and turbulent character of this fluid flow.

The AtmoFlow experiment payload is currently in development for operation on the ISS.

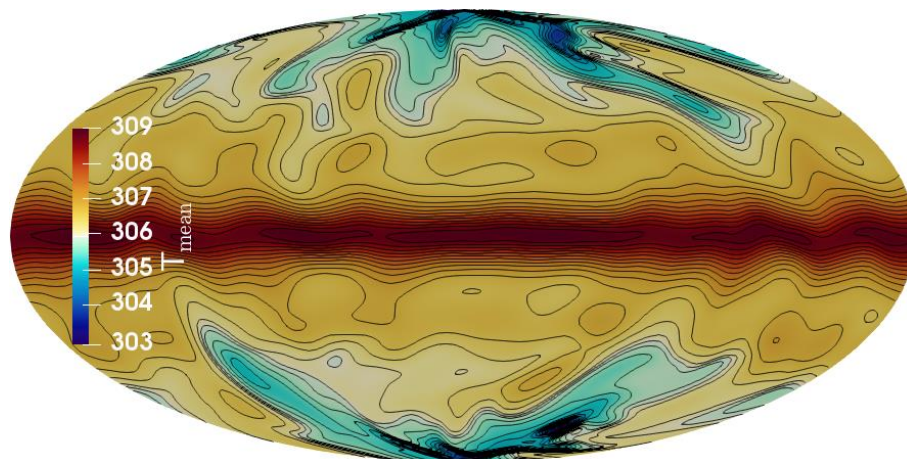


Fig. 2: Numerical simulations of the solid body rotation case at time stamp $t=2180s$ for $Ra=1.9 \times 10^6$ and $Ta=3.2 \times 10^6$.

Bibliography:

- [1] F. Zaussinger, P. Canfield, A. Froitzheim, V. Travnikov, P. Haun, M. Meier, A. Meyer, P. Heintzmann, T. Driebe, and C. Egbers. AtmoFlow - investigation of atmospheric-like fluid flows under microgravity conditions. *Microgravity Science and technology*, accepted, (2019).
- [2] F. Zaussinger, P. Canfield, T. Driebe, C. Egbers, P. Heintzmann, V. Travnikov, A. Froitzheim, P. Haun, and M. Meier. AtmoFlow - Simulating atmospheric flows on the International Space Station. Part II: Experiments and numerical simulations. In *69th IAC conference proceedings*, volume 18.A2.7.18-69. International Astronautical Federation, (2018).
- [3] P. Canfield, F. Zaussinger, C. Egbers, and P. Heintzmann. AtmoFlow - Simulating atmospheric flows on the International Space Station. Part I: Experiment and ISS-implementation concept. In *69th IAC conference proceedings*, volume 18.A2.6.15-69. International Astronautical Federation, (2018).

D Computer Technology

D1 High performance computing at the BTU - using the CFTM² support to scale your program to big data and to make it fast.

Andreas Krebs (CFTM²)

The activities of the Center for Flow and Transport Modelling and Measurement (CFTM²) can be characterized by three topics:

- (a) Consulting for numerical modelling with the focus on scientific computing and code parallelization, notably software libraries like LAPACK, ARPACK, ScaLAPACK, MPI, OpenMP, SuperLU,
- (b) Operation of a massive parallel computer located at the BTU,
- (c) Co-ordination of the HLRN activities at the BTU.

Ad (b): Operation of a massive parallel computer located at the BTU

As the old system heraklit with 32 compute nodes a 12 single thread cores started in January 2011, it is close to the end of its life-cycle. The CFTM² and the IT-Services analyzed the requirements of the BTU institutes using an opinion poll and deduced a call for tenders for a new heterogeneous HPC cluster. The new computer will cover the needs of three different user groups and will serve as a complement to the services offered by the HLRN (see (c)). The decision was taken in favor of the following combination of components:

- 1 compute node offers 1 TeraByte RAM with 2 * Intel Xeon Gold 6148 a 20 Cores. This node will allow for big CPLEX computations.
- 1 compute node provides two acceleration card (GPU). This node is a IBM Power AC922 with 2*POWER9 (16 cores) CPUs
- 2 NVidia Tesla V100 GPU connected by NVLink 2.0 with the CPU.
- This machine is complementary to the HLRN in the sense that GPU parallelization is available for the BTU staff.
- This parallelization is needed by the chair "Graphical systems". But also the fluid flow software OpenFOAM can benefit from GPU parallelization.
- 6 compute nodes allow for bigger MPI computations with up to 6*24 cores with 8 GigaByte/core RAM.
- 3 data nodes allow for parallel file I/O using IBM Spectrum Scale (cf. GPFS).
- The communication network operates with 20 GB/s. It is extensible so that the whole HPC cluster can be extended by further compute nodes.

The machine will be available to the BTU staff from July 2019 presumably.

Ad (c): Coordination of the HLRN activities at the BTU.

As the fundraising and the maintainance of a high performance computer exceeds the financial and the administrative potential of a single research institution and also of a single federal state, the North German states Berlin, Bremen, Hamburg, Mecklenburg-West Pomerania, Lower Saxony, and Schleswig-Holstein decided to manage supercomputing collectively in 2001 and founded the North-German Supercomputing Alliance (HLRN). The HLRN operates a distributed supercomputer system hosted at Konrad-Zuse-Zentrum for information technology Berlin (ZIB) and at the Gesellschaft für Datenverarbeitung Göttingen (GWDG).

The following projects got support in the frame of the abovely mentioned topics. The currency NPL (Norddeutsche Parallelrechner-Leistungseinheit) can be converted to Euro using the factor 0.26 Euro/NPL for the group of scientific users.

- Amir Shahipour, Andreas Krebs: Large scale structures in fully developed turbulent pipe flow (HLRN project no. bbi00011). The HLRN granted 750 kNPL for this project + 800 kNPL for its continuation of this project in 2018/2019.
- Florian Zaussinger: A very close look on white dwarfs II (HLRN project no. bbi00008). The HLRN granted 513 kNPL for the continuation of this project.
- Götz Seibold, Mattis Noell, Andreas Krebs: Excitations in disordered superconductors: Inclusion of long-range Coulomb interactions (HLRN project no. bbp00013). The HLRN granted 100 kNPL for this project.
- Markus Kober, Arnold Kühhorn: Transient implicit thermo-mechanical FEM simulations for extremely detailed models of airplane engines (HLRN project no. bbi00012). The HLRN granted 300 kNPL for this project + 200 kNPL for its continuation.

The following project prepared successfully a proposal using initial accounts at the HLRN. The HLRN provides 10 kNPL for a period of one year for the preparation phase.

- Uwe Harlander, Gabriel Meletti: Numerical Investigations on Stratified Rotational Instabilities (HLRN project no. bbi00013). The HLRN granted 275 kNPL for this project in 2019.

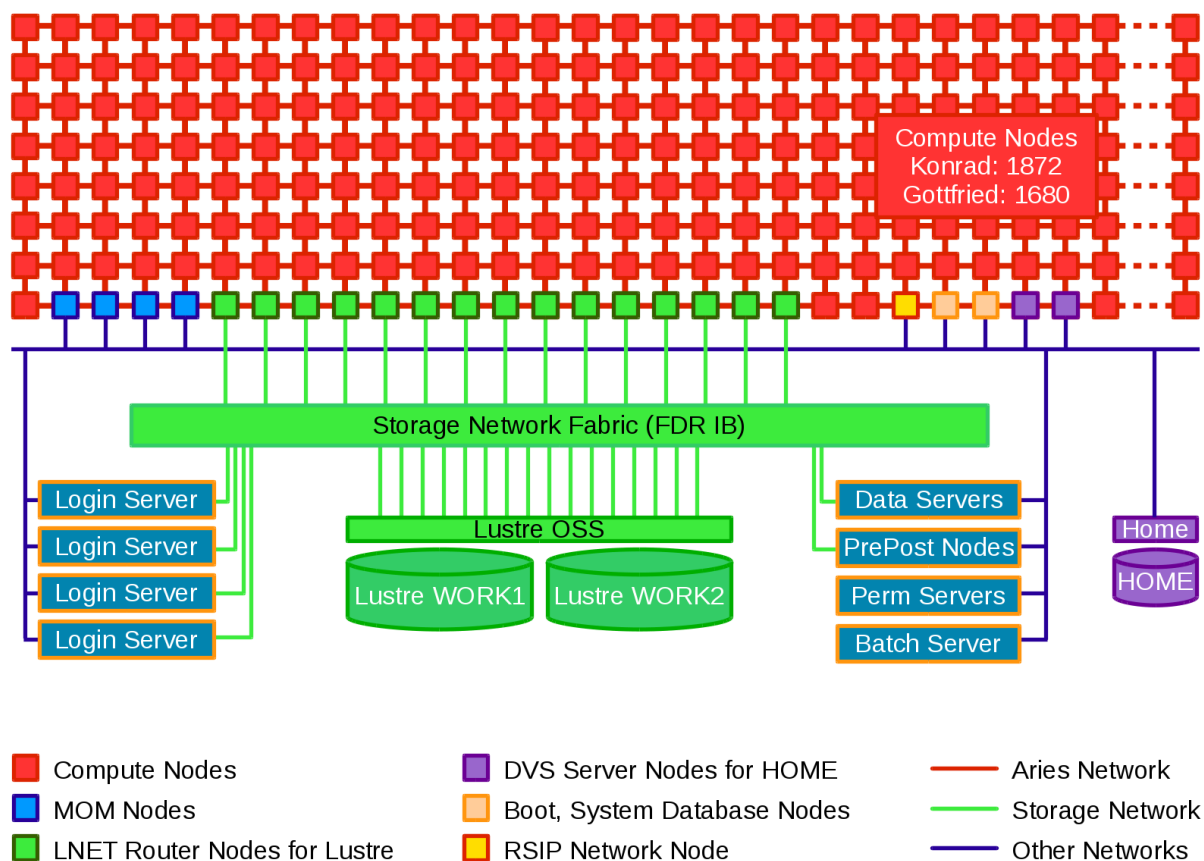


Figure 1: Node types and network overview of HLRN III HPC cluster, a Cray XC 30 (Image: Courtesy of HLRN and Cray)

Veröffentlichungen, Konferenzbeiträge und Vorträge/ Publications, contributions to conferences and invited lectures

Veröffentlichungen in reviewten Zeitschriften 2018/2019

Zanoun, E.-S., Öngüner, E., Shahirpour, A., Merbold, S., Egbers, Ch., 2018,
Spectral Analysis of Large Scale Structures in Fully Developed Turbulent Pipe Flow
PAMM. Proc. Appl. Math. Mech. **17**, 647-650, DOI 10.1002/pamm.201710293

Selvam, K., Öngüner, E., Peixinho, J., Zanoun, E.-S., Egbers, Ch., 2018,
Wall pressure in developing turbulent pipe flows
Journal of Fluids Engineering, **140(8)**, 081203 (2018)

Meier, M., Jongmanns, M., Meyer, A., Seelig, T., Egbers, Ch., Mutabazi, I., 2018,
Flow Pattern and Heat Transfer in a Cylindrical Annulus Under 1 g and Low-g Conditions:
Experiments.
Microgravity-Science and Technology, <https://doi.org/10.1007/s12217-018-9649-y>

Zaussinger, F., Haun, P., Neben, M., Seelig, T., Travnikov, V., Egbers, Ch., Yoshikawa, H.,
Mutabazi, I., 2018,
Dielectrically driven convection in spherical gap geometry.
Phys. Rev. Fluids **3**, 093501, <https://doi.org/10.1103/PhysRevFluids.3.093501>

Rodda, C., Bocia, I. D., Le Gal, P., Vincze, M., Harlander, U., 2018,
Baroclinic, Kelvin and inertia-gravity waves in the barostat instability experiment.
Geophysical & Astrophysical Fluid Dynamics, DOI10.1080/03091929.2018.1461858

Seelig, T., Gellert, M., Harlander, U., 2018,
Experimental investigation of stratorotational instability using a thermally stratified system:
instability, waves and associated momentum flux.
Geophysical & Astrophysical Fluid Dynamics, DOI10.1080/03091929.2018.1488971

Zaussinger, F., Kupka, F., Montgomery, M., Egbers, Ch., 2018,
Numerical simulation of DA white dwarf surface convection.
12th International Conference on Numerical Modeling of Space Plasma Flows: ASTRONUM-2017,
26–30 June 2017, Saint-Malo, France,
Journal of Physics: Conference Series, Volume 1031, conference 1, DOI: 10.1088/1742-
6596/1031/1/012013

Zaussinger, F, Haun, P., Neben, M., Seelig, T., Travnikov, V., Egbers, C., Yoshikawa, H., Mutabazi,
I., 2018,
Dielectrically driven convection in spherical gap geometry,
Physical Review Fluids **3**, 093501, American Physical Society, DOI: 10.1103/PhysRevFluids.3.
093501

Meyer, A., Crumeyrolle, O., Mutabazi, I., Meier, M., Jongmanns, M., Renoult, M.-C., Seelig, T.,
Egbers, C., 2018,
Flow Patterns and Heat Transfer in a Cylindrical Annulus under 1g and low-g Conditions: Theory
and Simulation, **Microgravity Science and Technology**, Springer,
ISSN: 0938-0108 (Print), 30 (2018) pp 653–662, DOI: 10.1007/s12217-018-9636-3

Veröffentlichungen, Konferenzbeiträge und Vorträge/ Publications, contributions to conferences and invited lectures

Veröffentlichungen in reviewten Zeitschriften 2018/2019

Nowak, T., Merbold, S., Egbers, Ch., Schacht, R., 2018,
Numerical Study with Experimental Validation of Thermal Coupling Phenomena with Flip-Chip
Assembled Test Dies on PCB, **IEEE Journal**, DOI: 10.1109/THERMINIC.2018.8593313, eISBN
978-1-5386-6759-0.

Zaussinger, F., 2018,
A dynamic beam model for the motility of *Listeria monocytogenes*.
Acta Mechanica, Vol. **229**, [Issue 12](#), pp 4927–4944, doi:10.1007/s00707-018-2277-1

U. Harlander, I.D. Borcia, A. Krebs. 2018,
Nonnormality increases variance of gravity waves trapped in a tilted box.
Geophys. & Astrophys. Fluid Dyn. DOI:10.1080/03091929.2018.1549660, 2018.

A. Ghasemi V, M. Klein, A. Will, and U. Harlander. 2018,
Mean flow generation by an intermittently unstable boundary layer over a sloping wall.
J. Fluid Mech., **853**, 111-149, 2018.

Th. v. Larcher, S. Viazzo, U. Harlander, M. Vincze, and A. Randriamampianina. 2018,
Instabilities and small-scale waves within the Stewartson layers of a thermally driven rotating
annulus.
J. Fluid Mech., **841**, 380-407, 2018.

Kupka, F., Zaussinger, F., Montgomery, M. H., 2018,
Mixing and overshooting in surface convection zones of DA white dwarfs: First results from
ANTARES.
Monthly Notices of the Royal Astronomical Society, Vol. **474**, Issue 4, 11 March 2018, Pages
4660–4671, <https://doi.org/10.1093/mnras/stx3119>

Seelig, T., Meyer, A., Gerstner, P., Meier, M., Jongmanns, M., Baumann, M., Heuveline, V., Egbers,
Ch., 2019,
Dielectrophoretic force-driven convection in annular geometry under Earth's gravity.
Int. J. Heat and Mass Transfer, Volume **139**, August 2019, Pages 386-398
<https://doi.org/10.1016/j.ijheatmasstransfer.2019.04.068>

Sesterhenn, J., Shahirpour, A., 2019,
A characteristic dynamic mode decomposition.
Theor. Comput. Fluid Dyn. pp 1–25, ISSN: 0935-4964, DOI: <https://doi.org/10.1007/s00162-019-00494-y>

Zanou, E.-S., Egbers, Ch., Örlp, R., Fiorini, T., Bellani, G. & Talamelli, A., 2019,
Experimental evaluation of the mean momentum and kinetic energy balance equations in turbulent
pipe flows at high Reynolds number.
J. Turbulence, <https://doi.org/10.1080/14685248.2019.1628968>

**Veröffentlichungen, Konferenzbeiträge und Vorträge/
Publications, contributions to conferences and invited lectures**

Veröffentlichungen in reviewten Zeitschriften 2018/2019

Froitzheim, A., Merbold, S., Ostilla-Mónico, R., Egbers, Ch., 2019
Angular momentum transport and flow organisation in Taylor-Couette flow at radius ratio of $\eta=0,357$,
Phys. Rev Fluids (submitted)

Froitzheim, A., Ezeta, R., Huisman, S., Merbold, S., Sun, Ch., Lohse, D., Egbers, Ch., 2019
Small-scale statistics of momentum transport and underlying flow structures in turbulent Taylor-Couette flow, **J. Fluid Mech.** (submitted)

**Veröffentlichungen, Konferenzbeiträge und Vorträge/
Publications, contributions to conferences and invited lectures**

Veröffentlichungen in Büchern 2018/2019

Öngüner, E.
Experiments in Pipe Flows at Transitional and Very High Reynolds Numbers
Dissertationsschrift BTU Cottbus-Senftenberg, **Cuvillier Verlag** Göttingen, 2018, ISBN-13-978-3-73699-783-7

Zanoun, E.-S., Öngüner, E., Egbers, C., Bellani, G., and Talamelli, A., 2019 “One-Dimensional Flow Spectra and Cumulative Energy from Two Pipe Facilities,” **Progress in Turbulence**, Springer (in press)

Veröffentlichungen, Konferenzbeiträge und Vorträge/ Publications, contributions to conferences and invited lectures

Veröffentlichungen in Tagungsbänden und Vorträge / Poster 2018/2019

Mutabazi, I., Kang, C., Meyer, A., Jongmanns, M., Meier, M., Egbers, Ch.
Thermoelectric convection in dielectric liquids in a cylindrical annulus under parabolic flight conditions
International Conference on Rayleigh Bénard Turbulence, May 14-18, 2018, Enschede, NL

Jongmanns, M., Meyer, A., Meier, M., Kang, C., Mutabazi, I., Egbers, Ch.
Experiments on thermoelectric convection in dielectric liquids in a cylindrical annulus under parabolic flight conditions
International Conference on Rayleigh Bénard Turbulence, May 14-18, 2018, Enschede, NL

Seelig, T., Jongmanns, M., Meyer, A., Meier, M., Egbers, Ch.
Onset of dielectrophoretic force-driven convection in annular geometry under Earth's gravity
20th International Couette-Taylor Workshop, 11-13 July 2018, Marseille, France

Meyer, A., Yoshikawa, H., Mutabazi, I., Egbers, Ch.
Effect of the dielectrophoretic force in a rigidly rotating cylindrical annulus
20th International Couette-Taylor Workshop, 11-13 July 2018, Marseille, France

Meyer, A., Jongmanns, M., Meier, M., Seelig, T., Kang, C., Mutabazi, I., Egbers, Ch.
Experiments on thermoelectric convection induced in a cylindrical annulus under microgravity conditions
20th International Couette-Taylor Workshop, 11-13 July 2018, Marseille, France

Egbers, C., Zaussinger, F., Haun, P., Canfield, P., Travnikov, V., Froitzheim, A., 2018,
Convection in the spherical gap under micro-gravity conditions: From Earth's mantle to atmospheric flows.
20th International Couette Taylor Workshop, July 11 - 13th, 2018 Marseille France

Rodda, C., Borcia, I. D., Hien, S., Achatz, U., Le Gal, P., Harlander, U.
Numerical and experimental study of inertia-gravity waves in the differentially heated rotating annulus
European Geosciences Union General Assembly 2018, Vienna, Austria, 8–13 April 2018

Hasanuzzaman, G., Merbold, S., Motuz, V., Egbers, Ch., Cuvier, C., Foucat, J-M
Experimental investigation of active control in turbulent boundary layer using uniform blowing
5th International Conference on Experimental Fluid Mechanics ICEFM 2018 Munich

Zanoun, E.-S., Motuz, Egbers, Ch., Keller, J., Dörner, K.
Stereoscopic-PIV and Hot Wire Measurements in Pipe Flow at Relatively High
5th International Conference on Experimental Fluid Mechanics ICEFM 2018 Munich

Merbold, S., Froitzheim, A., Egbers, Ch.
Torque in turbulent Taylor-Couette flow for small radius ratios
5th International Conference on Experimental Fluid Mechanics ICEFM 2018 Munich

Veröffentlichungen, Konferenzbeiträge und Vorträge/ Publications, contributions to conferences and invited lectures

Veröffentlichungen in Tagungsbänden und Vorträge / Poster 2018/2019

Froitzheim, A. Merbold, S., Egbers, Ch., Ezeta, R., Lohse, D., Sun, C.

Large scale vortices in the Taylor-Couette flow

12th European Fluid Mechanics Conference, September 7-9, 2018, Vienna

Shahirpour, A., Sesterhenn, J., Egbers, Ch.

A Characteristic Dynamic Mode Decomposition to capture large-scale coherent structures in fully developed turbulent pipe flow

12th European Fluid Mechanics Conference, September 7-9, 2018, Vienna

Zaussinger F., Haun P., Mutabazi I., Egbers Ch.

Dielectrically driven thermal convection

12th European Fluid Mechanics Conference, September 7-9, 2018, Vienna

Jongmanns, M., Meier, M. Meyer, A., Egbers, Ch.

Bestimmung von Strömungsmustern in einem Zylinderspalt mit radialem elektrischen Kraftfeld unter Schwerelosigkeit

26. GALA - Fachtagung Experimentelle Strömungsmechanik, 4. - 6. September 2018, Rostock, ISBN 978-3-9816764-5-7

Zaussinger F., Egbers, Ch., P., Heintzmann, P., Canfield, P.

ATMOFLOW - Simulating atmosphere flows on the international space station. Part I: Experiment and implementation concept

69th International Astronautical Congress, 1 - 5 October 2018, Bremen, Germany

Zaussinger F., Egbers, Ch., Driebe, T., Heintzmann, P., Canfield, P., Meier, M., Travnikow, V., Froitzheim A., Haun, P.

ATMOFLOW - Simulating atmosphere flows on the international space station. Part II: Experiments and numerical simulations

69th International Astronautical Congress, 1 - 5 October 2018, Bremen, Germany

Meier, M., Egbers, Ch, Mutabasi, I., Meyer, A., Seelig, T., Jongmanns, M.

Enhanced Heat transfer in a cylindrical annulus under 1g and low-g conditions

69th International Astronautical Congress, 1 - 5 October 2018, Bremen, Germany

Egbers, Ch.

Convection in a spherical gap under micro-gravity conditions: From Earth's mantle to atmospheric flow simulations

Wissenschaft auf der Internationalen Raumstation ISS, 29. - 31. Oktober 2018, **Wilhelm und Else Heraeus-Stiftung**, Physikzentrum Bad Honnef, Germany

Zanoun, E.-S., Öngüner, E., Egbers, Ch., Belani, G., Talamelli, A.

One-Dimensional Flow Spectra and Cumulative Energy from Two Pipe Facilities

iTi 2018 Conference on Turbulence VIII, September 5–7, 2018, Bertinoro, Italy

**Veröffentlichungen, Konferenzbeiträge und Vorträge/
Publications, contributions to conferences and invited lectures**

Veröffentlichungen in Tagungsbänden und Vorträge / Poster 2018/2019

Borcia, I.D., Borcia, R., Bestehorn, M., Xu, W., Harlander, U.
Surface waves generated by libration in a circular channel
12th European Fluid Mechanics Conference, September 7-9, 2018, Vienna

Nowak, T., Merbold, S., Egbers, Ch., Schacht, R.
Numerical Study with Experimental Validation of Thermal Coupling Phenomena with Flip-Chip
Assembled Test Dies on PCB (Poster)
24th INT. WORKSHOP on Thermal Investigations of ICs and Systems, September 2018,
Stockholm, ISBN 978-1-5386-6759-0

Nowak, T., „Thermisch konduktive und konvektive Kopplungseffekte von Silizium-Flip-Chips auf
einer Leiterplatte“; **IMAPS Herbstkonferenz**, 2018, München.

I. Borcia, I., Borcia, R., Bestehorn, M., Richter, S., Xu, W., Harlander, U.
Horizontal Faraday instability and parametric excitation in a circular channel
GAMM-Tagung 2019, 90th Annual Meeting of the International Association of Applied
Mathematics and Mechanics, February 18-22, 2019, Vienna, Austria
ISBN 978-3-903024-84-7

A. Shahirpour,
CISM-ECCOMAS International Summer School on: "Coherent Structures in Unsteady Flows:
Mathematical and Computational Methods", June 3, 2019 — June 7, 2019, Udine, Italy,
Coordinator: George Haller (ETH Zürich, Institute for Mechanical Systems, Zürich, Switzerland),
<http://www.cism.it/courses/C1904/>

Master-, Bachelorarbeiten, Dissertationen, Habilitationen Examinations, theses and habilitations

Dissertationen, Habilitationen:

M.Sc. Matthias Neben:

3D CFD der Gas-Partikel-Strömung in einer Laval-Düse zur Vorhersage mechanischer Erosion.
Dissertationsschrift BTU Cottbus-Senftenberg, 2019

M.Sc. Andreas Froitzheim:

Angular momentum transport and pattern formation in medium- and wide-gap turbulent Taylor-Couette flow: An experimental study.
Dissertationsschrift BTU Cottbus-Senftenberg, 2019

Dipl.-Phys. Sebastian Merbold:

Experimental investigation on turbulent transport in Taylor-Couette flow.
Dissertationsschrift BTU Cottbus-Senftenberg, 2019

M.Sc. Marcel Jongmanns:

Flow control of thermal convection using thermos-electro-hydrodynamic forces in a cylindrical annulus.

Dissertationsschrift BTU Cottbus-Senftenberg, 2019

Master-, Bachelorarbeiten, Dissertationen, Habilitationen Examinations, theses and habilitations

Masterarbeiten (2018)

- David Wilkniß:
Numerische Simulation eines Experiments zur Untersuchung von atmosphärischen Strömungen.
- Luisa Runge:
Gestaltung und Simulation einer Strömungsmaschine zum Einsatz auf dem Läufer einer Synchronmaschine.
- Daniel Haase:
Operating Windows Maschinenteknik im Fokus der Maschinendiagnose.
- Sven Haase:
Wiederherstellbarkeit des Betriebspunktes bei Verdichtertests.
- Kevin Wilkniß:
Doppelt-diffusive Schichtbildung über einer geheizten Platte.
- Jacob Böhnke:
Numerische Untersuchungen zur Optimierung der Strömung an einer Zapfluftstelle eines modernen Hochdruck-Verdichters in Flug-Triebwerksanwendung.
- Michael Wiederhold:
Numerische Simulation der Spaltströmung eines Radialgleitlagers im Abgasturbolader.
- Vilko Ostmann:
Planung und Konstruktion einer modularen Experimentalzelle zur Untersuchung thermoelektro-hydrodynamischer Konvektion in einer rechtwinkligen Kavität.
- Martin Richter:
Experimentelle Untersuchungen eines differentiell drehenden Taylor-Couette-Systems mit weitem Spalt.

Bachelorarbeiten (2019)

- Mustafa Al Kawwas:
Investigation into the drift rates of the GeoFlow II experiment.
- Max Schrader:
Vergleichsstudie verschiedener gasdynamischer Folienlagervarianten mit numerischer Modellbildung und Auswertung des Schmierespalts und der Foliensteifigkeitsverteilung.
- Matthias Strangfeld:
Untersuchung einer Leckage in einer Rohrströmung bei hohen Reynolds-Zahlen.

Anfahrt / How to get there?

Sie erreichen uns per

You can reach us by

Flugzeug:	über	<u>Flughäfen Berlin</u> (Tegel oder Schönefeld) <u>Flughafen Dresden</u>	Airplane:	via	<u>Airports Berlin</u> (Tegel or Schönefeld) <u>Airport Dresden</u>
Bahn:	über	<u>Berlin</u> <u>Dresden</u> <u>Leipzig</u>	Train:	via	<u>Berlin</u> <u>Dresden</u> <u>Leipzig</u>
Auto:	über	<u>Berlin</u> A10 Schönefelder Kreuz, A13 Richtung Dresden A15 Richtung Cottbus Abfahrt Cottbus-West	Car:	via	<u>Berlin</u> A10 Schönefelder Kreuz, A13 direction Dresden A15 direction Cottbus Exit Cottbus-West
	über	<u>Dresden</u> A4 Kreuz Dresden Nord A13 Richtung Berlin A15 Richtung Cottbus Abfahrt Cottbus-West		via	<u>Dresden</u> A4 Cross Dresden North A13 direction Berlin A15 direction Cottbus Exit Cottbus-West

